Università Politecnica delle Marche

Research Doctorate in Life and Environmental Sciences
Curriculum of Marine Biology and Ecology
Cycle XVI

Application of nanotechnologies in aquaculture

Supervisor:
Prof. Ike Olivotto

Ph.D. candidate:
Giulia Chemello

Co-Supervisor:
Prof. Giuseppe Radaelli

Supervisor
Prof. Ike Olivotto
Professor of Aquaculture, Reproduction and Development
of ornamental and commercial species
Department of Life and Environmental Sciences
Università Politecnica delle Marche (Ancona, Italy)

Co-supervisor
Prof. Giuseppe Radaelli
Professor of Anatomy of Domestic Animals
Department of Comparative Biomedicine and Food Science
Università degli Studi di Padova (Legnaro, Italy)

All'amore e al sostegno di chi in questo percorso c'è stato,

c'era già e ci sarà.

Contents

Chapter 3

Safety assessment of antibiotic administration by magnetic nanoparticles in *ex vivo* zebrafish and gilthead sea bream liver and intestine cultures

Chapter 4

A novel photocatalytic purification system for fish culture

Chapter 5

Larvicidal activity of a new photosensitizer complex tested on *Aedes aegypti* larvae

Abstract

Nanotechnology represents the ability to control and manipulate the matter at the atomic and molecular level and therefore hold a great potential to create new materials with enhanced properties.

Nanoparticles (NPs) play an important role in nanotechnology advances, unique NPs characteristics have accelerated the growth in the production of nanoscale materials and the rapid increase of their application in many areas. The major advantages of NPs are represented by their small size and high surface/volume ratio, which make them the key promoters of several industries and research sectors growth. Aquaculture represents the fastest growing food-producing sector in the world and significantly contributes to the world's supply of fish for human consumption. In order to guarantee a sustainable growth that meets the global needs, aquaculture activity has to overcome some disadvantageous aspects deriving from its own practices, such as the high amount of organic compounds in untreated wastewater, the large use of antibiotics and the proliferation of disease vectors. Nanotechnology application could offer different solutions to solve such issues and ensure the sustainable development of aquaculture activity.

Thanks to a multidisciplinary approach that includes molecular, chemical and microscopy analysis, this study was able to test the innovative and safe application of two different types of nanotechnology on different aquaculture aspects.

This project addresses five topics that are described in different chapters as follows:

1. In chapter one, I focused on a new methodology for oxytetracycline (OTC) administration through the use of iron oxide nanoparticles called SAMNs (made of maghemite γ-Fe_2O_3) in zebrafish (*Danio rerio*) through the formation of the new SAMNs@OTC complex.

Adult female zebrafish exposure to SAMNs allowed to test their efficacy as OTC delivery vector. The accumulation of OTC into zebrafish organs and the interaction with the biological environment were evaluated excluding possible toxic effects at a morphological and molecular level. This new OTC administration method seems much more efficient than the traditional way of exposure and has the potentiality to reduce antibiotic utilization and possible environmental impacts.

2. The second chapter described the process known as "protein hitch-hiking" as the mechanism of OTC transfer and accumulation observed in the first chapter. After bare SAMNs and SAMNs@OTC had been incubated in sea bream (*Sparus aurata*) blood serum, successive analysis determined the selective binding of SAMNs and SAMNs@OTC with the apolipoprotein A1, a known carrier of lipids and low-polarity molecules to fish ovary. Within the organism, the selective binding of apolipoprotein A1, which can be considered as an endogenous targeting signal, could lead to the organotropic and delivery of OTC in the fish ovary.
3. In the third chapter, the same oxytetracycline (OTC) delivery method previously studied in *in vivo* experiments reported in Chapter 1was tested using fish organ cultures from zebrafish and gilthead sea bream. This paper demonstrated that the complex SAMNs@OTC herein used may represent a valid and safe way to deliver OTC in organ cultures. However, the discrepancy observed between these results and those obtained from *in vivo* exposure highlighted different important factors which reveal that *in vivo* studies replacement with *ex vivo* models are not always able to represent the typical interaction complexity of a biological system. The main differences between *in vivo* and *ex vivo*

exposure are represented by the simplicity of the organ culture system used in this study compared to the biological complexity of the animal *in toto* as well as the two different experiment exposure times (hours *vs* days) and the direct contact of the NPs suspended in the culture medium with the organ cultures

4. The fourth chapter compared, for the first time, the effects on fish culture of a classical mechanical, biological, UV purification system to a TiO_2-PCD one, with particular emphasis on water chemistry and physiological responses in adult zebrafish. The photocatalytic system showed excellent efficiency in removing nitrogen compounds from water. Physiological analysis including histological and molecular assays demonstrated that no significant biological alterations/effects were detectable in cultured fish.
5. At last, the fifth chapter focused on assessing the efficacy of an innovative complex made of magnetic nanoparticle and a photosensitizer molecule (under evaluation for patentability) in relation to mosquitoes' proliferation control. *Aedes aegypti* larvae were exposed to the complex in water solution and the larvicidal activity of the nanomaterial and photosensitizer molecule alone were compared to the new complex. In particular, tissues accumulation of the complex was evaluated by optic and transmission electron microscopy (TEM).

Introduction

Nanotechnology

Nanoparticles (NPs) are conventionally defined as particles with at least one or more dimensions between 1 and 100 nm that show properties we cannot attribute to bulk samples of the same material (Auffan *et al.,* 2009). Nanotechnology investigates the integration of these nanoscale particles into larger material components and systems, keeping the control and construction of new and improved materials at the nanoscale. The peculiar properties of NPs have accelerated the growth rate growth in nanomaterials (NMs) production and the increase of their application in many areas, capturing the attention of researchers, governments, and industries worldwide.

Natural NPs have always existed on our planet, but only with the development of tools (such as scanning tunneling microscope (STM) and Atomic Force Microscope (AFM)), able to accurately detect the microscopic matter, scientists were able to study and manipulate NMs.

The term nanotechnology indeed was first introduced by Professor Norio Taniguchi from the University of Sciences in Tokyo, in 1974, in his thesis entitled "*On the basic concept of Nano – Technology"*, where he precisely described the formation of materials with dimensions of a nanometer (Demetzos, 2016).

Before Taniguchi's definition, the starting point of the new field we now regard to as nanotechnology was introduced by the famous physicist Richard P. Feynman during a talk at the Annual Meeting of the American Physical Society at the Californian Institute of Technology in 1959. In his speech entitled "*There's plenty of room at the bottom"* Feynman lectured about the problem of manipulating and controlling things on a small scale (Winkelmann & Editors, 2016) which is indeed the basic concept of nanotechnology studies.

Some years after Feynman's speech, the National Science Foundation (NSF) established in 1991 its first program dedicated to NPs and from 1997-1998 funded a cross-disciplinary program entitled ''Partnerships in Nanotechnology'' (Roco, 2011).

Governments and companies set up funds for research and development to support the rapid worldwide expansion of nanotechnology market which now includes more than 1.000 commercially available products containing nanomaterials or made using nanotechnology (Klaine *et al.*, 2012).

Such a rapid advancement of nanotechnology has laid the groundwork for innovation in different fields, including health, agriculture, food, transport, energy, electronics and communications, resulting in a significant increase of novel nanomaterials development (Roco, 2011).

Nanoparticles characteristic and synthesis

NPs can be spherical, tubular or irregularly shaped, and can exist in fused, aggregated or agglomerated forms (Grillo, Rosa and Fraceto, 2015). They can be categorized into carbon-based materials such as fullerenes and carbon nanotubes and inorganic nanoparticles including the ones based on metal oxides (zinc oxide, iron oxide, titanium dioxide and cerium oxide), metals (gold, silver and iron) and quantum dots (cadmium sulfide and cadmium selenide) (Ju-Nam and Lead, 2008).

Currently, NPs are commonly classified in two main categories based on their origins: non-engineered and engineered NPs. The formers are found in the environment and derive from natural events such as terrestrial dust storms, erosion, volcanic eruptions and forest fires. We can also consider as non-engineered NPs those accidentally produced and introduced into the environment by human activities such as combustion products or generated by combustion engines, power plants and other thermos-degradation systems

(Cupaioli *et al.*, 2014). On the other hand, the development of nanotechnology is responsible for human exposure to a new NPs category: the engineered NPs. Engineered NPs are intentionally produced by humans using different materials, such as metals (including Ag, Zn, Au, Ni, Fe and Cu), metal oxides (TiO_2, Fe_3O_4, SiO_2, CeO_2 and Al_2O_3), non-metals (silica and quantum dots), carbon (nanotubes and fullerene), polymers (alginate, chitosan, hydroxymethylcellulose, polyhydroxyalkanoates and poly-e-caprolactone) and lipids (soybean lecithin and stearic acid) (Grillo, Rosa and Fraceto, 2015). The synthesis of engineered NPs produces homogenous materials with controlled characteristics, which exhibit intermediate features between atoms' and corresponding bulk materials'. Small size and high surface/volume ratio strongly determine NPs chemical-physical properties, reactivity, and interactions with the environment.

As an example, the melting behavior is one of the chemical-physical parameters that differentiates nanoscale from the corresponding bulk material. Small particles have lower melting points than bulk material due to an increase of surface and internal ratio atoms as the size of particles decreases. Moreover, NPs shape strongly influences their interactions with the environment. For instance, the charge distribution on the surface of spherical inorganic NPs is quite different from that of rod or urchin shaped particles (Hutter *et al.*, 2010). The chemical-physical characteristics of NPs also determine their biodistribution, biological effects and, consequently, their toxicity. In the case of engineered NPs for drug delivery, the chemical-physical characteristics influence drug loading, drug release, NPs stability and cellular uptake. NPs size, shape and composition strongly influence their interaction with biological systems. The high surface/volume ratio and the chemistry of NPs surfaces promote their aggregation and interaction with biomolecules such as proteins and DNA (Ludwig K. Limbach *et al.*, 2005). Due to their size, NPs

should be easily uptaken by living organisms; smallest NPs penetrate the cellular barrier (such as Blood-Brain Barrier) more rapidly than larger ones (Chen *et al.*, 2010).

Together with size, the shape also interferes with NPs biodistribution and tissue-specific accumulation. Recent evidence show that sub-micrometric discoidal particles accumulate in lungs, liver, heart, and spleen more than spherical and cylindrical particles (Decuzzi *et al.*, 2010).

In addition, the hydrophobicity of NPs influences their capacity to bind proteins. It has been hypothesized that interaction of NPs with proteins might alter protein conformation leading to exposure of new epitopes and/or abnormal functions (Mu *et al.*, 2009).

To obtain particles with specific characteristics at the nanoscale size, different production procedures have been discovered and developed. NPs production methods can be classified into top-down and bottom-up categories. Top-down approaches involve the size-reduction of large particles to the nanometer range. This can be achieved by milling or high-pressure homogenization (Chan and Kwok, 2011). The two major types of high-pressure homogenization are microfluidization and piston-gap homogenization. Microfluidization is essentially air-jet milling, in which the particles are fragmented by collision in a high-pressure air jet. On the other hand, piston-gap homogenization involves forcing a liquid suspension at high pressure through a narrow channel or gap inside a pipe (Chan and Kwok, 2011).

A major drawback of the top-down approach is the imperfection obtained at the surface structure, which in metallic NPs, for example, can significantly impact NPs physical properties and surface chemistry (Thakkar, Mhatre and Parikh, 2010).

Conversely, bottom-up methods generate nanoparticles by building them from drug molecules in solution. This can be achieved by controlled precipitation

(or crystallization) and evaporation. These processes can occur in the bulk solution or in droplets, depending on the technique.(Chan and Kwok, 2011).

NPs in biomedicine

Nanotechnology application in the biomedical field shows interesting advancements in several specific areas such as drug targeting, biodiagnostics, bioimaging, and genetic manipulation (Chatterjee *et al.*, 2014). Novel directions include, for example, theranostics (nanosystems capable of diagnosis, drug delivery and monitoring therapeutic responses all in a single tool) and plasmonic photothermal therapy (PPT) (Giner-Casares *et al.*, 2016). To date, NPs biomedical applications include drug and gene delivery, labeling, pathogen or protein detection, probing of DNA structure, tissue engineering, hyperthermia treatments and magnetic resonance imaging (MRI) contrast agents (Hoet *et al.*, 2004).

The major advantages of nanoparticles over larger sized particles are represented by their small size and high surface/volume ratio, which make them the key promoters of the development in biomedical research. A wide variety of organic and inorganic NPs is currently used for biological applications. Semiconductor quantum dots are commercially available and offer a viable alternative to fluorescently labeled particles, whereas iron oxide nanoparticles, due to their favorable features, are the only type of magnetic NPs approved for clinical use by the Food and Drug Administration (Wilczewska *et al.*, 2012). They are currently used in magnetic resonance imaging (MRI) as contrast enhancers in place of conventional gadolinium-based contrast agents (Chatterjee *et al.*, 2014).

A more novel group in terms of their use in biomedicine are plasmonic nanoparticles, which offer many advantages in biomedical research due to their unique characteristics that allow the display of localized surface plasmon

resonance (LSPR) bands in the UV-visible-near IR (infrared) spectral range (Giner-Casares *et al.*, 2016). Whereas, carbon NPs, magnetic NPs and those based on solid lipid are considered as promising carriers for drug delivery. In particular, metal-based NPs hold the potential to carry large drug doses as well as increase drugs circulatory half-life (Ahmad *et al.*, 2010).

Among all the techniques improved by NPs, it is surprising how nanotechnology revolutionized drug delivery procedures. The development of NPs suspensions containing medicines has made it possible to increase the therapeutic index of many components (improvement of the activity and reduction of toxicity) by selectively directing them towards the target tissues or cells (Couvreur, 2013).

The high surface area allows NPs modification to improve drugs pharmacokinetic properties (increase vascular circulation lifetime, bioavailability improvement). Thanks to the increased vascular circulation lifetime also the efficacy of the drug showed a significant increase; the enhancement of drug bioavailability means that a significantly lesser dosage than bulk drugs could effectively exert the effects.

The possibility to modify NPs surface not only helps in targeted drug delivery but can also solve the secondary purpose of monitoring drug release.

Different approaches include solid core drug delivery systems (SCDDS), which consist in coating a solid NP with a fatty acid shell to contain the drug of interest. This methodology works at relatively low temperature and pressure, making it especially useful in the case of heat-sensitive or labile drugs (Swain *et al.*, 2014). Porous NPs can also be used as a drug delivery matrix. For example, mesoporous silica particles can be applied to control the release of different substances (Strømme *et al.*, 2009).

Finally, current research has focused on taking advantages of NPs electronic, magnetic and optical properties to improve the efficiency of signal detection, transmission, and amplification.

One of the most difficult obstacle to deal with NPs biomedical application is the toxicity expressed by some type of NPs which also present, at the same time, suitable properties to their application in several biomedical techniques. Because of their easy penetration across biomembranes and interference with basal metabolic reactions, they could damage structures within the cell.

Apart from their toxicity, NPs also tend to accumulate in the body, therefore, their accumulation could have serious consequences, if not in the near future most likely after a chronic exposure.

To overcome these problems, instead of simple NPs, core/shell structured NPs are often applied thanks to their additional advantages. Core-shell NPs possess a core made of a material coated with another material on top of it. In biomedical applications, these NPs show peculiar properties such as minor cytotoxicity, higher dispersion, higher biocompatibility, better conjugation with other bioactive molecules and increased thermal and chemical stability. Shell layers act as a nontoxic coating as well as to improve the core material property (Couvreur, 2013).

These NPs open the way to the synthesis of novel drug carriers with enhanced properties such as increased residence time, increased bioavailability, and reduction of dosing quantity and frequency of administration along with a higher specificity.

Nanotoxicology

Nanotechnology contribution and benefits in many research and industrial fields are widely demonstrated, however it is recognized that its application may raise new challenges in safety and ethical domains. As described in the previous paragraph, a broad range of engineered NPs has been designed to be introduced into the body for diagnostic and therapeutic purposes (Thanh and Green, 2010; Reddy *et al.*, 2012; Nalwa, 2014).

To find application in biomedicine, as well as in many other sectors, NPs should satisfy specific criteria, the most important of which is the lack of toxicity. In *in vivo* application, besides the absence of toxic effects, NPs must avoid non-specific interactions with plasma proteins and either avoid or allow uptake by the reticuloendothelial system (RES) depending on the application and to efficiently reach their target. NPs also have to maintain colloidal stability under physiological conditions including a wide range of pH (Thanh and Green, 2010).

Progress in the development of new types of engineered NPs often results in the creation of new materials with unexpected physical and chemical characteristics and consequently in unique and often unknown biological effects.

While the toxicity of many bulk materials is well understood, the concentration or size at which NPs begin to exhibit new toxic effects are still not clear (Sharifi *et al.*, 2012). There is a considerable gap between the available data on NMs production and their toxicity evaluation. Engineered NPs that accidentally reach the environment represent a further problem, because biological systems did not evolve, and are therefore unprepared to deal, with their presence (Moore, 2006).

Therefore, to take advantage of NPs properties, deeper studies have been performed over the past two decades to determine whether the potential

benefits of nanotechnology could be exploited without any adverse impact on human health as well as on the environment.

NPs cellular uptake

To date, most of NPs toxicity and ecotoxicity studies have been conducted without determining the uptake mechanisms (Zhao and Wang, 2012). A proper knowledge of the experimental conditions that influence the transport and uptake across cell membranes would improve our understanding of their toxicity as well as their properties and applications.

NPs can enter the organism through six principal routes: intravenous, transdermal, subcutaneous, inhalation, intraperitoneal and oral (Ryman-Rasmussen, Riviere and Monteiro-Riviere, 2007). NPs accidental uptake by inhalation or ingestion is likely to be the principal way in terrestrial organisms, whereas in aquatic animals there could be other routes of entry such as direct passage across gills and other external surface epithelia such as olfactory organs or body wall (Moore, 2006).

NPs bioaccumulation in aquatic organisms is already demonstrated and several data are available from different studies which analyzed NPs absorption in different aquatic species. The results revealed that the accumulation can occur in various organs (liver, intestine, gills, brain, and spleen) depending on NPs type and exposure routes (Ramsden *et al.*, 2009; Shaw, Al-Bairuty and Handy, 2012; Hao *et al.*, 2013; Piccinetti *et al.*, 2014; Shang, Nienhaus and Nienhaus, 2014). Knowledge of NPs bioaccumulation is essential to detect and quantify the organisms' uptake capacity as well as their distribution within tissues, cell and subcellular compartments (Gomes *et al.*, 2012).

When NPs enter the organism, absorption occurs through the interaction among biological components such as proteins and cells, they can distribute

into various organs where they remain with unchanged, modified or metabolized structure for an uncertain amount of time before passing to other organs or be excreted (Sharifi *et al.*, 2012).

Cell membranes tend to be impermeable to many large particles, usually, only particles in the range of 10 nm to 30 nm in size can cross the membrane through diffusion (Lead and Smith, 2009), the cell membrane acts as a barrier separating the external environment from the inside of the cell. One mechanism to overcome this barrier, which is already exploited with success by viruses is endocytosis (Smith and Helenius, 2004). Endocytosis and diffusion have been proposed as mechanisms for the uptake into cells of NPs with similar size as viruses (Kettler *et al.*, 2014).

Endocytic mechanisms are normally involved in key physiological functions such as intracellular digestion and cellular immunity; endocytic pathways can either lead to the endosomal and lysosomal compartments (conventional endocytosis) or else *via* cell-surface lipid raft-associated domains (known as caveolae) which avoids the degradative fate of material entering the endosomal/lysosomal system (Fig.1) (Pelkmans and Helenius, 2002; Na *et al.*, 2003; Panyam and Labhasetwar, 2003; Panyam *et al.*, 2003). This second pathway, in medical nanotechnology, is the main route through which many NPs are designed to enter target cells (Na *et al.*, 2003; Panyam and Labhasetwar, 2003; Panyam *et al.*, 2003).

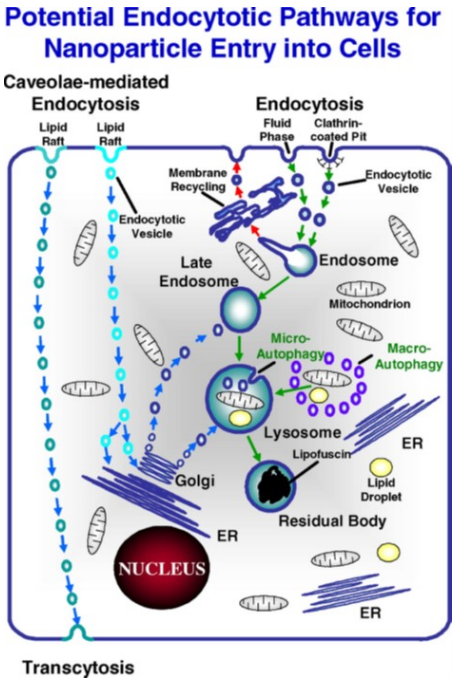

Figure 1. *Possible endocytosis pathways exploited by manufactured NPs to enter the cell. Endocytosis via clathrin-coated pits (receptor-mediated) or uncoated pits (fluid phase) transfers materials to the lysosomal degradative compartment, while caveolar endocytosis can result in translocation to the endoplasmic reticulum (ER), Golgi or through the cell by transcytosis* (Moore, 2006).

NPs internalization in cells is mainly influenced by NPs different physical and chemical properties along with the conditions of the exposure medium of the cells. Recent studies have focused on *in vivo* biodistribution of engineered nanostructures in relation to their physical parameters such as size, shape, surface charge, surface functional groups, and hydrophilicity.

NPs size, for example, may affect their uptake efficiency, kinetics, internalization mechanism and subcellular distribution. A size-dependent uptake in different cell lines has been observed for gold, mesoporous silica, polystyrene and iron oxide NPs, with the maximum cellular uptake at NPs

core size in the range of 30-50 nm, which suggests that there is an optimal size for active uptake (Shang, Nienhaus and Nienhaus, 2014).

The effects of nanoparticle shape on its internalization were also examined and it was found that spherical particles of similar size were taken up 500% more than rod-shaped particles; this can be explained by a greater membrane wrapping time required for the elongated particles (Verma and Stellacci, 2010). Finally, it was observed that NPs surface charge determines aggregation in the blood or interaction with oppositely- and like-charged cell membrane surfaces. Many studies demonstrated that cationic and neutral NPs show the highest transport efficiency compared to negatively charged NPs due to the charge attraction between the positive NPs and negative cell membrane surface, thus increasing the rate and extent of absorption (Murugan *et al.*, 2015).

NPs toxicity effects

The majority of toxicity tests suggested that generation of ROS (reactive oxygen species) and consequent oxidative stress are the most frequent effects caused by NPs exposure, which consequently mediate a series of pathological events such as inflammation, genetic damage, inhibition of cell division and cell death (Manke, Wang and Rojanasakul, 2013).

ROS are physiologically produced in trace amounts in response to various stimuli, free radicals occur as essential byproducts of mitochondrial respiration (Manke, Wang and Rojanasakul, 2013). Inflammatory phagocytes such as neutrophils and macrophages induce oxidative reactions as a defense mechanism against environmental pollutants, tumor cells and microbes (Manke, Wang and Rojanasakul, 2013).

Conversely, high ROS levels are normally indicative of oxidative stress and can damage cells by lipid peroxidation, proteins alteration, DNA damages or

interfering with signaling functions and modulating gene transcription (Schieber and Chandel, 2014).

The mechanism for ROS generation is different for each NP type and to date, the exact cellular mechanism is not completely understood and must be elucidated. One mechanism of NP-induced oxidative stress occurs during the dissolution of iron-based NPs, which catalyzes ROS generation and formation of OOH• and OH• radicals from H_2O_2 via the Fenton reaction (Sharifi *et al.*, 2012). Furthermore, some inert NPs do not give rise to spontaneous ROS production, yet are capable of inducing ROS production under biological conditions, based on the ability of the NPs to target mitochondria (Tian Xia *et al.*, 2006).

Many evidence demonstrate the ability of different types of NPs to induce oxidative stress and, consequently, negative effects. For instance, CNT-induced oxidative stress activates cell signaling pathways resulting in increased expression of pro-inflammatory and fibrotic cytokines (Li *et al.*, 2010). Some NPs have been shown to activate inflammatory cells such as macrophages and neutrophils resulting in an increased production of ROS (Kennedy *et al.*, 2009). Other NPs such as titanium dioxide, zinc oxide, cerium oxide, and silver NPs have been shown to deposit on the cell surface or inside the subcellular organelles and induce oxidative stress signaling cascades that eventually result in oxidative stress to the cell (Manke, Wang and Rojanasakul, 2013). Oxidative stress associated with TiO_2 NPs, for example, results in early inflammatory responses, such as an increase in polymorph nuclear cells, impaired macrophage phagocytosis, and/or fibro proliferative changes in rodents (Bermudez *et al.*, 2004). TiO_2 NPs also can cause proinflammatory effects in human endothelial cells (Sharifi *et al.*, 2012). Carbon NPs have been shown to induce oxidative stress in fish brain cells and pulmonary inflammation in rats (Warheit *et al.*, 2003; Oberdörster, 2004).

In vivo and *in vitro* nanotoxicity

Both in vivo and in vitro tests have been developed to evaluate the toxicity of several NPs, focusing on gaining a comprehensive understanding of the relationship between NPs properties and their potential toxicity or application in different fields.

Although any experimental analysis can be performed with cells obtained from either in vivo or in vitro experimentation, it is necessary to highlight the constant debate of the advantages and disadvantages of both methods.

In vitro methods produce specific and quantitative measurements of toxicity and are extremely valid for initially evaluating the expected biocompatibility of new NPs. Different techniques can be used to assess NMs toxicity, including *in vitro* assays for cell viability/proliferation, mechanistic assays (ROS generation, apoptosis, necrosis, DNA damages), microscopic evaluation of intracellular localization (SEM-EDS, TEM, AFM, fluorescence spectroscopy, MRI, VEDIC microscopy), gene expression analysis, high-throughput systems, *in vitro* hemolysis and genotoxicity (Arora, Rajwade and Paknikar, 2012).

In vitro methods are ideal for nanotoxicology research because they can produce reproducible results rapidly and inexpensively without the use of animals. Some examples of these techniques include the lactate dehydrogenase (LDH) assay performed to test cell membrane integrity, the MTT assay of mitochondrial function and immunochemistry markers for apoptosis and necrosis (Sharifi *et al.*, 2012). These methods, however, show some disadvantages: they provide little information on the mechanism or cause of cellular toxicity and death. Some colorimetric assays such as Live/Dead, Trypan Blue, and Neutral Red just discriminate live from dead cells but provide little information regarding the mechanisms of cell death (Sharifi *et al.*, 2012). Moreover, recent studies suggest that classical cell-based

assays designed for testing chemicals may not provide reliable data since nanomaterials can interfere with assay components and readout systems (Kroll *et al.*, 2012). The accuracy and precision of colorimetric assays for NPs *in vitro* toxicity, for example, are affected by the interaction between NPs and dyes. It has been demonstrated that carbon nanotubes (CNTs) adsorb MTT formazan and other dyes such as Neutral Red and Alamar Blue producing conflicting results, while the high adsorption capacity of carbon nanomaterials generates false-positive data resulting in an overestimation of their toxicity (Casey *et al.*, 2007; Kroll *et al.*, 2012).

On the other hand, *in vivo* models allow the study of aspects that cannot be otherwise observed through *in vitro* systems. Factors such as route of administration, biodistribution, biodegradability, long-term disposition, induction of developmental defects and activation of the immune system, are all major issues in determining *in vivo* nanotoxicity and cannot be properly studied by an *in vitro* approach (i.e. primary cell cultures, tissues and organ cultures) (Rizzo *et al.*, 2013).

Although i*n vivo* tests can provide information on the carcinogenicity, pulmonary, dermal and gastrointestinal toxicity related to the initial deposition of nanomaterials by considering various exposure routes, they are time-consuming, more expensive and raise ethical issues. Moreover, cultured human and animal cells can be better controlled and therefore provide more reproducible data than *in vivo* systems, although requiring a high standardization to maximize data reproducibility (Clift, Gehr and Rothen-Rutishauser, 2011).

At present, it is evident that one of the major gaps in the knowledge of nanotoxicity studies is the lack of correlation between *in vivo* and *in vitro* tests, which leads to discrepancy in experimental conditions.

Therefore, a proper development of *in vitro* assays as predictive tools to evaluate NPs toxicity is an important goal during early product development. If correctly validated, these initial screening tests would result useful since they are simpler, faster and less expensive than their *in vivo* counterparts are. Moreover, successful development of *in vitro* toxicity systems should reduce animal use and animal stress used in hazard screening.

Aquaculture

While the rearing of aquatic animals and plants may seem a relatively new activity, aquaculture actually represents an ancient practice that is nearly 4000-year old. Pond culture of Tilapia nilotica is engraved in an Egyptian tomb dating before 2000 B.C. and the husbandry of carp may have been the source of fresh fish for the emperor in China around 1000 B.C (Iwama, 2009). This misconception may be due to the fact that aquaculture production, as well as its utilization in human consumption, has dramatically increased in the last 3 decades. Global aquaculture production has more than doubled since 2000, increasing from 41.7 million tons to reach a new estimate of over 90.4 million tons in 2012, with production growing at an annual average rate of 6.7% since then (FAO, 2017). Such a growth is the results of the production areas expansion, increase of knowledge in husbandry systems and advancement in production technologies, but most importantly entails an increased exploitation of natural resources and hence raises concerns on environmental distress (Samuel-Fitwi *et al.*, 2012).

Numerous are the benefits deriving from aquaculture activity:

- Production of high-quality food, increase of household food supply and improvement of nutrition.
- Strengthened marginal economies by the increase in employment and reduction of food prices.

- Improvement of water resources and nutrient management at household or community levels.
- Preservation of aquatic biodiversity through re-stocking and recovering of protected species.
- If done sustainably, management and preservation of wild stock stressed by commercial and sports fisheries.
- Stimulation of research and technology development.
- Increased education and environmental awareness.

With a global population of nearly seven billion people, the demand for aquatic food is destined to increase and a further expansion and intensification of aquaculture production are required. To guarantee a sustainable growth that meets the global needs, aquaculture activity should overcome some disadvantageous aspects deriving from its own practice which may cause negative effects on the production itself and may have negative environmental impacts.

One of the major negative aspects that characterize intensive aquaculture practices is the large amount of uneaten feed and fish feces present in untreated wastewater (Brune et al. 2003; Piedrahita 2003; Gutierrez-Wing and Malone 2006). These waters are particularly rich in organic compounds such as nitrogen and organic nitrogen is potentially toxic for aquatic organisms especially in its anionized form NH_3 (Hu *et al.*, 2017). To date, an efficient maintenance of the water quality in fish tanks is accomplished through "open-systems", which consist of aquaculture facilities characterized by a constant water flow taken from a natural source (basin, lake, river, sea, and lagoon) and restituted to the main water body.

In this way, large amounts of water are used daily with substantial costs and the actual risk of organic nutrient-rich waters (nitrogen compounds,

phosphorus, dissolved organic carbon and organic matter) affecting the aquatic environment (Turcios and Papenbrock, 2014).

It is not rare that high amounts of organic compounds released from aquaculture intensive systems lead to eutrophication phenomena contributing to an increase in primary productivity and often generating undesirable changes in the structure and function of aquatic ecosystems (Marinho-Soriano *et al.*, 2011). Some of the consequences deriving from the eutrophication (caused by fish farms input of organic matter), of aquatic environment, are the decrease of benthic diversity (Wu, 1995; Karakassis *et al.*, 2000) and the alteration of sediment's characteristics (Wu *et al.*, 1994; Cancemi, De Falco and Pergent, 2003). Cancemi and collaborators (2003) observed the influence of a fish farm in a littoral bay of Corsica on the surrounding ecosystem, in particular, they observed the effects on the *Posidonia oceanica* seagrass meadows. The input of organic matter deriving from the cages caused an alteration of the bottom sediment, a high epiphyte biomass (due to the nutrient enrichment) and a plant/epiphyte competition that lead to leaf fragility and a decrease in light availability.

Also salmon farming was demonstrated to cause marked changes in species number and diversity, faunal abundance, and distribution of benthic fauna (Brown, Gowen and McLusky, 1987; Findlay, Watling and Mayer, 1995).

Disease emergence is an important constraint to the growth of aquaculture, poor water quality, and high stocking density often promote outbreaks of pathogens and their potential spread in the bordering areas with serious impacts on wild populations (Thompson *et al.*, 2002). For example, crayfish plague, introduced from the USA, has eradicated native crayfish from a large area of Europe (Alderman, 1996). Movement of stocks for aquaculture purposes have been demonstrated to increase the risk of spreading pathogens (Naylor *et al.*, 2000). In Europe, for example, serious epidemics of

furunculosis and *Gyrodactylus salaris*, in stocks of Atlantic salmon, have been linked to movements of fish for aquaculture and re-stocking (McVicar, 1997). It has already been demonstrated that Norwegian cod and salmon farms are the principal cause of spreading pathogens from farmed fish to wild populations (Johansen *et al.*, 2011).

Once again, many epidemics have been reported in some of the most important salmon farming regions of the world, including Chile, where infectious salmon anemia virus (ISAV) caused the most important disease and economic crisis in the history of the country's salmon industry (2007-2009) (Mardones *et al.*, 2014). There are evidence that anthropogenic activities, such as movement of live or harvested fish or their byproduct, may have played a more important role than the environmental or passive transmission in this outbreak (Mardones *et al.*, 2014).

Many of these problems have been faced using large amounts of antibiotics. Their wide and frequent use has resulted in antibiotic resistance in many fish pathogens (Defoirdt, Sorgeloos and Bossier, 2011), and their massive release into the environment through faeces and uneaten antibiotic-enriched feed, causing an increased environmental antibiotic resistance (Rhodes *et al.*, 2000; Miranda and Zemelman, 2002; Petersen *et al.*, 2002).

Finally, another hazard, often associated to aquaculture practices, of public health interest, is represented by the proliferation of mosquitoes and others disease vectors, that may harbor their eggs and larvae on fish tanks (Erondu and Anyanwu, 2011). Mosquitoes larvae indeed feed on suspended particles or carcasses of their own or related species while floating at water surface (Merritt, Dadd and Walker, 1992).Several mosquito species are known to be vectors of many arboviruses which are important causes of human disease epidemics. Malaria, dengue, Japanese encephalitis, yellow fever, Rift Valley fever, Venezuelan equine encephalitis, and Ross River to name just a few of

these diseases (Penilla *et al.*, 1998; Gubler, 2002). The geographic distribution of some mosquito vectors and some viruses have expanded globally, accompanied by more frequent and larger epidemics, e.g., dengue fever, for this reasons the controls of mosquitoes spread is of crucial importance (Gubler, 2002).

Nanotechnology could offer different solutions to overcome the problems that affect the aquaculture industry, e.g. water treatment, control of aquatic diseases, fishpond sterilization and nano-feed for fish. Some of these issues have already been investigated in the last years. For example, in aquaculture systems, fish feeding is commonly supplied as pellet food, and NPs are used to enclose or coat (nano-encapsulation technology) nutrients that would normally degrade, such as fatty acids, or have limited assimilation efficiency across the fish gut because of their poor solubility. To date, the antimicrobial properties of NPs such as titanium and silver NPs are exploited to reduce the build-up of bacteria in aquaculture systems (Sondi and Salopek-Sondi, 2004; Martínez-Castañón *et al.*, 2008; Martinez-Gutierrez *et al.*, 2010).

However, some others issue still need to be addressed or better investigated, and nanotechnology can offer an alternative method to guarantee water quality in aquaculture systems and can be used as drug delivery matrix that guarantees a more efficient antibiotic and vaccine delivering system as already demonstrated in human biomedicine.

Therefore, the present Ph.D. thesis examines for the first time, the possible application of different nanomaterials to antibiotic delivery, water treatment and control of mosquitoes' proliferation in aquaculture systems.

Model organisms

The present Ph.D. project was conducted using different aquatic organisms (at different development stages) as experimental models, for the purpose of evaluating the effect of new nanomaterials in organisms showing different levels of complexity.

Escherichia coli

Class: Gammaproteobacteria
Order: Enterobacterales
Family: Enterobacteriaceae
Genus: Escherichia

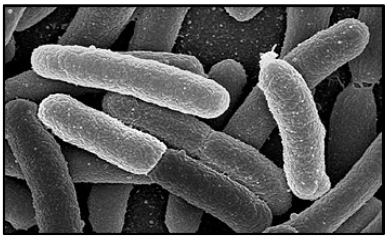

Escherichia coli is one of the most versatile gram-negative bacterial species. It alternates between its primary and secondary habitats respectively the gut of vertebrates (where it lives as a commensal), and water and sediment (which are reached after excretion from the host). It may also behave as an intra- and extra-intestinal pathogen in humans and many other animal species (Clermont *et al.*, 2011). Such a variability is due to the high genome plasticity deriving from gene loss and gain and horizontal transfer (Touchon *et al.*, 2009). *E. coli* has a core genome of less than 2000 genes, but the total number of 10000 allows a large number of different gene combinations and, therefore, the diverse phenotypes observed (Rasko *et al.*, 2008; Touchon *et al.*, 2009).
Based on genomic information, the species has been divided into six different phylogenetic groups, denoted as A, B1, B2, C, D, and E (Touchon *et al.*, 2009). These subgroups include saprophytic (A) and pathogenic (in particular B2, D) types and are often considered to be the result of long evolution process (van Elsas *et al.*, 2011).

Pathogenic strains responsible for intestinal infections include enteropathogenic *E. coli* (EPEC), enterohemorrhagic *E. coli* (EHEC), enterotoxigenic *E. coli* (ETEC), enteroaggregative *E. coli* (EAEC), enteroinvasive *E. coli*, diffusely adherent *E. coli*, necrotoxic *E. coli*, and cell-detaching *E. coli* (Hamelin *et al.*, 2007). Although pathogenic *E. coli* have been more commonly recognized as intestinal pathogens, extraintestinal infections are also a major source of morbidity and mortality (Russo, 2003). *E. coli* is commonly known as an important component of the gastrointestinal microflora; however, its presence as a key component of the microbial communities is crucial in the aquatic environment, especially in the sediment banks, soil and beach sands (Pachepsky and Shelton, 2011). Thanks to this and to the amount of information about its genetics, *E. coli* is used as a model organism in different studies to detect and test bacterial antibiotic-resistance in the aquatic environment (Costanzo, Murby and Bates, 2005; Sjölund *et al.*, 2008; Kümmerer, 2009; Gullberg *et al.*, 2011). Determining the presence of antibiotic-resistant bacteria in an environmental reservoir is vital, as the environmental source is not only a way of dissemination of antibiotic-resistant microorganisms among human and animals but also the route through which resistance genes are introduced into natural bacterial ecosystems (Amaya *et al.*, 2012).

Aedes aegypti

Class: Insecta

Order: Diptera

Family: Culicidae

Genus: Aedes

Aedes aegypti is a tropical mosquito originating from Africa that probably spread because of international trade by sea routes through the fifteenth to the seventeenth centuries (Jansen and Beebe, 2010). Unlike many other mosquito species, *A. aegypti* is a day-biting mosquito and often feeds on multiple hosts during a single gonotrophic cycle. Females preferentially lay eggs in manmade or artificial containers including water tanks, flower vases, pot plant bases, discarded tires, buckets or other containers typically found in close proximity of or in houses (Christophers, 1960).

After the hatching, larvae feed on microorganisms and particulate organic matter. When larvae have acquired enough energy and size, metamorphosis to pupae occurs. Pupae do not feed but just undergo morphological changes to the adult flying mosquito. The entire life cycle lasts 8-10 days at room temperature, depending on the level of feeding.

Aedes aegypti is one of the species responsible for the transmission of yellow fever, dengue fever and dengue hemorrhagic fever (Cheng, 2003). It was also identified as one of Zika virus vectors (urban transmission) together with other species of *Aedes* genus (Ioos *et al.*, 2014).

There are several aspects that make the controlling of mosquito populations a difficult task: for instance, eggs can endure desiccation for up to one year; there is no effective technique to control the eggs in water containers (Russell, Kay and Shipton, 2001); because of their high domestication, adults can rest indoor in inaccessible places, making air larvicidal useless (Ciccia, Coussio

and Mongelli, 2000). Finally, the prolonged application of common larvicidal substances and insect growth regulators such as organophosphates has fostered several environmental and health concerns, including widespread larval resistance, disruption of natural biological control systems, outbreaks of other insect species and undesirable effects on non-target organisms (Sen-Sung Cheng *et al.*, 2004).

Danio rerio

Class: Actinopterygii
Order: Cypriniformes
Family: Cyprinidae
Subfamily: Danioninae
Genus: Danio

Zebrafish (*Danio rerio*) is a small tropical freshwater cyprinoid fish hailing from India. Over the years, it has gained an increasing importance as vertebrate model in the fields of developmental biology, genetics, functional genomics, aquatic toxicology, neuroscience and many other areas of biomedical research (Arunachalam *et al.*, 2013).

The main advantages of using zebrafish as an experimental model over other organisms derive from its high fecundity, short generation time, rapid development (hatching occurs after 2-3 days post fertilization), external fertilization, translucent embryos (suitable for observation of internal organs with conventional microscopy) and an extensive amount of information made available by genome and transcriptome sequencing (Teraoka, Dong and Hiraga, 2003). In addition, tissue types (kidney, spleen, liver, blood brain barrier) and immunogenic and physiological responses to common xeno-

substances such as oxidative stress and to foreign bodies are comparable to those of higher vertebrates (Rubinstein, 2003).

The transparent chorion enables an easy observation of development and a detailed knowledge of its life cycle, both for embryonic stages (Kimmel *et al.*, 1995) and postembryonic development (Parichy *et al.*, 2009). This has facilitated the identification of genes with important roles in development by mutagenesis screens.

Starting from the 1950s, zebrafish has been used for toxicity tests of synthetic chemicals and natural products (Battle and Hisaoka, 1952), metals (e.g., zinc, selenium, mercury, and copper) (Niimi and LaHam, 1975; Dave and Xiu, 1991; Senger *et al.*, 2006; Johnson, Carew and Sloman, 2007) and organic solvents (e.g., phenol, aniline, and cyclohexane) (Vittozzi and De Angelis, 1991). Thanks to the inexpensive costs associated to zebrafish maintenance and handling, successive studies on different areas of toxicology were performed to understand the adverse effects of chemicals and to predict results in humans. These studies demonstrated that zebrafish is suitable for chemical screening and displays good dose responsiveness to toxicity (Zhang *et al.*, 2003).

In recent years, along with nanotechnology development, the necessity of quick, cheap and easy protocols to conservatively assess the toxicity of nanomaterials, especially those used in biomedicine, has increasingly occurred. Zebrafish, as model organism, allows the performance of nanotoxicity tests for a wide range of nanomaterials including metal nanoparticles, carbon-based nanomaterials, and polymers, many of which are already being incorporated into nanopharmaceuticals (Fako and Furgeson, 2009).

Sparus aurata

Class: Actinopterygii

Order: Perciformes

Family: Sparidae

Genus: Sparus

Gilthead sea bream (*Sparus aurata*) is a marine teleost occupying the Mediterranean Sea and the Atlantic coasts of Europe. It is a euryhaline species moving, in early spring, towards protected coastal waters (lagoon, pond, and basins) in search for abundant food and milder temperatures while in late autumn returns to the open sea for feed purposes and because of its sensitivity to low temperatures. It is mainly carnivorous (shellfish, including mussels and oysters), occasionally herbivorous.

Gilthead sea bream is a protandrous hermaphrodite, being a functional male in the first two years and changing sex at approximately 30 cm in length. During the male phase, bisexual gonads are functionally testicles, with asynchronous spermatogenesis and no functional ovarian areas (Kadmon, Yaron and Gordin, 1985). Ovarian development is also asynchronous, and females are batch spawners that can lay 20.000-80.000 eggs per day for a period of up to 3 months. In the Mediterranean, they reproduce between October and December. The eggs are spherical and pelagic, with a diameter slightly lower than 1 mm and a single large oil droplet. The planktonic larval stage lasts about 50 days at 17-18° C.

Gilthead sea bream is economically a very important species for the Greek, and the Mediterranean in general, aquaculture (Grigorakis *et al.*, 2002). The husbandry of this species has grown over the past two decades (FAO, 2010) and more than 200000 tons per year is now produced in the Mediterranean Sea (Arechavala-Lopez *et al.*, 2013). Improvements in larval production

techniques, formulation of specialized feeds, use of cages as the main rearing technique and the substantial financing from the European Union allowed a rapid increase of sea bream production (Rodgers and Furones, 1998).

Unfortunately, high-density production techniques inevitably have led to issues related to disease spreading problems in the entire Mediterranean marine aquaculture industry. Many species of marine parasites proliferate as commensal species and cause severe problems when poor on-site conditions, bad husbandry or adverse environmental factors occur (Rodgers and Furones, 1998). In particular, the most critical period in sea bream production is the larval stage, when bacterial infections commonly cause mass mortalities during the rearing (Carnevali *et al.*, 2004). Good management techniques are therefore necessary to afford the high production rates and different studies testing innovative techniques to improve culture quality have been already performed (Hulata, 2001; Carnevali *et al.*, 2004; Avella *et al.*, 2010).

Nanomaterials

Surface-active magnetic nanoparticles (SAMNs)

SAMNs are magnetic nanoparticles constituted of maghemite (γ-Fe_2O_3) with a mean diameter of 10 ± 2 nm (Sinigaglia *et al.*, 2012). They were provided by the University of Padua, Italy, where a novel synthesis method that is entirely carried out in water without the need of any organic solvent or surfactant was developed (Magro *et al.*, 2010). This new method offers several advantages: simplicity, low costs, high yield scale and, above all, it is an organic solvent free process and thus ecologically green. The final synthesis product after drying and curing at 400°C for 2 hours is a red-brown powder (Magro *et al.*, 2010). Bare SAMNs are dispersible in water, and their suspensions are stable for several months. Because of their unique physical and chemical properties, these NPs present a high average magnetic moment

and their surface shows peculiar binding properties which make them suitable to be reversibly derivatized with selected organic molecules (Magro *et al.*, 2012).

As a result, these NPs could be applied to biology and medicine, drug delivery systems, medical imaging, and protein purification (Venerando *et al.*, 2013).

SAMNs have been successfully bound to different molecules of biotechnological interest such as biotin and avidin (Magro *et al.*, 2012), bovine serum amine oxidase (Sinigaglia *et al.*, 2012), curcumin (Magro *et al.*, 2014) and rhodamine (Venerando *et al.*, 2013), showing the ability of forming a stable complex with all the target molecules. Furthermore, SAMNs cytotoxicity has been already studied by testing their effect on HeLa cells culture and demonstrating that they can be safely used at concentrations up to 100 µg/mL (Venerando *et al.*, 2013).

In this Ph.D. project, SAMNs were bound to different molecules forming new original complexes (see Chapter 1, 2 and 3).

Titanium dioxide NPs (TiO_2)

This project included also the study of a new purification system based on TiO_2 photocatalytic degradation (PCD). The filtration system consisted of an external mechanical purification system solely (EHEIM© experience 250; flow rate: 700 L/h) and a 36 W UVC sterilizer (Panaque©, Italy) equipped with 4 steel plates around the UV lamp (PCD filtration system).

The preparation method of titania paste is described in chapter 4. Final titania films obtained were deposited on stainless steel plates successively calcined in oven. Four plates were then inserted around a 36 W UVC (254 nm) lamp (Panaque©, Italy) at a 0.5 cm distance from the quartz bulb.

References

Ahmad, M. Z. *et al.* (2010) 'Metallic nanoparticles: technology overview & drug delivery applications in oncology', *Expert Opinion on Drug Delivery*. Taylor & Francis, 7(8), pp. 927–942. doi: 10.1517/17425247.2010.498473.

Alderman, D. J. (1996) 'Geographical spread of bacterial and fungal diseases of crustaceans.', *Revue scientifique et technique (International Office of Epizootics)*, 15(2), pp. 603–32.

Amaya, E. *et al.* (2012) 'Antibiotic resistance patterns of Escherichia coli isolates from different aquatic environmental sources in Leon, Nicaragua', *Clinical Microbiology and Infection*. Blackwell Publishing Ltd, 18(9), pp. E347–E354. doi: 10.1111/j.1469-0691.2012.03930.x.

Arechavala-Lopez, P. *et al.* (2013) 'Differentiating the wild or farmed origin of Mediterranean fish: a review of tools for sea bream and sea bass', *Reviews in Aquaculture*, 5(3), pp. 137–157. doi: 10.1111/raq.12006.

Arora, S., Rajwade, J. M. and Paknikar, K. M. (2012) 'Nanotoxicology and in vitro studies: The need of the hour', *Toxicology and Applied Pharmacology*, 258(2), pp. 151–165. doi: 10.1016/j.taap.2011.11.010.

Arunachalam, M. *et al.* (2013) 'Natural History of Zebrafish (*Danio rerio*) in India', *Zebrafish*. Mary Ann Liebert, Inc. 140 Huguenot Street, 3rd Floor New Rochelle, NY 10801 USA , 10(1), pp. 1–14. doi: 10.1089/zeb.2012.0803.

Auffan, M. *et al.* (2009) 'Towards a definition of inorganic nanoparticles from an environmental, health and safety perspective', *Nature Nanotechnology*. Nature Publishing Group, 4(10), pp. 634–641. doi: 10.1038/nnano.2009.242.

Avella, M. A. *et al.* (2010) 'Application of multi-species of Bacillus in sea bream larviculture', *Aquaculture*, 305(1–4), pp. 12–19. doi: 10.1016/j.aquaculture.2010.03.029.

Battle, H. I. and Hisaoka, K. K. (1952) 'Effects of Ethyl Carbamate (Urethan) on the Early Development of the Teleost Brachydanio rerio', *Cancer Research*, 12(5).

Bermudez, E. *et al.* (2004) 'Pulmonary Responses of Mice, Rats, and Hamsters to Subchronic Inhalation of Ultrafine Titanium Dioxide Particles', *Toxicological Sciences*. Oxford University Press, 77(2), pp. 347–357. doi: 10.1093/toxsci/kfh019.

Brown, J. R., Gowen, R. J. and McLusky, D. S. (1987) 'The effect of salmon

farming on the benthos of a Scottish sea loch', *Journal of Experimental Marine Biology and Ecology*, 109(1), pp. 39–51. doi: 10.1016/0022-0981(87)90184-5.

Brune, D. E. *et al.* (no date) 'Intensification of pond aquaculture and high rate photosynthetic systems'. doi: 10.1016/S0144-8609(03)00025-6.

Cancemi, G., De Falco, G. and Pergent, G. (2003) 'Effects of organic matter input from a fish farming facility on a Posidonia oceanica meadow', *Estuarine, Coastal and Shelf Science*, 56(5–6), pp. 961–968. doi: 10.1016/S0272-7714(02)00295-0.

Carnevali, O. *et al.* (2004) 'Administration of probiotic strain to improve sea bream wellness during development', *Aquaculture International*, 12, pp. 377–386.

Casey, A. *et al.* (2007) 'Spectroscopic analysis confirms the interactions between single walled carbon nanotubes and various dyes commonly used to assess cytotoxicity', *Carbon*, 45(7), pp. 1425–1432. doi: 10.1016/j.carbon.2007.03.033.

Chan, H.-K. and Kwok, P. C. L. (2011) 'Production methods for nanodrug particles using the bottom-up approach', *Advanced Drug Delivery Reviews*, 63(6), pp. 406–416. doi: 10.1016/j.addr.2011.03.011.

Chatterjee, K. *et al.* (2014) 'Core/shell nanoparticles in biomedical applications', *Advances in Colloid and Interface Science*, 209, pp. 8–39. doi: 10.1016/j.cis.2013.12.008.

Chen, Y.-S. *et al.* (2010) 'Size-dependent impairment of cognition in mice caused by the injection of gold nanoparticles', *Nanotechnology*. IOP Publishing, 21(48), p. 485102. doi: 10.1088/0957-4484/21/48/485102.

Cheng, S. (2003) 'Bioactivity of selected plant essential oils against the yellow fever mosquito Aedes aegypti larvae', *Bioresource Technology*, 89(1), pp. 99–102. doi: 10.1016/S0960-8524(03)00008-7.

Christophers, S. (1960) 'Aëdes aegypti (L.) the Yellow Fever Mosquito: its Life History, Bionomics and Structure.', *Aëdes aegypti (L.) the Yellow Fever Mosquito: its Life History, Bionomics and Structure.* London : The Syndics of the Cambridge University Press, Bentley House, 200, Euston Road, N.W.I.

Ciccia, G., Coussio, J. and Mongelli, E. (2000) 'Insecticidal activity against Aedes aegypti larvae of some medicinal South American plants', *Journal of Ethnopharmacology*, 72(1–2), pp. 185–189. doi: 10.1016/S0378-8741(00)00241-5.

Clermont, O. *et al.* (2011) 'Animal and human pathogenic Escherichia coli strains share common genetic backgrounds', *Infection, Genetics and Evolution*, 11(3), pp. 654–662. doi: 10.1016/j.meegid.2011.02.005.

Clift, M. J. D., Gehr, P. and Rothen-Rutishauser, B. (2011) 'Nanotoxicology: a perspective and discussion of whether or not in vitro testing is a valid alternative', *Archives of Toxicology*. Springer-Verlag, 85(7), pp. 723–731. doi: 10.1007/s00204-010-0560-6.

Costanzo, S. D., Murby, J. and Bates, J. (2005) 'Ecosystem response to antibiotics entering the aquatic environment', *Marine Pollution Bulletin*, 51(1–4), pp. 218–223. doi: 10.1016/j.marpolbul.2004.10.038.

Couvreur, P. (2013) 'Nanoparticles in drug delivery: Past, present and future', *Advanced Drug Delivery Reviews*, pp. 21–23. doi: 10.1016/j.addr.2012.04.010.

Cupaioli, F. A. *et al.* (2014) 'Engineered nanoparticles. How brain friendly is this new guest?', *Progress in Neurobiology*, 119, pp. 20–38. doi: 10.1016/j.pneurobio.2014.05.002.

Dave, G. and Xiu, R. (1991) 'Toxicity of mercury, copper, nickel, lead, and cobalt to embryos and larvae of zebrafish,Brachydanio rerio', *Archives of Environmental Contamination and Toxicology*. Springer-Verlag, 21(1), pp. 126–134. doi: 10.1007/BF01055567.

Decuzzi, P. *et al.* (2010) 'Size and shape effects in the biodistribution of intravascularly injected particles', *Journal of Controlled Release*, 141(3), pp. 320–327. doi: 10.1016/j.jconrel.2009.10.014.

Defoirdt, T., Sorgeloos, P. and Bossier, P. (2011) 'Alternatives to antibiotics for the control of bacterial disease in aquaculture', *Current Opinion in Microbiology*, pp. 251–258. doi: 10.1016/j.mib.2011.03.004.

Demetzos, C. (no date) *Pharmaceutical nanotechnology : fundamentals and practical applications*.

Erondu, E. and Anyanwu, P. (2011) 'Potential hazards and risks associated with the aquaculture industry', *African Journal of Food, Agriculture, Nutrition and Development*, 4(13). doi: 10.4314/ajfand.v4i13.71775.

Fako, V. E. and Furgeson, D. Y. (2009) 'Zebrafish as a correlative and predictive model for assessing biomaterial nanotoxicity', *Advanced Drug Delivery Reviews*, 61(6), pp. 478–486. doi: 10.1016/j.addr.2009.03.008.

FAO (2010) *The state of world fisheries and aquaculture 2010*. Food and Agriculture Organization of the United Nations.

FAO (2017) *http://www.fao.org/fishery/statistics/software/fishstatj/en*.

Findlay, R. H., Watling, L. and Mayer, L. M. (1995) 'Environmental impact of salmon net-pen culture on marine benthic communities in Maine: A case study', *Estuaries*. Springer-Verlag, 18(1), p. 145. doi: 10.2307/1352289.

Giner-Casares, J. J. *et al.* (2016) 'Inorganic nanoparticles for biomedicine: where materials scientists meet medical research', *Materials Today*, 19(1), pp. 19–28. doi: 10.1016/j.mattod.2015.07.004.

Gomes, T. *et al.* (2012) 'Accumulation and toxicity of copper oxide nanoparticles in the digestive gland of Mytilus galloprovincialis', *Aquatic Toxicology*, 118–119, pp. 72–79. doi: 10.1016/j.aquatox.2012.03.017.

Grigorakis, K. *et al.* (2002) 'Comparison of wild and cultured gilthead sea bream (Sparus aurata); composition, appearance and seasonal variations', *International Journal of Food Science and Technology*. Blackwell Science Ltd, 37(5), pp. 477–484. doi: 10.1046/j.1365-2621.2002.00604.x.

Grillo, R., Rosa, A. H. and Fraceto, L. F. (2015) 'Engineered nanoparticles and organic matter: A review of the state-of-the-art', *Chemosphere*, 119, pp. 608–619. doi: 10.1016/j.chemosphere.2014.07.049.

Gubler, D. J. (2002) 'The Global Emergence/Resurgence of Arboviral Diseases As Public Health Problems', *Archives of Medical Research*, 33, pp. 330–342.

Gullberg, E. *et al.* (2011) 'Selection of Resistant Bacteria at Very Low Antibiotic Concentrations', *PLoS Pathogens*. Edited by M. Lipsitch. Public Library of Science, 7(7), p. e1002158. doi: 10.1371/journal.ppat.1002158.

Gutierrez-Wing, M. T. and Malone, R. F. (no date) 'Biological filters in aquaculture: Trends and research directions for freshwater and marine applications'. doi: 10.1016/j.aquaeng.2005.08.003.

Hamelin, K. *et al.* (2007) 'Occurrence of Virulence and Antimicrobial Resistance Genes in Escherichia coli Isolates from Different Aquatic Ecosystems within the St. Clair River and Detroit River Areas', *Applied and Environmental Microbiology*, 73(2), pp. 477–484. doi: 10.1128/AEM.01445-06.

Hao, L. *et al.* (2013) 'Bioaccumulation and sub-acute toxicity of zinc oxide nanoparticles in juvenile carp (Cyprinus carpio): A comparative study

with its bulk counterparts', *Ecotoxicology and Environmental Safety*, 91, pp. 52–60. doi: 10.1016/j.ecoenv.2013.01.007.

Hoet, P. H. *et al.* (2004) 'Nanoparticles – known and unknown health risks', *Journal of Nanobiotechnology*. BioMed Central, 2(1), p. 12. doi: 10.1186/1477-3155-2-12.

Hu, J. *et al.* (2017) 'Study on treatment of aquaculture wastewater using a hybrid constructed wetland', *IOP Conference Series: Earth and Environmental Science*. IOP Publishing, 61(1), p. 12015. doi: 10.1088/1755-1315/61/1/012015.

Hulata, G. (2001) 'Genetic manipulations in aquaculture: a review of stock improvement by classical and modern technologies', *Genetica*. Kluwer Academic Publishers, 111(1/3), pp. 155–173. doi: 10.1023/A:1013776931796.

Hutter, E. *et al.* (2010) 'Microglial Response to Gold Nanoparticles', *ACS Nano*. American Chemical Society, 4(5), pp. 2595–2606. doi: 10.1021/nn901869f.

Ioos, S. *et al.* (2014) 'Current Zika virus epidemiology and recent epidemics', *Médecine et Maladies Infectieuses*, 44(7), pp. 302–307. doi: 10.1016/j.medmal.2014.04.008.

Iwama, G. K. (2009) 'Interactions between aquaculture and the environment', *http://dx.doi.org/10.1080/10643389109388413*. Taylor & Francis Group . doi: 10.1080/10643389109388413.

Jansen, C. C. and Beebe, N. W. (2010) 'The dengue vector Aedes aegypti: what comes next', *Microbes and Infection*, 12(4), pp. 272–279. doi: 10.1016/j.micinf.2009.12.011.

Johansen, L.-H. *et al.* (2011) 'Disease interaction and pathogens exchange between wild and farmed fish populations with special reference to Norway', *Aquaculture*, 315, pp. 167–186. doi: 10.1016/j.aquaculture.2011.02.014.

Johnson, A., Carew, E. and Sloman, K. (2007) 'The effects of copper on the morphological and functional development of zebrafish embryos', *Aquatic Toxicology*, 84(4), pp. 431–438. doi: 10.1016/j.aquatox.2007.07.003.

Ju-Nam, Y. and Lead, J. R. (2008) 'Manufactured nanoparticles: An overview of their chemistry, interactions and potential environmental implications', *Science of the Total Environment*, 400(1–3), pp. 396–414. doi: 10.1016/j.scitotenv.2008.06.042.

Kadmon, G., Yaron, Z. and Gordin, H. (1985) 'Sequence of gonadal events and oestradiol levels in Sparus aurata (L.) under two photoperiod regimes', *Journal of Fish Biology*, 26(5), pp. 609–620. doi: 10.1111/j.1095-8649.1985.tb04301.x.

Karakassis, I. *et al.* (2000) 'Impact of cage farming of fish on the seabed in three Mediterranean coastal areas', *ICES Journal of Marine Science*. Oxford University Press, 57(5), pp. 1462–1471. doi: 10.1006/jmsc.2000.0925.

Kennedy, I. M. *et al.* (2009) 'Uptake and inflammatory effects of nanoparticles in a human vascular endothelial cell line.', *Research report (Health Effects Institute)*, (136), pp. 3–32.

Kettler, K. *et al.* (2014) 'Cellular uptake of nanoparticles as determined by particle properties, experimental conditions, and cell type', *Environmental Toxicology and Chemistry*, 33(3), pp. 481–492. doi: 10.1002/etc.2470.

Kimmel, C. B. *et al.* (1995) 'Stages of embryonic development of the zebrafish', *Developmental Dynamics*. Wiley Subscription Services, Inc., A Wiley Company, 203(3), pp. 253–310. doi: 10.1002/aja.1002030302.

Klaine, S. J. *et al.* (2012) 'Paradigms to assess the environmental impact of manufactured nanomaterials', *Environmental Toxicology and Chemistry*. John Wiley & Sons, Inc., 31(1), pp. 3–14. doi: 10.1002/etc.733.

Kroll, A. *et al.* (2012) 'Interference of engineered nanoparticles with in vitro toxicity assays', *Archives of Toxicology*. Springer-Verlag, 86(7), pp. 1123–1136. doi: 10.1007/s00204-012-0837-z.

Kümmerer, K. (2009) 'Antibiotics in the aquatic environment – A review – Part II', *Chemosphere*, 75(4), pp. 435–441. doi: 10.1016/j.chemosphere.2008.12.006.

Lead, J. R. and Smith, E. (Emma L. . (2009) *Environmental and human health impacts of nanotechnology*. Wiley.

Li, J. J. *et al.* (2010) 'Nanoparticle-induced pulmonary toxicity', *Experimental Biology and Medicine*. SAGE PublicationsSage UK: London, England, 235(9), pp. 1025–1033. doi: 10.1258/ebm.2010.010021.

Ludwig K. Limbach, † *et al.* (2005) 'Oxide Nanoparticle Uptake in Human Lung Fibroblasts: Effects of Particle Size, Agglomeration, and Diffusion at Low Concentrations'. American Chemical Society . doi: 10.1021/ES051043O.

Magro, M. *et al.* (2010) 'Maghemite nanoparticles and method for preparing

thereof.'

Magro, M. *et al.* (2012) 'Avidin Functionalized Maghemite Nanoparticles and Their Application for Recombinant Human Biotinyl-SERCA Purification', *Langmuir*. American Chemical Society, 28(43), pp. 15392–15401. doi: 10.1021/la303148u.

Magro, M. *et al.* (2014) 'A magnetically drivable nanovehicle for curcumin with antioxidant capacity and MRI relaxation properties', *Chemistry - A European Journal*, 20(37), pp. 11913–11920. doi: 10.1002/chem.201402820.

Manke, A., Wang, L. and Rojanasakul, Y. (2013) 'Mechanisms of nanoparticle-induced oxidative stress and toxicity.', *BioMed research international*. Hindawi Publishing Corporation, 2013, p. 942916. doi: 10.1155/2013/942916.

Mardones, F. O. *et al.* (2014) 'The role of fish movements and the spread of infectious salmon anemia virus (ISAV) in Chile, 2007–2009', *Preventive Veterinary Medicine*, 114(114), pp. 37–46. doi: 10.1016/j.prevetmed.2014.01.012.

Marinho-Soriano, E. *et al.* (2011) 'Bioremediation of aquaculture wastewater using macroalgae and Artemia', *International Biodeterioration & Biodegradation*, 65(1), pp. 253–257. doi: 10.1016/j.ibiod.2010.10.001.

Martínez-Castañón, G. A. *et al.* (2008) 'Synthesis and antibacterial activity of silver nanoparticles with different sizes', *Journal of Nanoparticle Research*. Springer Netherlands, 10(8), pp. 1343–1348. doi: 10.1007/s11051-008-9428-6.

Martinez-Gutierrez, F. *et al.* (2010) 'Synthesis, characterization, and evaluation of antimicrobial and cytotoxic effect of silver and titanium nanoparticles', *Nanomedicine: Nanotechnology, Biology and Medicine*, 6(5), pp. 681–688. doi: 10.1016/j.nano.2010.02.001.

McVicar, A. (1997) 'Disease and parasite implications of the coexistence of wild and cultured Atlantic salmon populations', *ICES Journal of Marine Science*. Oxford University Press, 54(6), pp. 1093–1103. doi: 10.1016/S1054-3139(97)80014-8.

Merritt, R. W., Dadd, R. H. and Walker, E. D. (1992) 'Feeding Behavior, Natural Food, and Nutritional Relationships of Larval Mosquitoes', *Annual Review of Entomology*. Annual Reviews 4139 El Camino Way, P.O. Box 10139, Palo Alto, CA 94303-0139, USA , 37(1), pp. 349–374. doi: 10.1146/annurev.en.37.010192.002025.

Miranda, C. D. and Zemelman, R. (2002) 'Antimicrobial multiresistance in bacteria isolated from freshwater Chilean salmon farms', *The Science of the Total Environment*, 293, pp. 207–218.

Moore, M. N. (2006) 'Do nanoparticles present ecotoxicological risks for the health of the aquatic environment?', *Environment International*, 32(8), pp. 967–976. doi: 10.1016/j.envint.2006.06.014.

Mu, Q. *et al.* (2009) 'Characterization of Protein Clusters of Diverse Magnetic Nanoparticles and Their Dynamic Interactions with Human Cells', *The Journal of Physical Chemistry C*. American Chemical Society, 113(14), pp. 5390–5395. doi: 10.1021/jp809493t.

Murugan, K. *et al.* (2015) 'Parameters and characteristics governing cellular internalization and trans-barrier trafficking of nanostructures.', *International journal of nanomedicine*. Dove Press, 10, pp. 2191–206. doi: 10.2147/IJN.S75615.

Na, K. *et al.* (2003) 'Self-assembled nanoparticles of hydrophobically-modified polysaccharide bearing vitamin H as a targeted anti-cancer drug delivery system', *European Journal of Pharmaceutical Sciences*, 18(2), pp. 165–173. doi: 10.1016/S0928-0987(02)00257-9.

Nalwa, H. S. (2014) '<I>A Special Issue on</I> Reviews in Biomedical Applications of Nanomaterials, Tissue Engineering, Stem Cells, Bioimaging, and Toxicity', *Journal of Biomedical Nanotechnology*, 10(10), pp. 2421–2423. doi: 10.1166/jbn.2014.2034.

Naylor, R. L. *et al.* (2000) 'Effect of aquaculture on world fish supplies', *Nature*. Nature Publishing Group, 405(6790), pp. 1017–1024. doi: 10.1038/35016500.

Niimi, A. J. and LaHam, Q. N. (1975) 'Selenium Toxicity on the Early Life Stages of Zebrafish (*Brachydanio rerio*)', *Journal of the Fisheries Research Board of Canada*. NRC Research Press Ottawa, Canada , 32(6), pp. 803–806. doi: 10.1139/f75-105.

Oberdörster, E. (2004) 'Manufactured nanomaterials (fullerenes, C60) induce oxidative stress in the brain of juvenile largemouth bass.', *Environmental health perspectives*. National Institute of Environmental Health Science, 112(10), pp. 1058–62. doi: 10.1289/ehp.7021.

Pachepsky, Y. A. and Shelton, D. R. (2011) '*Escherichia Coli* and Fecal Coliforms in Freshwater and Estuarine Sediments', *Critical Reviews in Environmental Science and Technology*. Taylor & Francis Group, 41(12), pp. 1067–1110. doi: 10.1080/10643380903392718.

Panyam, J. and Labhasetwar, V. (2003) 'Biodegradable nanoparticles for drug and gene delivery to cells and tissue', *Advanced Drug Delivery Reviews*, 55(3), pp. 329–347. doi: 10.1016/S0169-409X(02)00228-4.

Panyam, J. *et al.* (2003) 'Fluorescence and electron microscopy probes for cellular and tissue uptake of poly(d,l-lactide-co-glycolide) nanoparticles', *International Journal of Pharmaceutics*, 262(1–2), pp. 1–11. doi: 10.1016/S0378-5173(03)00295-3.

Parichy, D. M. *et al.* (2009) 'Normal table of postembryonic zebrafish development: Staging by externally visible anatomy of the living fish', *Developmental Dynamics*. Wiley-Liss, Inc., 238(12), pp. 2975–3015. doi: 10.1002/dvdy.22113.

Pelkmans, L. and Helenius, A. (2002) 'Endocytosis Via Caveolae', *Traffic*. Munksgaard International Publishers, 3(5), pp. 311–320. doi: 10.1034/j.1600-0854.2002.30501.x.

Penilla, P. R. *et al.* (1998) 'Resistance management strategies in malaria vector mosquito control. Baseline data for a large-scale field trial against Anopheles albimanus in Mexico', *Medical and Veterinary Entomology*. Blackwell Science Ltd, 12(3), pp. 217–233. doi: 10.1046/j.1365-2915.1998.00123.x.

Petersen, A. *et al.* (2002) 'Impact of integrated fish farming on antimicrobial resistance in a pond environment.', *Applied and environmental microbiology*. American Society for Microbiology, 68(12), pp. 6036–42. doi: 10.1128/AEM.68.12.6036-6042.2002.

Piccinetti, C. C. *et al.* (2014) 'Transfer of Silica-Coated Magnetic (Fe3O4) Nanoparticles Through Food: A Molecular and Morphological Study in Zebrafish.', *Zebrafish*, 0(0), pp. 1–13. doi: 10.1089/zeb.2014.1037.

Piedrahita, R. H. (2003) 'Reducing the potential environmental impact of tank aquaculture effluents through intensification and recirculation', *Aquaculture*, 226, pp. 35–44. doi: 10.1016/S0044-8486(03)00465-4.

Ramsden, C. S. *et al.* (2009) 'Dietary exposure to titanium dioxide nanoparticles in rainbow trout, (Oncorhynchus mykiss): no effect on growth, but subtle biochemical disturbances in the brain', *Ecotoxicology*. Springer US, 18(7), pp. 939–951. doi: 10.1007/s10646-009-0357-7.

Rasko, D. A. *et al.* (2008) 'The pangenome structure of Escherichia coli: comparative genomic analysis of E. coli commensal and pathogenic isolates.', *Journal of bacteriology*. American Society for Microbiology, 190(20), pp. 6881–93. doi: 10.1128/JB.00619-08.

Reddy, L. H. *et al.* (2012) 'Magnetic Nanoparticles: Design and Characterization, Toxicity and Biocompatibility, Pharmaceutical and Biomedical Applications', *Chemical Reviews*. American Chemical Society, 112(11), pp. 5818–5878. doi: 10.1021/cr300068p.

Rhodes, G. *et al.* (2000) 'Distribution of oxytetracycline resistance plasmids between aeromonads in hospital and aquaculture environments: implication of Tn1721 in dissemination of the tetracycline resistance determinant tet A.', *Applied and environmental microbiology*. American Society for Microbiology, 66(9), pp. 3883–90. doi: 10.1128/AEM.66.9.3883-3890.2000.

Rizzo, L. Y. *et al.* (2013) 'In Vivo Nanotoxicity Testing using the Zebrafish Embryo Assay.', *Journal of materials chemistry. B, Materials for biology and medicine*. Europe PMC Funders, 1. doi: 10.1039/C3TB20528B.

Roco, M. C. (2011) 'The long view of nanotechnology development: the National Nanotechnology Initiative at 10 years', *Journal of Nanoparticle Research*. Springer Netherlands, 13(2), pp. 427–445. doi: 10.1007/s11051-010-0192-z.

Rodgers, C. J. and Furones, M. D. (1998) 'Disease Problems in Cultured Marine Fish in the Mediterranean.', *Fish Pathology*. The Japanese Society of Fish Pathology, 33(4), pp. 157–164. doi: 10.3147/jsfp.33.157.

Rubinstein, A. L. (2003) 'Zebrafish: From disease modeling to drug discovery', *Current Opinion in Drug Discovery & Development Current Drugs ISSN*, 6(2), pp. 218–223.

Russell, B. M., Kay, B. H. and Shipton, W. (2001) 'Survival of <I>Aedes aegypti</I> (Diptera: Culicidae) Eggs in Surface and Subterranean Breeding Sites During the Northern Queensland Dry Season', *Journal of Medical Entomology*, 38(3), pp. 441–445. doi: 10.1603/0022-2585-38.3.441.

Russo, T. (2003) 'Medical and economic impact of extraintestinal infections due to Escherichia coli: focus on an increasingly important endemic problem', *Microbes and Infection*, 5(5), pp. 449–456. doi: 10.1016/S1286-4579(03)00049-2.

Ryman-Rasmussen, P.J., Riviere, J. E., Monteiro-Riviere, N.A. (2007) 'Variables Influencing Interactions of Untargeted Quantum Dot Nanoparticles with Skin Cells and Identification of Biochemical Modulators'. American Chemical Society . doi: 10.1021/NL070375J.

Samuel-Fitwi, B. *et al.* (2012) 'Sustainability assessment tools to support aquaculture development', *Journal of Cleaner Production*, 32, pp. 183–192. doi: 10.1016/j.jclepro.2012.03.037.

Schieber, M. and Chandel, N. S. (2014) 'ROS Function in Redox Signaling and Oxidative Stress', *Current Biology*, 24(10), pp. R453–R462. doi: 10.1016/j.cub.2014.03.034.

Senger, M. R. *et al.* (2006) 'In vitro effect of zinc and cadmium on acetylcholinesterase and ectonucleotidase activities in zebrafish (Danio rerio) brain', *Toxicology in Vitro*, 20(6), pp. 954–958. doi: 10.1016/j.tiv.2005.12.002.

Sen-Sung Cheng, † *et al.* (2004) 'Chemical Composition and Mosquito Larvicidal Activity of Essential Oils from Leaves of Different Cinnamomum osmophloeum Provenances'. American Chemical Society . doi: 10.1021/JF0497152.

Shang, L., Nienhaus, K. and Nienhaus, G. (2014) 'Engineered nanoparticles interacting with cells: size matters', *Journal of Nanobiotechnology*, 12(1), p. 5. doi: 10.1186/1477-3155-12-5.

Sharifi, S. *et al.* (2012) 'Toxicity of nanomaterials', *Chem. Soc. Rev.* The Royal Society of Chemistry, 41(6), pp. 2323–2343. doi: 10.1039/C1CS15188F.

Shaw, B. J., Al-Bairuty, G. and Handy, R. D. (2012) 'Effects of waterborne copper nanoparticles and copper sulphate on rainbow trout, (Oncorhynchus mykiss): Physiology and accumulation', *Aquatic Toxicology*, 116–117, pp. 90–101. doi: 10.1016/j.aquatox.2012.02.032.

Sinigaglia, G. *et al.* (2012) 'Catalytically active bovine serum amine oxidase bound to fluorescent and magnetically drivable nanoparticles.', *International journal of nanomedicine*. Dove Press, 7, pp. 2249–59. doi: 10.2147/IJN.S28237.

Sjölund, M. *et al.* (2008) 'Dissemination of multidrug-resistant bacteria into the Arctic.', *Emerging infectious diseases*. Centers for Disease Control and Prevention, 14(1), pp. 70–2. doi: 10.3201/eid1401.070704.

Smith, A. E. and Helenius, A. (2004) 'How Viruses Enter Animal Cells', *Science*, 304(5668).

Sondi, I. and Salopek-Sondi, B. (2004) 'Silver nanoparticles as antimicrobial agent: a case study on E. coli as a model for Gram-negative bacteria', *Journal of Colloid and Interface Science*, 275(1), pp. 177–182. doi: 10.1016/j.jcis.2004.02.012.

Strømme, M. *et al.* (2009) 'Mesoporous silica-based nanomaterials for drug delivery: evaluation of structural properties associated with release rate', *Wiley Interdisciplinary Reviews: Nanomedicine and Nanobiotechnology*. John Wiley & Sons, Inc., 1(1), pp. 140–148. doi: 10.1002/wnan.13.

Swain, P. *et al.* (2014) 'Antimicrobial activity of metal based nanoparticles against microbes associated with diseases in aquaculture', *World Journal of Microbiology and Biotechnology*. Springer Netherlands, 30(9), pp. 2491–2502. doi: 10.1007/s11274-014-1674-4.

Teraoka, H., Dong, W. and Hiraga, T. (2003) 'Zebrafish as a novel experimental model for developmental toxicology', *Congenital Anomalies*, 43(2), pp. 123–132. doi: 10.1111/j.1741-4520.2003.tb01036.x.

Thakkar, K. N., Mhatre, S. S. and Parikh, R. Y. (2010) 'Biological synthesis of metallic nanoparticles', *Nanomedicine: Nanotechnology, Biology and Medicine*, 6(2), pp. 257–262. doi: 10.1016/j.nano.2009.07.002.

Thanh, N. T. K. and Green, L. A. W. (2010) 'Functionalisation of nanoparticles for biomedical applications', *Nano Today*, 5, pp. 213–230. doi: 10.1016/j.nantod.2010.05.003.

Thompson, F. L. *et al.* (2002) 'Importance of biofilm for water quality and nourishment in intensive shrimp culture', *Aquaculture*, 203, pp. 263–278.

Tian, X. *et al.* (2006) 'Comparison of the Abilities of Ambient and Manufactured Nanoparticles To Induce Cellular Toxicity According to an Oxidative Stress Paradigm'. American Chemical Society . doi: 10.1021/NL061025K.

Touchon, M. *et al.* (2009) 'Organised Genome Dynamics in the Escherichia coli Species Results in Highly Diverse Adaptive Paths', *PLoS Genetics*. Edited by J. Casadesús. American Society for Microbiology, 5(1), p. e1000344. doi: 10.1371/journal.pgen.1000344.

Turcios, A. and Papenbrock, J. (2014) 'Sustainable Treatment of Aquaculture Effluents—What Can We Learn from the Past for the Future?', *Sustainability*. Multidisciplinary Digital Publishing Institute, 6(2), pp. 836–856. doi: 10.3390/su6020836.

van Elsas, J. D. *et al.* (2011) 'Survival of Escherichia coli in the environment: fundamental and public health aspects.', *The ISME journal*. Nature Publishing Group, 5(2), pp. 173–83. doi: 10.1038/ismej.2010.80.

Venerando, R. *et al.* (2013) 'Magnetic Nanoparticles with Covalently Bound Self-Assembled Protein Corona for Advanced Biomedical

Applications', *The Journal of Physical Chemistry C*. American Chemical Society, 117(39), pp. 20320–20331. doi: 10.1021/jp4068137.

Verma, A. and Stellacci, F. (2010) 'Effect of Surface Properties on Nanoparticleâ€"Cell Interactions', *Small*, 6(1), pp. 12–21. doi: 10.1002/smll.200901158.

Vittozzi, L. and De Angelis, G. (1991) 'A critical review of comparative acute toxicity data on freshwater fish', *Aquatic Toxicology*, 19(3), pp. 167–204. doi: 10.1016/0166-445X(91)90017-4.

Warheit, D. B. *et al.* (2003) 'Comparative Pulmonary Toxicity Assessment of Single-wall Carbon Nanotubes in Rats', *Toxicological Sciences*. Oxford University Press, 77(1), pp. 117–125. doi: 10.1093/toxsci/kfg228.

Wilczewska, A. Z. *et al.* (2012) 'Nanoparticles as drug delivery systems', *Pharmacological Reports*, 64(5), pp. 1020–1037. doi: 10.1016/S1734-1140(12)70901-5.

Winkelmann, K. and Editors, B. B. (no date) 'Global Perspectives of Nanoscience and Engineering Education'.

Wu, R. S. S. (1995) 'Pergamon O025-326X(95)OOlOO-X The Environmental Impact of Marine Fish Culture: Towards a Sustainable Future', *Marine Pollution Bulletin*, 31, pp. 4–12.

Wu, R. S. S. *et al.* (1994) 'Impact of marine fish farming on water quality and bottom sediment: A case study in the sub-tropical environment', *Marine Environmental Research*, 38(2), pp. 115–145. doi: 10.1016/0141-1136(94)90004-3.

Zhang, C. *et al.* (2003) 'Zebrafish: An Animal Model for Toxicological Studies', in *Current Protocols in Toxicology*. Hoboken, NJ, USA: John Wiley & Sons, Inc., p. 1.7.1-1.7.18. doi: 10.1002/0471140856.tx0107s17.

Zhao, C.M. and Wang, W.X. (2012) 'Size-Dependent Uptake of Silver Nanoparticles in Daphnia magna', *Environmental Science & Technology*. American Chemical Society, 46(20), pp. 11345–11351. doi: 10.1021/es3014375.

Chapter 1

Oxytetracycline delivery in adult female zebrafish by iron oxide nanoparticles

Chemello G, Piccinetti CC, Randazzo B, Carnevali O, Maradonna F, Magro M, Bonaiuto E, Vianello F, Radaelli G, Fifi AP, Gigliotti F, Olivotto I.

Zebrafish 2016, 13 (6): 495-503.

1.1 Introduction

The development of intensive aquaculture practices has led to the growth of several bacterial diseases, which requires an increasing use of antibiotics. According to statistics, the annual consumption of antibiotics in the Europe Union is about 5,000 tons[1]. Anyway, the worldwide effective use of antibiotics in aquaculture is not easy to determine, especially in developing countries where a proper regulation for their administration is missing[2]. Because of their low absorption rate and no effective metabolization rate by fish, antibiotics are usually administered at high dosages[3]. As a consequence, antibiotics are often excreted in their original form directly into the environment[4]. The considerable release of antibiotics in the aquatic environment has been associated with the emergence of antibiotic resistance in bacterial fish pathogens, with the alteration of the microbiota of the aquatic ecosystems[5] and a constant presence in surface waters in the ng/L to mg/L range[6]. These relatively low concentrations can cause uncertain ecological effects and be a potential threat to aquatic organisms as a consequence of a chronic exposure to these substances[1]. These concerns have led to the development of more strict regulations for the use of antibiotics in the aquaculture sector and, at date, some countries (Europe, North America, and Japan), licensed the use of a few antibiotics for fish treatment[2].

Among the approved antibiotics, oxytetracycline (OTC) is one of the most commonly used in aquaculture[7]. It belongs to the tetracycline class of broad-spectrum antibiotics with bacteriostatic effects and can be administered both orally or added to the water[8]. OTC is poorly absorbed by fish and Yonar [8] reported that 70-80% of OTC was intact in exposed animals. OTC generally accumulates in skin, liver, and intestine[9–11]. For example Malvisi and collaborators[9], in 1996, reported a 1.82±1.26 μg/g OTC skin concentration in seabass exposed for 14 days to a medicated diet containing 75 mg OTC/kg

body weight, while a 13.9±9.5 µg/g OTC concentration was detected in the liver of sea bass (*Dicentrarchus labrax*) 128 hours after intravascular administration of 40 mg/kg of OTC[11].

It is clear that alternative strategies for a better management of antibiotic administration are of primary interest to improve absorption rates and, as a consequence, to reduce the release in the aquatic environment[12–14]. Metal NPs, including superparamagnetic iron oxide NPs, are interesting materials that can be used in a wide range of biomedical applications, including drug delivery, magnetic resonance imaging, and hyperthermal treatment of tumors[15]. Among these materials, the two magnetic forms of iron oxide, magnetite (Fe_3O_4) and maghemite (c-Fe_2O_3), are considered suitable for *in vivo* applications[15,16] since their surface can be easily functionalized to meet a number of requirement. Besides enabling selective binding of different bioactive molecules, magnetic NPs functionalized for biomedical applications must retain their magnetic properties, be nontoxic, hydrophilic, and biocompatible, and remain stable in aqueous colloidal suspensions.

Many drug-nanocarriers were proposed to protect the drug from rapid degradation and/or clearance, by enhancing drug concentration in target tissues[17]. As a consequence, a lower drug dose is usually required with a reduction of toxic collateral effects for patients or damage to the environment[18].

The present study investigates for the first time to our knowledge, a new methodology for OTC administration through the use of iron oxide nanoparticles (constituted of maghemite γ-Fe_2O_3) in zebrafish (ZF). ZF is a widely used model for biomedical, developmental biology, genetics, toxicology and aquaculture studies due to its high reproduction rate and the abundant information that has recently become available from genome sequencing[19,20].

OTC was administered in water solution or nanoparticles-bound at a final concentration of 4 mg/L for 28 days. OTC accumulation in different tissues was determined by HPLC (High Pressure Liquid Chromatography) analysis; liver, gills and intestine integrity was examined by histological analysis and stress and growth markers were analyzed by Real Time PCR.

1.2 Materials and Methods

1.2.1 Ethics

All procedures involving animals were conducted in line with Italian legislation on experimental animals and were approved by the Health Ministry's Department of Veterinary Public Health and by the ethics committee of Università Politecnica delle Marche (Authorization N 640/2015-PR). Optimal rearing conditions were applied throughout the study, and all efforts were made to minimize animal suffering by using an anesthetic (MS222; Sigma-Aldrich).

1.2.2 Synthesis of Surface Active Maghemite Nanoparticles (SAMNs)

Bare nanoparticles called Surface Active Maghemite Nanoparticles (SAMNs) constituted of stoichiometric maghemite (γ-Fe_2O_3) were synthesized as described by[21,22]. Briefly summarizing: $FeCl_3 \cdot 6H_2O$ (10.0 g, 37 mmol) was dissolved in MilliQ grade water (800 mL) under vigorous stirring at room temperature, to allow the reduction reaction occurrence $NaBH_4$ solution (2 g, 53 mmol) in ammonia (3.5 %, 100 mL, 4.86 mol/mol Fe) was quickly added to the solution. The final synthesis product resulted in a red-brown nanopowder composed of maghemite nanoparticles with a mean diameter of 11 ± 2 nm that showed a magnetic response when exposed to a magnetic field.

1.2.3 Formation of the complex magnetic nanoparticles and oxytetracycline (SAMNs@OTC)

Oxytetracycline hydrochloride (O5875-Sigma-Aldrich, Italy) (20 mg/L) was incubated with various NPs concentrations (0.1, 0.2, 0.5, 1.0, 1.5 and 2.0 g/L) in H_2O at room temperature. This solution was stored, under overnight constant agitation, to promote complex formation. Then, magnetic NPs were separated from the aqueous solution with the assistance of a magnet. Finally, OTC concentration in the supernatants was checked by spectrophotometry using Varian Cary 60 instrument (Agilent Technologies, CA, USA).

1.2.4 Fish

Adults female AB ZF were kept in a ZF system (Tecniplast, Varese, Italy) at 28°C, 14L/10D photoperiod, pH 7.0, NO_2 and NH_3 < 0.03 mg/L and fed with a commercial pellet (Blueline, Italy) twice daily (2% body weight) for one month. The experiment started after this first period of acclimation.

1.2.5 Experimental design

Adult ZF (600 animals) were kept in 12 tanks (100 L) divided into 4 experimental groups each of 150 fish (50 fish per tank) and exposed to the following conditions for 28 days: control (3x 50 fish tanks) (28°C, 14L/10D photoperiod pH 7.0, NO_2 and NH_3 < 0.03 mg/L; total 150 fish) ; group A (3x 50 fish tanks): fish exposed to 4 mg/L OTC *via* water (same chemical-physical conditions of control group); group B (3x 50 fish tanks): fish exposed to 100 mg/L SAMNs@OTC equivalent to a concentration of 4 mg OTC (same chemical-physical conditions of control group); group C (3x 50 fish tanks): fish exposed to 100 mg/L SAMNs (same chemical-physical conditions of control group).

Samplings were performed at 0, 14 and 28 days after the beginning of the treatment. Fish were collected and anesthetized with a lethal dose of MS222 (1 g/L) (Sigma-Aldrich) and liver, brain, digestive tract, skin, ovary and *in toto* fish were sampled and properly stored for further analysis.

1.2.6 High Pressure Liquid Chromatography (HPLC) analysis

Extraction procedure

About 100 mg of each tissue sample (in triplicate) were weighed, triturated and homogenized in a blender, placed in a plastic tube and dissolved in 1 ml of ultrapure water acidified with 1% phosphoric acid. The tube was vigorously mixed for 2 minutes, treated in an ultrasonic bath for 5 minutes and then centrifuged at 13000 rpm for 10 minutes. The supernatant was collected and filtered through a 0.2 µm membrane filters and stirred before injection into the chromatograph. A 20µL aliquot was injected.

HPLC analysis

The separation conditions for the OTC were a mobile phase flow of 0.8 mL/min containing acetonitrile acidified with 0.1% phosphoric acid and ultrapure water acidified with 1% phosphoric acid (15:85, v/v) filtered through a 0.45 µm nylon filter under vacuum and degassed by ultra-sonication. Column oven temperature was 25°C and ultraviolet detector operated at a wavelength of 360 nm. The quantitation was accomplished by using an analytical calibration curve built with six concentration levels in the range 20 – 250 µg/L (OTC). Extraction recoveries were determined by spiking untreated biological samples (100 mg) with a fortification solution at LOQ and LOD levels: 500 and 100 µg/kg.

The HPLC system (Agilent 1100 series with Chemstation) used for analysis consists of a quaternary pump (Agilent 1100 series), a vacuum degasser, an injector and a wave-length ultraviolet detector (Agilent 1100 series). The

chromatographic column was an analytical reversed-phase Zorbax Eclipse XDB C18, 4.6 x 150 mm, 5µm.

Method validation

The method was *"in-house*" validated using the following performance criteria: linearity, sensitivity, and selectivity, detection and quantification limits, accuracy and precision. The solution for calibration and fortification were prepared in ultrapure water acidified with 1% phosphoric acid and stored at temperature ≤ -18°C.

Linearity, sensitivity and selectivity, detection and quantification limits were established by the analytical curve (20, 40, 50, 80, 100 and 250 µg/L of OTC). The limit of quantification (LOQ) was obtained from the calibration curve and calculated using the following expression: $y = ax + b$, where y is the peak area of OTC and x is the amount of OTC in µg/mL; then the limit of quantification (LOQ) was expressed in µg/kg by the following formula: OTC (µg/L) × V_{ex} (mL) / W (g), where V_{ex} is the extraction volume and W is the untreated sample weight. The limit of detection (LOD) was the lowest amount of an analyte in a sample that can be detected but not necessarily quantitated as an exact value and it was 100 µg/kg. The precision of the method, expressed as the relative standard deviation of peak area measurements (n=5), was evaluated by the recovery data obtained (accuracy) at the LOQ concentration level (RSD% = 6.51). The accuracy of the method, expressed as percent recovery, was determined at 500 µg/kg that was the LOQ concentration level (Mean Recovery 95.5%).

1.2.7 Histological analysis

Ten samples of the intestine, liver, and gills, randomly collected at each sampling time from control, group A, B, C were fixed by immersion in 4% paraformaldehyde and stored at 4°C overnight. Samples were then washed in PBS 1X, dehydrated in an ethanol series and embedded in paraffin. Slides of 4 µm sections (cut with a microtome LEICA) were stained with Mayer's hematoxylin and eosin stain and examined under photomicroscope (Olympus Vanox photomicroscope, Japan).

1.2.8 RNA extraction and cDNA synthesis

Total RNA extraction from single ZF livers (5 replicates randomly collected at each sampling time from control, A, B and C groups) was optimized using the RNeasy_Minikit (Qiagen, Italy) following the manufacturer's protocol. Total RNA extracted was eluted in 20 µl RNase-free water (Qiagen, Italy). Final RNA concentration was determined by the NanoPhotometer P-Class (Implen, Germany). RNA integrity was verified by ethidium bromide staining of 28S and 18S ribosomal RNA bands on 1% agarose gel. RNA was stored at -80°C until use. Total RNA was treated with DNAse (10 IU at 37°C for 10 min; MBI Fermentas). Then, 3µg RNA were used for cDNA synthesis with the iScript cDNA Synthesis Kit (Bio-Rad) following the producers' instructions.

1.2.9 Real-Time PCR

PCRs were performed with SYBR Green in an iQ5 iCycler thermal cycler (both from Bio-Rad), in triplicate. Reactions were set on a 96-well plate by mixing, for each sample, 1 µL cDNA diluted 1:20, 5 µL of 2x concentrated iQ TM SYBR Green Supermix containing SYBR Green as the fluorescent intercalating agent, 0.3 µM forward primer, and 0.3 µM reverse primer. The

thermal profile for all reactions was 3 min at 95°C, followed by 45 cycles of 20 s at 95°C, 20 s at 60°C, and 20s at 72°C. Fluorescence was monitored at the end of each cycle. Dissociation curve analysis showed a single peak in all cases.

Relative quantification of the expression of genes involved in fish stress response (*hnf4a, hsp70.1*, *sod1*, *sod2*, *gsta.1*) and growth (*igf1*, *igf2a,* and *mstnb*) was performed using *rplp0* and *actbl* as the housekeeping genes to standardize the results (Table 1). Data were analyzed using the iQ5 optical system software version 2.0, including Genex Macro iQ5 Conversion and Genex Macro iQ5 files (all from Bio-Rad).

Amplification products were sequenced, and homology was verified. No amplification product was detected in negative controls and no primer-dimer formation was found in control templates. Modification of gene expression is reported with respect to controls. Primer sequences were designed using Primer3 (210 v. 0.4.0) starting from ZF sequences available in ZFIN. Primers were used at a final concentration of 10 pmol/μL.

1.2.10 Statistical analysis

HPLC and real-time PCR data were analyzed by two-way ANOVA analysis of variance, both followed by Tukey's post-test. The statistical software package Prism5 (GraphPad Software) was used for analyses. Significance was set at $p < 0.05$.

1.3 Results

1.3.1 OTC content by High Pressure Liquid Chromatography (HPLC) analysis.

At T0, OTC was not detectable in all analyzed tissues (control, group A, B, and C) (Fig. 1a-f). In addition, the same result was observed in all control and group C samples at T1 and T2 (Fig. 1a-f).

On the contrary, during the whole experimental time, in all group A and B samples an OTC accumulation was evident (Fig. 1a, c, d, e, f), with the exception of group B livers exposed to SAMNs@OTC complex in which OTC was not detectable (Fig. 1b).

The highest concentration of OTC was recorded in group A and B intestine samples (Fig. 1a). At T1 there were no significant differences ($p > 0.05$) between the two experimental groups and the mean concentration was 10.00±0.30 μg/g and 9.97±0.80 μg/g, for group A and B, respectively. At T2 the mean concentration was 14.10±0.800 μg/g and 9.95±0.67 μg/g, for group A and B, respectively. Group A concentration was significantly ($p <0.05$) higher than group B.

In brain samples (Fig. 1c) of both group A and B no significant differences ($p >0.05$) in OTC concentration were detected at both sampling times (0.039±0.02 μg/g and 0.37±0.04 μg/g at T1, 0.37±0.03 μg/g and 0.43±0.06 μg/g at T2 in group A and B, respectively).

On the contrary, group B ovary, skin and *in toto* samples (exposed to SAMNs@OTC complex) (Fig. 1d, e, f group B) showed a significantly higher (approximately 10 times magnitude increase) OTC concentration ($p <0.05$) respect to those exposed to OTC *via* water (Fig. 1d, e, f group A).

1.3.2 Histological analysis

The histological analysis of liver (Fig. 2a, b, c, d) gills (Fig. 2e, f, g, h) and intestine (Fig. 2i, l, m, n) did not show any significant difference in the morphological structure of the analyzed tissues. All the samples showed a normal structural and morphological integrity without evidence of steatosis, inflammation, vacuolation, oedema, cellular atrophy or necrosis.

1.3.3 Real-Time PCR results

Real time PCR analysis were performed on genes involved in fish growth (*igf1*, *igf2a,* and *mstnb*) and stress response (*hnf4a*, *hsp70.1*, *sod1*, *sod2*, *gsta.1*). Results showed that naked NPs administration (group C) did not cause significant variations in the expression of all the analyzed genes respect to control, during the whole experimental period (Fig. 3c, f, i) (Fig. 4c, f) (Fig. 5i, n, q). On the contrary, both *via* water and *via* SAMNs@OTC complex OTC administered was able to act on the expression of some of the genes analyzed.

Growth factors

Regarding *Igf1* gene expression, no significant ($p > 0.05$) differences respect to control were detected in all group A samples (Fig. 3a). On the contrary, in group B, exposed to the SAMNs@OTC complex, a time-dependent significant increase in *igf1* gene expression was observed ($p < 0.05$) (Fig. 3b) during the experiment, respect to control. A similar result was observed for *igf2a* gene expression for both group A and B (Fig. 3d, 3e respectively). Finally, both *via* water (group A) and SAMNs@OTC (group B) exposure induced a significant ($p < 0.05$) time-related decrease of *mstnb* mRNA levels ($p < 0.05$) compared to control (Fig. 3g, h).

Stress and detoxification stress markers

In group A samples, *hnf4a* gene expression showed a significant lower gene expression at both T1 and T2 with respect to control (p <0.05) (Fig. 4a), while in group B, no significant differences were observed with respect to control at T1 and T2 (p >0.05) (Fig 4b).

Regarding *hsp70.1,* a significantly lower (p <0.05) gene expression was observed in both group A (Fig. 4d) and B (Fig. 4e) respect to control, at both T1 and T2. In particular, group B showed a significant time-related decrease of this gene expression (p <0.05).

As concerns *sod1* gene expression, an opposite change in gene expression was detected in group A and B. A significant increase (p <0.05) of *sod1* gene expression was observed in group A respect to control (Fig. 5g), while for group B samples, a significant reduction (p <0.05) in *sod1* gene expression was detected both at T1 and T2 (Fig. 5h).

As regards, *sod2* gene expression group A samples were characterized by a significant down-regulation (p <0.05) compared to control, at both T1 and T2 (Fig. 5l). Group B gene expression did not show any significant difference (p >0.05) respect to control during the whole time of exposure (Fig. 5m).

Finally, an opposite trend in *gsta.1* expression was observed between group A and B; a significant decrease was observed in group A (p <0.05) (Fig. 5o) while a significant time-related increase of *gsta.1* expression was evident in group B (p <0.05) (Fig. 5p).

1.4 Discussion

In the present study, the possible application of synthetic iron oxide NPs (SAMNs) for OTC administration in ZF was evaluated. At date, there is a strong need for the development of new and alternative administration methods for this antibiotic in the aquaculture sector, because of its wide use[23],

very low absorption rate[8] and its high release into the environment through the faeces and waste waters [24].

NPs are materials characterized by different chemical composition, which have been reported to be potentially toxic for aquatic organisms[25,26]. However, toxicity relies on their composition, size, physical and chemical properties[27]. In particular, iron oxide NPs have been reported to have no toxicity in *in vivo* and *in vitro* systems[15,16,28]. The same results were confirmed in the present study, evidencing, by a multidisciplinary approach, that iron oxide NPs (naked or as a complex with OTC) exposure did not cause any significant stress response in treated fish.

All the different experimental conditions tested in this study, had no effects on the structural and morphological integrity of gills, liver, and intestine of treated ZF. These tissues were selected because of their importance in ecotoxicological studies[29,30]. In addition, as expected[31] molecular analysis revealed that especially SAMNs@OTC complex exposure had a greater growth promoter action with respect to *via* water treatment. This result can be easily related to the OTC concentrations detected by HPLC in the different organs, which were higher in fish exposed to the SAMNs@OTC complex with respect to *via* water exposure and are discussed later on in this same section.

Previous studies showed that OTC can be responsible for the induction of toxicity in fish liver, by altering the activity of enzymes involved in stress response[32,33]. As already demonstrated by Nakano et al., (2015)[34] OTC exposure is able to cause a significant decrease in *hsp70* gene expression; the same result was observed in the liver of both group A and B fish of the present study. The liver is, in fact, an important storage organ which primary function in fish is detoxification[35]. Regarding detoxification genes, it is clear that in the present study naked NPs had no effects on their gene expression. However, group A and B results often show opposite trends. This could be related to the

activation of different defense/detoxification mechanisms related to the administration method and/or the different OTC concentrations detected in the samples analyzed.

As expected OTC administration, both *via* water and through NPs, caused an accumulation in target tissues of ZF. For both treatments, HPLC analysis showed that the intestine was the main accumulation organ. On the contrary, the lowest OTC concentrations were observed in the brain and, surprisingly, in the liver of the treated fish. The low OTC concentration detected in the brain can easily be explained by the hydrophilic characteristics of OTC[36], its high molecular weight (496.89 g/mol Sigma-Aldrich, CAS#O5875-50G) and the presence of a blood-brain barrier characterized by tight junctions and selective transporters which restrict paracellular diffusion of molecules with high molecular weight[37].

Results obtained from liver samples were not obvious. No OTC was detected in all liver samples of SAMNs@OTC (group B) exposed fish. In addition, in fish exposed to 4 mg/L OTC (*via* water), the liver antibiotic concentration was very low during the whole experimental time, especially if compared to previous experiments reporting that the liver is one of the main accumulation organs of OTC[38–40]. These results, as already demonstrated in grass carp[41], could be explained by the occurrence of a very active and fast detoxification mechanism in the liver, and its high vascularization that guarantees a fast absorption rate as well as fast disposal mechanisms[41]. However, the total absence of OTC in the liver of group B fish exposed to SAMNs@OTC complex lays the foundation for new hypotheses. First, it has to be underlined that the binding of OTC on SAMNs is very stable. Attempts to obtain the release of OTC from SAMNs surface were unsuccessfully carried out using absolute ethanol, and 2M NH_4OH which led only to a partial release of OTC, as already tested for the release of bound substances on iron oxide NPs[42,43].

As a consequence, a first hypothesis is that OTC was not released by the NPs because the liver did not provide the proper chemical-physical environment for its release. For this reason, the absence of OTC in the liver could be explained by the inability of HPLC to detect the complex SAMNs@OTC. The second hypothesis, which is now under study, is that SAMNs@OTC complex, within the organism, was able to bind to other macromolecules as already observed in complex media [17,44,45]. Some of these macromolecules are released into the blood stream and could serve as a carrier for SAMNs@OTC promoting their accumulation in other organs. In the present study, while *via* water treatment did not cause a significant OTC accumulation in the ovary and skin of treated fish, SAMNs@OTC treatment caused a ten times higher OTC concentration in the same target organs. It is known that ZF presents an asynchronous ovary and spawns every day [46]. Oocyte maturation is supported by vitellogenesis that occurs in the liver through the production of vitellogenin that is secondly released into the blood stream before reaching the ovary [1]. Vitellogenin is a high molecular mass glycolipophosphoprotein which is usually encoded by multiple vg genes in several species including fish [1]. It could be speculated that SAMNs@OTC could be able to bind to vitellogenin, and secondly be incorporated into the oocytes, after reaching the ovary through the blood stream. This new administration method is thus very promising for the treatment of those diseases characterized by vertical transmission. An example is the treatment of *Piscirickettsia salmonis* for which OTC is usually used [47].

1.5 Conclusions

The present study represents an important first step for the development of a new OTC administration method able to guarantee a higher absorption of the antibiotic in ZF. In fact, group B fish revealed a ten times higher OTC accumulation respect to group A (exposed *via* water). As a consequence, this new administration method seems much more efficient respect to the traditional way of exposure, reduces antibiotic utilization and possible environmental impacts. However, the dynamics related to OTC release from the SAMNs@OTC complex, are still not clear and need further investigations.

References

1. Zhang Q, Cheng J, Xin Q. Effects of tetracycline on developmental toxicity and molecular responses in zebrafish (*Danio rerio*) embryos. Ecotoxicology 2015; 24: 707–719.
2. Defoirdt T, Sorgeloos P, Bossier P. Alternatives to antibiotics for the control of bacterial disease in aquaculture. Curr Opin Microbiol 2011; 14: 251–258.
3. Sapkota A, Amy R, Kucharski M, Burke J, McKenzie S, Walker P, et al. Aquaculture practices and potential human health risks: Current knowledge and future priorities. Environ Int 2008; 34: 1215–1226.
4. Burridge L, Weis J S, Cabello F, Pizarro J, Bostick K. Chemical use in salmon aquaculture: A review of current practices and possible environmental effects. Aquaculture 2010; 306: 7–23.
5. Muñoz-Atienza E,Gómez-Sala B,Araújo C, Campanero C, Del Campo R, Hernández PE et al. Antimicrobial activity, antibiotic susceptibility and virulence factors of Lactic Acid Bacteria of aquatic origin intended for use as probiotics in aquaculture. BMC Microbiol 2013; 13: 15.
6. Hoa PTP, Managaki S, Nakada N, Takada H, Shimizu A, Anh DH et al. Antibiotic contamination and occurrence of antibiotic-resistant bacteria in aquatic environments of northern Vietnam. Sci Total Environ 2011; 409: 2894–2901.
7. Rigos G, Nengas I, Tyrpenou AE, Alexis M, Troisi GM. Pharmacokinetics and bioavailability of oxytetracycline in gilthead sea bream (*Sparus aurata*) after a single dose. Aquaculture 2003; 221: 75–83.
8. Yonar ME. The effect of lycopene on oxytetracycline-induced oxidative stress and immunosuppression in rainbow trout (Oncorhynchus mykiss, W.). Fish Shellfish Immunol 2012; 32: 994–1001.
9. Malvisi J, Della Rocca G, Anfossi P, Giorgetti G. Tissue distribution and residue depletion of oxytetracycline in sea bream (*Sparus aurata*) and sea bass (*Dicentrarchus labrax*) after oral administration. Aquaculture 1996; 147: 159–168.

10. Namdari R, Abedini S, Law FCP. Tissue distribution and elimination of oxytetracycline in seawater chinook and coho salmon following medicated-feed treatment. Aquaculture 1996; 144: 27–38.
11. Rigos G, Nengas I, Tyrpenou AE, Alexis M, Troisi G M. Pharmacokinetics and tissue distribution of oxytetracycline in sea bass, *Dicentrarchus labrax*, at two water temperatures. Aquaculture 2002; 210: 59–67.
12. Teja AS, Koh PY. Synthesis, properties, and applications of magnetic iron oxide nanoparticles. Prog Cryst Growth Charact Mater 2009; 55: 22–45.
13. Bamrungsap S, Zhao Z, Chen T, Wang L, Li C, Fu T. Nanotechnology in therapeutics: a focus on nanoparticles as a drug delivery system. Nanomedicine 2012; 7: 1253–1271.
14. Couvreur P. Nanoparticles in drug delivery: Past, present and future. Adv Drug Deliv Rev 2013; 65: 21–23.
15. Piccinetti CC, Montis C, Bonini M, Laurà R, Guerrera MC, Radaelli G et al. Transfer of Silica-Coated Magnetic (Fe_3O_4) Nanoparticles Through Food: A Molecular and Morphological Study in Zebrafish. Zebrafish 2014; 00: 1–13.
16. Mahmoudi M, Sant S, Wang B, Laurent S, Sen T. Superparamagnetic iron oxide nanoparticles (SPIONs): Development, surface modification and applications in chemotherapy. Adv Drug Deliv Rev 2011; 63: 24–46.
17. Wilczewska AZ, Niemirowicz K, Markiewicz KH, Car H. Nanoparticles as drug delivery systems. Pharmacol Reports 2012; 64: 1020–1037.
18. Nevozhay D, Kanska U, Budzynska R, Boratynski J. Current status of research on conjugates and related drug delivery systems in the treatment of cancer and other diseases. Postepy Hig Med Dosw 2007; 61: 350–360.
19. Lu Y, Yin Y, Mayers BT, Xia Y. Modifying the Surface Properties of Superparamagnetic Iron Oxide Nanoparticles through a Sol-Gel Approach. Nano Lett 2002; 2: 183–186.
20. Yang P, Quan Z, Hou Z, Li C, Kang X, Cheng Z et al. A magnetic, luminescent and mesoporous core-shell structured composite material as drug carrier. Biomaterials 2009; 30: 4786–4795.

21. Magro M, Nodari L, Russo U, Valle G, Vianello F. Maghemite nanoparticles and method for preparing thereof 2012. Patent WO/2012/010200A1.

22. Magro M, Sinigaglia G, Nodari L, Tucek J, Polakova K, Marusak Z et al. Charge binding of rhodamine derivative to OH - stabilized nanomaghemite: Universal nanocarrier for construction of magnetofluorescent biosensors. Acta Biomater 2012; 8: 2068–2076.

23. Rigos G, Smith P. A critical approach on pharmacokinetics, pharmacodynamics, dose optimisation and withdrawal times of oxytetracycline in aquaculture. Rev Aquac 2015; 7: 77–106.

24. Lalumera GM, Calamari D, Galli P, Castiglioni S, Crosa G, Fanelli R. Preliminary investigation on the environmental occurrence and effects of antibiotics used in aquaculture in Italy. Chemosphere 2004; 54: 661–668.

25. Choi JE, Kim S, Ahn JH, Youn P, Kang JS, Park K, et al. Induction of oxidative stress and apoptosis by silver nanoparticles in the liver of adult zebrafish. Aquat Toxicol 2010; 100: 151–159.

26. Handy RD, Henry TB, Scown TM, Johnston BD, Tyler CR. Manufactured nanoparticles: their uptake and effects on fish--a mechanistic analysis. Ecotoxicology 2008; 17: 396–409.

27. Oberdörster G, Oberdörster E, Oberdörster J. Nanotoxicology: An emerging discipline evolving from studies of ultrafine particles. Environ Health Perspect 2005; 113: 823–839.

28. Hussain SM, Hess KL, Gearhart JM, Geiss KT, Schlager JJ. In vitro toxicity of nanoparticles in BRL 3A rat liver cells. Toxicol in Vitro 2005; 19: 975–983.

29. Costa PM, Carreira S, Costa MH, Caeiro S. Development of histopathological indices in a commercial marine bivalve (*Ruditapes decussatus*) to determine environmental quality. Aquat Toxicol 2013; 126: 442–454.

30. Ben Ameur W, De Lapuente J, El Megdiche Y, Barhoumi B, Trabelsi S, Camps L et al. Oxidative stress, genotoxicity and histopathology biomarker responses in mullet (*Mugil cephalus*) and sea bass (*Dicentrarchus labrax*) liver from Bizerte Lagoon (Tunisia). Mar Pollut Bull 2012; 64: 241–251.

31. Gonzalez Ronquillo M, Angeles Hernandez JC. Antibiotic and synthetic growth promoters in animal diets: Review of impact and analytical methods. Food Control 2016; doi:10.1016/j.foodcont.2016.03.001.

32. Bruno DW. An investigation into oxytetracycline residues in Atlantic salmon, Salmo salar L. J Fish Dis 1989; 12: 77–86.

33. Pari L, Gnanasoundari M, Influence of naringenin on oxytetracycline mediated oxidative damage in rat liver. Basic Clin Pharmacol Toxicol 2006; 98: 456–461.

34. Nakano T, Hayashi S, Nagamine N. Effect of excessive doses of oxytetracycline on stress-related biomarker expression in coho salmon. Environ Sci Pollut Res Int 2015; doi:10.1007/s11356-015-4898-4.

35. Olsson PE. Toxicology of Aquatic Pollution: Physiological, Molecular and Cellular Approaches Taylor EW, (ed), pp. 283 Cambridge University Press, 1996.

36. Zhao C, Pelaez M, Duan X, Deng H, O'Shea K, Fatta-Kassinos D et al. Role of pH on photolytic and photocatalytic degradation of antibiotic oxytetracycline in aqueous solution under visible/solar light: Kinetics and mechanism studies. Appl Catal B Environ 2013; 134-135: 83–92.

37. Kalaiarasi S, Arjun P, Nandhagopal S, Brijitta J, Iniyan AM, Vincent S et al. Development of biocompatible nanogel for sustained drug release by overcoming the blood brain barrier in zebrafish model. J Appl Biomed 2016; 14: 157–169.

38. Grondel JL, Nouws JFM, De Jong M, Schutte AR, Driessens F. Pharmacokinetics and tissue distribution of oxytetracycline in carp, *Cyprinus carpio* L., following different routes of administration. J Fish Dis 1987; 10: 153–163.

39. Herman RL, Collis D, Bullock GL. Oxytetracycline residues in different tissues of trout. Tech Pap 1969.

40. Reja A, Moreno L, Serrano JM, Santiago D, Soler F. Concentration-time profiles of oxytetracycline in blood, kidney and liver of tench (*Tinca tinca* L) after intramuscular administration. Vet Hum Toxicol 1996; 38: 344–7.

41. Zhang Q, Li X. Pharmacokinetics and residue elimination of oxytetracycline in grass carp, *Ctenopharyngodon idellus*. Aquaculture 2007; 272: 140–145.
42. Magro M, Campos R, Baratella D, Lima G, Holà K, Divoky C, et al. A magnetically drivable nanovehicle for curcumin with antioxidant capacity and MRI relaxation properties. Chem - A Eur J 2014; 20: 11913–11920.
43. Magro M, Baratella D, Jakubec P, Zoppellaro G, Tucek J, Aparicio C et al. Triggering Mechanism for DNA Electrical Conductivity: Reversible Electron Transfer between DNA and Iron Oxide Nanoparticles. Adv Funct Mater 2015; 25: 1822–1831.
44. Venerando R, Miotto G, Magro M, Dallan M, Baratella D, Bonaiuto E, et al. Magnetic nanoparticles with covalently bound self-assembled protein corona for advanced biomedical applications. J Phys Chem 2013; C 117: 20320–20331.
45. Miotto G, Magro M, Terzo M, Zaccarin M, Da Dalt L, Bonaiuto E, et al. Protein corona as a proteome fingerprint: The example of hidden biomarkers for cow mastitis. Colloids Surf B Biointerfaces 2016; 140: 40–9.
46. Spence R, Gerlach G, Lawrence C, Smith C. The behaviour and ecology of the zebrafish, Danio rerio. Biol Rev Camb Philos Soc2008; 83: 13–34.
47. Rozas M, Enríquez R. Piscirickettsiosis and Piscirickettsia salmonis in fish: a review. J Fish Dis 2014; 37: 163–88.

Tables

Gene	Forward primer (5'- 3')	Reverse primer (5'- 3')	ZFIN ID
hsp70.1	5'-TGTTCAGTTCTCTGCCGTTG -3'	5'-AAAGCACTGAGGGACGCTAA-3'	ZDB-GENE-990415-91
hnf4a	5'- ACGGTTCGGCGAGCTGCTTC-3'	5'-TCCTGGACCAGATGGGGGTGT-3'	ZDB-GENE- 030131-77
sod1	5'-GTCGTCTGGCTTGTGGAGTG-3'	5'-TGTCAGCGGGCTAGTGCTT-3'	ZDB-GENE-990415-58
sod2	5'-CCGGACTATGTTAAGGCCATCT-3'	5'-ACACTCGGTTGCTCTCTTTTCTCT-3'	ZDB-GENE-030131-42
gsta.1	5'-TTGAGGAAAAGGCCAAAGTG-3'	5'-AACACGGCCTTCACTGTTCT-3'	ZDB-GENE-040426-20
nr3c1	5'-CGCCTTTAATCATGGGAGAA-3'	5'-AGACCTTGGTCCCCTTCACT-3'	ZDB-GENE-050522-03
igf1	5'-GGCAAATCTCCACGATCTCTAC-3'	5'-CGGTTTCTCTTGTCTCTCTCAG-3'	ZDB-GENE-010607-2
igf2a	5'-GAGTCCCATCCATTCTGTTG-3'	5'-TCCTTTGTTTGTTGCCATTTG-3'	ZDB-GENE-991111-3
mstnb	5'-GGACTGGACTGCGATGAG-3'	5'-GATGGGTGTGGGGATACTTC-3'	ZDB-GENE-990415-65
rplp0	5'-CTGAACATCTCGCCCTTCTC-3'	5'-TAGCCGATCTGCAGACACAC-3'	ZDB-GENE-000629-1
actbl	5'-GGTACCCATCTCCTGCTCCAA-3'	5'-GAGCGTGGCTACTCCTTCACC-3'	ZDB-GENE-000329-1

Table 1. Primers sequences and ZFIN ID.

Figures

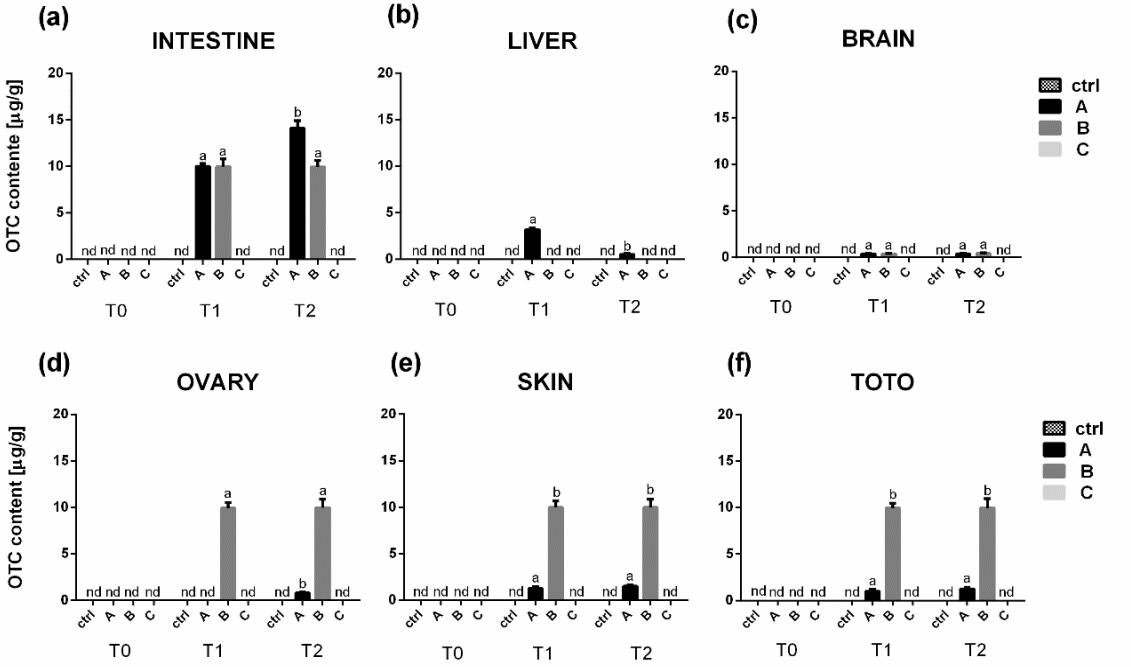

Figure 1. Mean OTC concentrations (expressed in µg/g of body weight) detected in ZF intestine **(a)**, liver **(b)**, brain **(c)**, ovary **(d)**, skin **(e)** and *in toto* fish **(f)**. HPLC analysis were performed at the beginning (T0), after 14 (T1) and 28 (T2) days of exposure. OTC content was measured in control group (ctrl), in fish exposed to 4mg/L of OTC (group A), in fish exposed to 100 mg/L of SAMNs@OTC complex (group B) and in fish exposed to 100 mg/L of SAMNs (group C). Not detectable (nd) indicates samples where OTC concentration was absent or lower than the limit of detection (LOD). Different letters indicate statistical significant differences among experimental groups ($p < 0.05$).

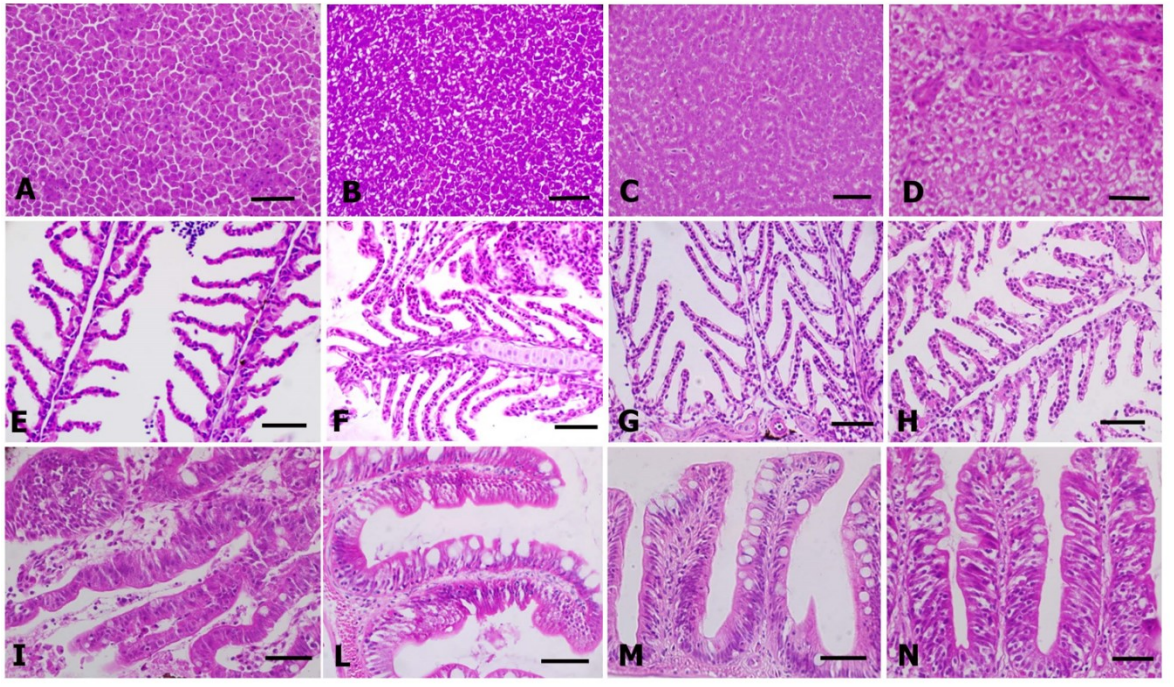

Figure 2. Example of histomorphology (day 28) of ZF: liver ctrl **(A)**, group A **(B)**, group B **(C)**, group C **(D)**; gills ctrl **(E)**, group A **(F)**, group B **(G)**, group C **(H)** and intestine ctrl **(I)**, group A **(L)**, group B **(M)**, group C **(N)**. Scale bars: 50μm. Control group (ctrl), fish exposed to 4mg/L of OTC (group A), fish exposed to 100 mg/L of SAMNs@OTC complex (group B) and fish exposed to 100 mg/L of SAMNs (group C).

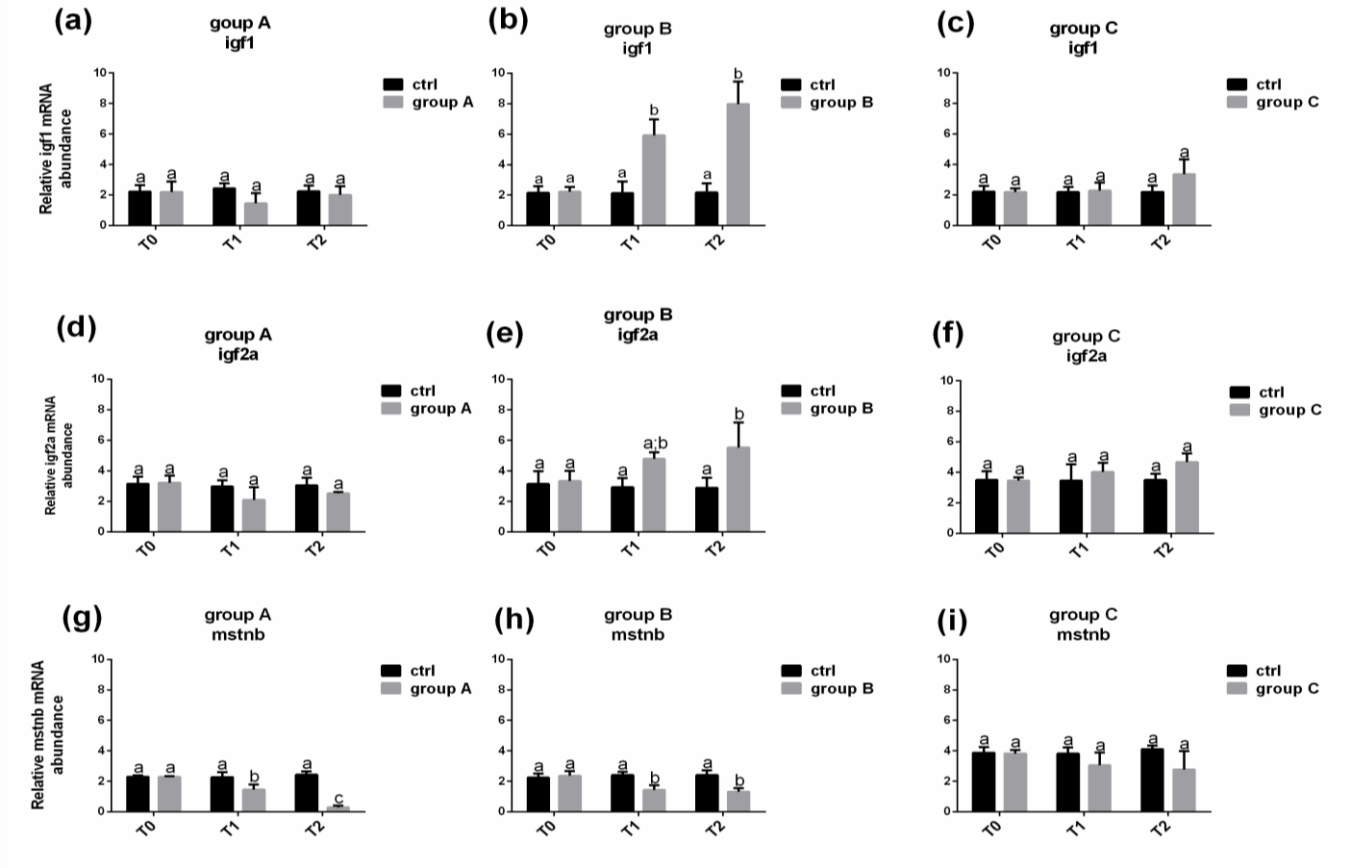
(a)
goup A
igf1
Relative igf1 mRNA abundance
ctrl
group A
(b)
group B
igf1
ctrl
group B
(c)
group C
igf1
ctrl
group C
(d)
group A
igf2a
Relative igf2a mRNA abundance
ctrl
group A
(e)
group B
igf2a
ctrl
group B
(f)
group C
igf2a
ctrl
group C
(g)
group A
mstnb
Relative mstnb mRNA abundance
ctrl
group A
(h)
group B
mstnb
ctrl
group B
(i)
group C
mstnb
ctrl
group C
T0
T1
T2

Figure 3. Relative mRNA levels of genes involved in fish growth (*igf1, igf2* and *mstnb*) analyzed in the liver at 0 (T0), 14 (T1) and 28 (T2) days of exposure. *Igf1, igf2a* and *mstnb* expression was analyzed in control (ctrl) and: group A (**a**, **d** and **g**); group B (**d**, **e** and **h**) and group C (**c**, **f** and **i**). Different letters indicate statistical significant differences among experimental groups ($p < 0.05$). Values are presented as mean ± SD (n=5). Control group (ctrl), fish exposed to 4mg/L of OTC (group A), fish exposed to 100 mg/L of SAMNs@OTC complex (group B) and fish exposed to 100 mg/L of SAMNs (group C).

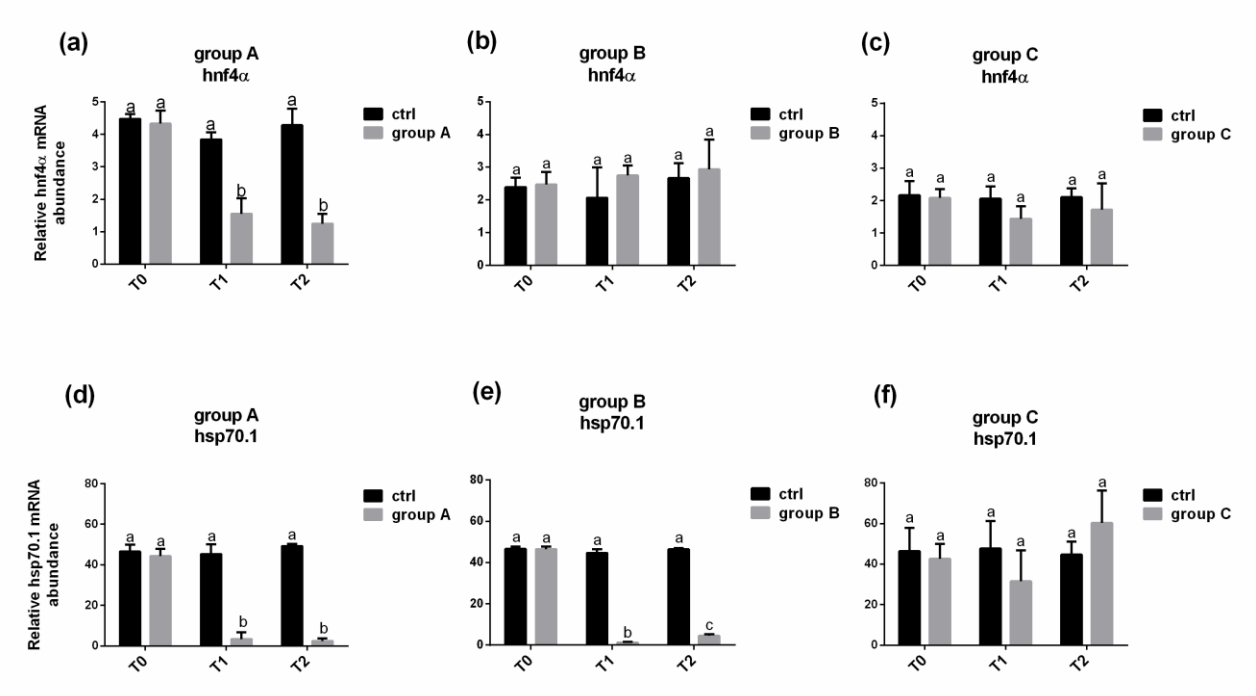

Figure 4. Relative mRNA levels of genes involved in stress response (*hnf4α* and *hsp70*) analyzed in livers at 0 (T0), 14 (T1) and 28 (T2) days of exposure. *Hnf4α* and *hsp70.1* expression was analyzed in control (ctrl) and: group A (**a**, **d**); group B (**b**, **e**) and group C (**c**, **f**). Different letters indicate statistical significant differences among experimental groups ($p < 0.05$). Values are presented as mean ± SD (n=5). Control group (ctrl), fish exposed to 4mg/L of OTC (group A), fish exposed to 100 mg/L of SAMNs@OTC complex (group B) and fish exposed to 100 mg/L of SAMNs (group C).

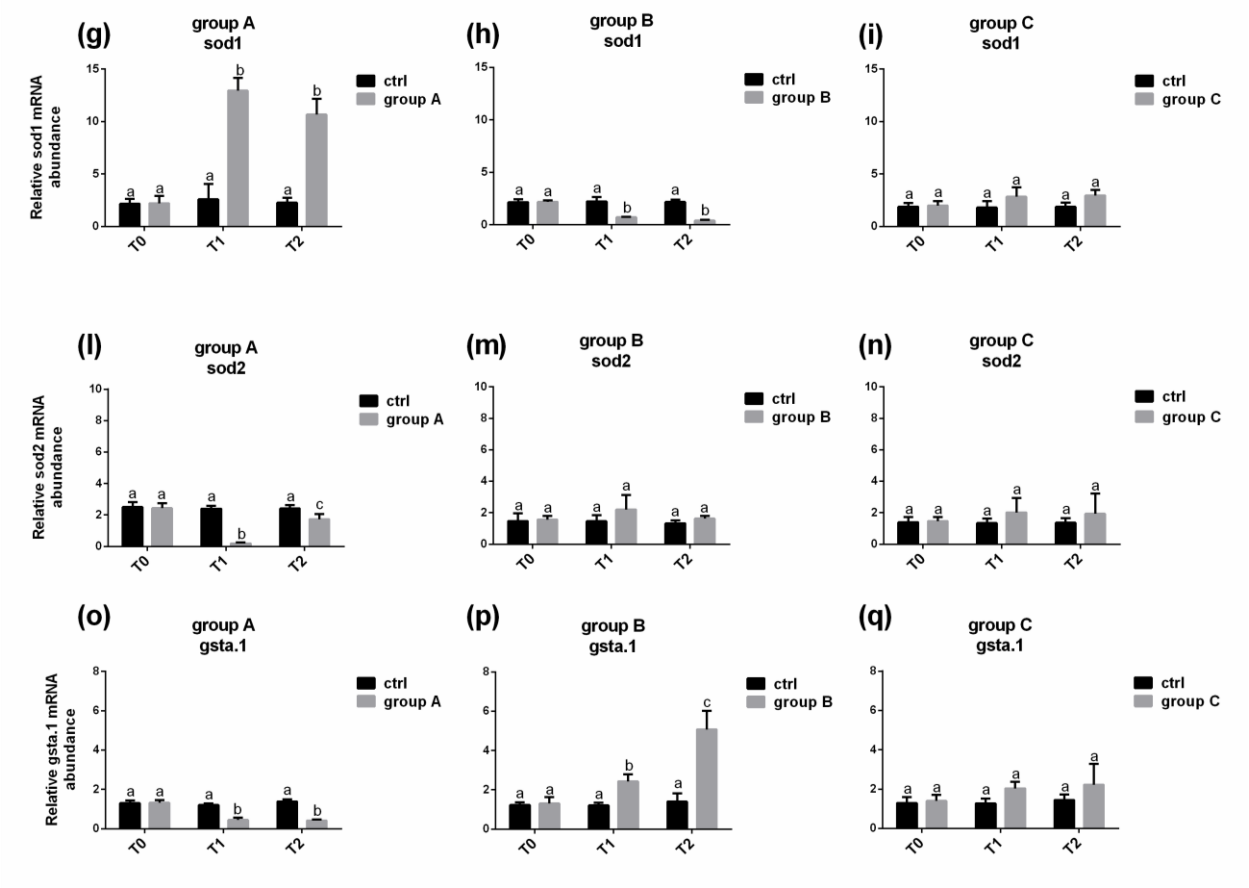
(g)
group A
sod1
Relative sod1 mRNA abundance
ctrl
group A
(h)
group B
sod1
ctrl
group B
(i)
group C
sod1
ctrl
group C
(l)
group A
sod2
Relative sod2 mRNA abundance
ctrl
group A
(m)
group B
sod2
ctrl
group B
(n)
group C
sod2
ctrl
group C
(o)
group A
gsta.1
Relative gsta.1 mRNA abundance
ctrl
group A
(p)
group B
gsta.1
ctrl
group B
(q)
group C
gsta.1
ctrl
group C
T0
T1
T2

Figure 5. Relative mRNA levels of genes involved in detoxification (*sod1, sod2*, and *gsta1*) analyzed in the liver at 0 (T0), 14 (T1) and 28 (T2) days of exposure. *Sod1*, *sod2,* and *gsta.1* expression was analyzed in control (ctrl) and: group A (**g**, **l** and **o**); group B (**h**, **m** and **p**) and group C (**i**, **n** and **q**). Different letters indicate statistical significant differences among experimental groups ($p< 0.05$). Values are presented as mean ± SD (n=5). Control group (ctrl), fish exposed to 4mg/L of OTC (group A), fish exposed to 100 mg/L of SAMNs@OTC complex (group B) and fish exposed to 100 mg/L of SAMNs (group C).

Chapter 2

Protein hitch-hiking by iron oxide nanoparticles as an emerging concept of organotropic drug targeting: mechanism and *in vivo* study

Magro M, Bonaiuto E, de Almeida Roger J, Chemello G, Baratella D, Pasquaroli S, Mancini L, Olivotto I, Zoppellaro I, Ugolotti J, Aparicio C, Fifi AP, Cozza G, Miotto G, Radaelli G, Zboril R, Vianello F.

Under revision

2.1 Introduction

Tuning the properties of nanostructured materials for applications in biologically oriented scenarios represents the current goal of the theranostics research. Envisioning from the bench-synthesis the final extent of *in vivo* protein-nanoparticle interactions is complicated[1] because during their metabolism an unavoidable array of unspecific interactions exists between the nanosystem and the biological molecules present in all living organism[2,3]. The knowledge of the nature and strengths of these interactions and their influence on the biological activity of the resulting nanobioconjugate constitute the essential know-how for the development of theranostic materials and drug carriers in biomedicine. Liposomes-encapsulated drugs and polymer-drug conjugates were the earliest nanotechnologies employed for biomedical applications, representing the foundation of advanced drug delivery[4,5]. Stimuli-responsive devices, including multiwalled carbon nanotubes and ultrasmall iron oxide nanoparticles, were proposed as new generation nanocarriers, allowing the triggered release of the transported drug[6]. Iron oxide nanoparticles have been studied in this context for decades, because they usually express an intrinsically low toxicity impact, making them compatible to be engineered for drug delivery, as contrast agent materials and even tailored for medical therapies (hyperthermia). Years ago, a novel synthetic procedure for the assembly of nanostructured superparamagnetic materials, in the size range around 10 nm, which presented distinctive surface properties[7] was developed. The synthesis of this material was based on iron oxide, completely carried out in water without the employment of any organic solvent or surfactant, which lead to the formation of nanoparticles (maghemite phase, γ-Fe_2O_3), characterized by unique surface chemical behavior. These nanoparticles, called SAMNs (surface active maghemite nanoparticles)[8] display high water stability (e.g. colloidal suspensions) that did not require

further surface modification or coating derivatization. SAMNs is a magnetic nanomaterial that shows great surface reactivity, thanks to the presence of solvent-exposed iron(III) atoms, and yet keeps the stable crystalline structure with high magnetic moment response (> 60 emu/g)[7]. From the combination of colloidal stability, excellent cell uptake[9], stability within the host cells[10], low toxicity[9] and excellent MRI contrast agent properties[8], these nanoparticles can be considered elective carriers and flexible magnetic vectors for drug delivery. In order to test the effective use of this material in real-world scenarios, the fate and potential ecotoxic effects of SAMNs@OTC were studied in terms of their environmental risks. For this reason, *Escherichia coli* (*E. coli*) ATCC 25922 was used as oxytetracycline sensitive strain model, in the presence of different concentrations of OTC, SAMNs, and SAMNs@OTC.

The application of these SAMNs was successfully validated in a previous *in vivo* study for the direct delivery of oxytetracycline (OTC) in zebrafish female (especially in the ovary) using SAMNs as mother-vector[11] (see Chapter 1). In the previous study the fate and biodistribution of OTC were analyzed, while in the present studied, samples deriving from the *in vivo* experiments were analyzed to detect the accumulation of SAMNs in zebrafish organs after the exposure to different experimental conditions (see Chapter 1).

Moreover, in this study, using gilthead sea bream (*Sparus aurata*) as model organism, a circulating protein displaying an affinity for SAMNs surface (Apolipoprotein A1) was demonstrated to target the SAMNs@OTC complex in a way it can shuttle them directly to the ovary. This mechanism is termed "protein hitch-hiking" and could offer a valid explanation for the results obtained in the previous *in vivo* study[11], in particular, the high OTC concentration observed in ovary samples can be justified by the formation of the bind between SAMNs@OTC and Apo A1. The strategy reported herein

represents a solid innovation for attaining the effective delivery of pharmaceutical compounds in the final context of personalized medicine[12].

2.2 Materials and Methods

2.2.1 Synthesis of surface active magnetic nanoparticles (SAMNs)

A typical synthesis of nanoparticles was already described and can be summarized as follows[7,13]: $FeCl_3 \cdot 6H_2O$ (10.0 g, 37 mmol) was dissolved in MilliQ grade water (800 mL) under vigorous stirring at room temperature. $NaBH_4$ solution (2 g, 53 mmol) in ammonia (3.5 %, 100 mL, 4.86 mol/mol Fe) was quickly added to the mixture. Soon after the reduction reaction occurrence, the temperature of the system was increased to 100 °C and kept constant for 2 hours. Then, the material was cooled to room temperature and aged in water, as prepared, for other 24 hours. This product was separated by the imposition of an external magnet (NdFeB) and washed several times with water. This material can be transformed into a red-brown powder (final synthesis product) by drying and curing at 400 °C for 2 hours. The resulting powder showed a magnetic response upon exposure to an external magnetic field. The final mass of product was 2.0 g (12.5 mmol) of Fe_2O_3 and a yield of 68 % was calculated. The resulting nanoparticulated material was characterized by Mössbauer spectroscopy, FT-IR spectroscopy, high resolution transmission electron microscopy (HR-TEM), XRD, magnetization measurements and resulted constituted of stoichiometric maghemite (γ-Fe_2O_3) with a mean diameter (davg) of 11 ± 2 nm, which can lead to the formation, upon ultrasound application in water (Bransonic, mod. 221, 48 kHz, 50 W) of a stable colloidal suspension, without any organic or inorganic coating or derivatization[7,13]. The surface of these bare maghemite nanoparticles shows peculiar binding properties and can be reversibly derivatized with selected organic molecules.

2.2.2 Oxytetracycline binding on magnetic nanoparticles

Oxytetracycline (20 mg/L) was incubated in the presence of various nanoparticle concentrations (0.1, 0.2, 0.5, 1.0, 1.5 and 2.0 g/L) in H_2O at room temperature. SAMN suspensions were previously treated by ultrasound (Bransonic, mod. 221, 48 kHz, 50 W) for 5 minutes, and then stored, under overnight constant agitation, to promote complex formation. Then, magnetic nanoparticles were separated from the aqueous solution with the assistance of a magnet (N35, 263-287 kJ m^{-3} BH, 1,170-1,210 mT flux density by Power Magnet, Germany) for 1 hour. SAMN@OTC was washed several times under constant agitation.

2.2.3 Exposure of *Escherichia coli* (*E. coli*)

ATCC 25922 *E. coli* were cultured in LB medium at 37°C under shaking. The broth-culture was diluted until an optic density of 1 x 108 CFU/mL and used to test different conditions: A) control for strain growth; B) 4 mg/L oxytetracycline; C) 2 mg/L oxytetracycline; D) 100 mg/L SAMNs; E) 50 mg/L SAMNs; F) 100 mg/L SAMN@oxytetracycline; G) 50 mg/L SAMN@oxytetracycline. After 3 and 18 hrs incubation at 37°C under shaking, serial dilutions (10^{-4}, 10^{-5}, 10^{-6} and 10^{-7}) of each sample were plated on LB agar and CFU/mL were counted after overnight incubation at 37°C. Each experiment was performed in triplicate.

2.2.4 Determination of iron content in biological samples

Total iron content in biological samples was determined by inductively coupled plasma atomic-emission spectrometry (ICP-AES) SPECTRO ARCOS (Spectro, Berwyn, PA, USA) following sample mineralization with nitric acid.

2.2.5 Optical microscopy

Ten samples of the intestine, liver, and gills, randomly collected at each sampling time from control, group A, B, C were fixed by immersion in 4% paraformaldehyde and stored at 4°C overnight. Samples were then washed in PBS 1X, dehydrated in an ethanol series and embedded in paraffin. Slides of 4 µm sections (cut with a microtome LEICA) were stained with Mayer's hematoxylin and eosin stain and examined under photomicroscope (Olympus Vanox photomicroscope, Japan).

2.2.6 Electron transmission microscopies (TEM)

The transmission electron microscope (TEM) micrographs of biological samples were acquired by a FEI Tecnai 12 microscope operating at 120 kV.

2.2.7 Test on zebrafish

All the information related to the experimental design and the collection procedures of zebrafish samples have been described in Chapter 1.

2.2.8 Incubation of SAMNs and SAMN@OTC in fish plasma

Male gilthead sea bream (n=5) were treated with E_2 (3.5 mg/animal, Sigma, St. Louis, MO) to induce an increase of plasma vitellogenin (VTG) levels. After 72 hrs, the animals were rapidly anesthetized in a tank containing water plus 100 mg/l of MS222 (Sigma), and blood samples were collected from the caudal vein with heparinized syringes in heparinized tubes containing PMSF (1 mM) to prevent protein proteolytic breakdown; the samples were then centrifuged (1,500g for 15 min at 4°C) and the plasma stored at -20°C. SAMNs or SAMN@OTC (50 µg) were incubated in fish blood serum (200 µL, 20 mg/mL average protein concentration) for 2 hours under end-over-end mixing. After incubation, magnetic nanoparticles were separated by the

application of an external magnet, the supernatants were removed, and, finally, magnetic nanoparticles bearing bound proteins were subjected to 2 washing cycles (200 μL) with water. Bound proteins were released from SAMNs surface by treatment at 95°C (5 min) in 250 mM TRIS, pH 8.5, 2% SDS, 50 mM DTT. Released proteins were analyzed by SDS gel electrophoresis. The most intense electrophoretic band was excised and digested by trypsin, and proteins were identified by mass spectrometry.

2.2.9 SDS-PAGE Electrophoresis

1-D SDS-PAGE was performed using Bis-Tris 4-12% polyacrylamide gels (NuPAGE, Invitrogen) with MES buffer, at 160 V constant tension for approximately 1 h (until the front line reached the end of the gel). Samples were dissolved in a solubilizing buffer (10% glycerol, 250 mM TRIS, pH 8.5, 2% SDS, 50 mM DTT, Coomassie Blue), heated for 10 min at 70°C, centrifuged for 1 min and then loaded onto the gel, together with molecular mass weight standards. After SDS-PAGE runs, gels were stained with Colloidal Coomassie and finally, gel images were acquired by a digital equipment (Kodak 4000MM)[14].

2.2.10 In gel digestion of proteins

Selected protein bands were manually excised from the gel and protein digestion was performed in gel, using sequencing grade modified trypsin (Promega, Madison, WI). Briefly, excised gel bands were repeatedly washed with 50% acetonitrile/40 mM NH_4HCO_3 and then dried under vacuum. Trypsin (20 μL, 12.5 ng/μL in 40 mM NH_4HCO_3) was added to each gel band and samples were incubated for 30 min at 4°C. Then, excess trypsin was discarded and replaced by 25 μL of 40 mM NH_4HCO_3, containing 10% acetonitrile. Digestion was carried out at 37°C, overnight. After trypsin

digestion, peptides were extracted from the gel with 50% acetonitrile/0.1% formic acid (25 µL), repeated twice. The final peptide mixtures were then dried under vacuum and finally resuspended with of 5% acetonitrile/0.1% formic acid (20 µL).

2.2.11 Protein identification by Mass Spectrometry (MS)

All samples were analyzed by LC-MS/MS using a 6520 Q-TOF mass spectrometer, coupled on-line with a 1200 series HPLC system through a Chip Cube Interface (Agilent Technologies, CA, USA). Each sample (4 µL) was loaded onto a C18 large capacity chip-column, integrating a 300 nL capacity trap-column, an RP column (75 µm × 150 mm), connection capillaries, and a nano-spray emitter. Solvent A was water containing 0.1 % formic acid, while solvent B was acetonitrile containing 0.1 % formic acid. Peptides were separated with a linear gradient of 0 – 50 % of solvent B in 50 min at a flow rate of 0.3 µL/min. Mass spectra were acquired in a data-dependent mode: MS/MS spectra of the 4 most intense ions were acquired for each MS scan in the 140 – 1,700 Da range. Scan speed was set to 3 MS spectra s^{-1} and 3 MS/MS spectra s^{-1}. Capillary voltage was set to 1,720 V and drying gas to 4 L/s. Raw data files were converted into Mascot Generic Format (MGF) files with MassHunter Qualitative Analysis Software (Agilent Technologies). MGF files were analyzed using Mascot Search Engine, server version 2.3 (Matrix Science, London, UK). Spectra were searched against the SwissProt database (May 2011 version, Taxonomy Mammalia, 65,453 entries) with the following parameters: enzyme specificity was set to trypsin with up to 2 missed cleavages, peptide and fragment tolerance were set to 6 ppm and 0.05 Da respectively. Deamidation (NQ), phosphorylation (ST), oxidation (MC) and propionamide (C) were selected as variable modification. Proteins were considered as positively identified if at least 3 peptides with individual

significant score ($p < 0.05$) were sequenced. The search was carried out also against the corresponding randomized database, which did not return any positive identification under the same strict conditions (i.e., at least 3 peptides sequenced with individual significant score).

2.3 Results and Discussion

2.3.1 Effects of SAMNs and SAMNs@OTC on *E. coli*

Bacteria play a key role in aquatic ecosystems, where they degrade and uptake carbon from the DOC pool and their biomass forms the basis of the aquatic food web; in addition, several bacteria species are involved in element cycles that represent the starting point for living aquatic organisms. However, bacterial communities are sensitive to disturbances, and alterations in community productivity and abundance may deeply affect the whole ecosystem[15]. Natural nanoparticles, including metal oxide nanoparticles, exist in all ecosystems and play important roles in biogeochemical processes. While living organisms have adapted to the presence of natural nanoparticles in the environment, the potential harmful properties of synthetic nanomaterials on ecosystems have to be evaluated. In the present study, in order to evaluate the interactions between nanoparticles (both naked SAMNs and SAMNs@OTC) and bacteria, *E. coli* (ATCC 25922) was used as OTC sensitive strain model, its growth was tested in the presence of different concentrations of OTC, SAMNs, and SAMNs@OTC (Table 1). *E. coli* growth in different conditions after 3 and 18 hrs incubation at 37°C. In particular, *E. coli* cultures were treated with OTC (2 and 4 mg/mL) and SAMNs (50 and 100 mg/mL). OTC completely suppressed *E. coli* growth (Table 1), conversely, as previously described for other iron oxide nanoparticles[16], SAMNs did not inhibit the growth of *E. coli*. Moreover, no interference with *E. coli* growth was observed in the presence of SAMNs@OTC (Table 1), highlighting that the binding on

SAMNs completely suppresses OTC toxicity for these bacteria, and evidencing the applicability of SAMNs for OTC water remediation. The absence of cytotoxicity of SAMNs@OTC can be attributable to the high stability of the complex.

2.3.2 Test on zebrafish.

In the previous study, performed on zebrafish (see Chapter 1), SAMNs@OTC complex was *in vivo* tested as drug carrier in order to provide a full insight into the fate of SAMNs@OTC as drug vector.

In this study, nanoparticles distribution into the host organism (zebrafish) was studied by Inductively Coupled Plasma-Atomic Emission Spectroscopy (ICPAES) (Table 2), in combination with optical and electron transmission microscopies (Fig.1) (Fig.2). In comparison with the basal level of the metal in controls, iron concentration in the population treated with SAMNs@OTC (as well as with naked SAMNs) resulted fivefold higher (Table 2). As SAMNs@OTC (and naked SAMNs) present a high colloidal stability in water, the internalization in fish via oral route was plausible. Accordingly, ICP-AES indicates that iron in the intestine of treated fishes was more than twenty times higher than in controls (Table 2). Optical micrographs showed the absence of macroscopic nanoparticles aggregates in the intestine (Fig. 1a), confirming the high colloidal behavior of the naked and OTC modified nanomaterial and suggesting their adsorption by the intestinal tissue. Electron microscopy images (Fig. 1b, c, d) of the same region evidenced the presence of isolated nanoparticles on the surface of intestine villi and adsorbed inside the enterocytes confirming the massive nanoparticle adsorption in the intestinal tract. In particular, ICP-AES (Table 2) indicates that about 50% of the nanoparticles resulted in the intestine, and the rest was adsorbed. Therefore, animal organs were explored by optical and electron microscopy

and representative images liver and ovary are reported in Fig. 2. Aggregates of SAMNs@OTC and SAMNs were absent in the liver parenchyma (data confirmed by ICP-AES), which showed no sign of alteration with respect to controls (Fig. 2a). Interestingly, isolated SAMNs@OTC complex and bare SAMNs or small nanoaggregates can be observed in small liver blood vessels (Fig. 2b, c). Moreover, the drug carrier, as well as bare SAMNs, were evidenced in the ovary (Fig. 2d).

These results together with those obtained from previous *in vivo* study which revealed the presence of OTC in the intestinal tract and ovary of animals treated with SAMNs@OTC, opened two different distribution scenarios from free or immobilized OTC administrations: the binding of OTC on SAMNs surface enabled the drug overcoming of the intestinal barrier and its biodistribution within the host organism, involving the prevention of drug loss before reaching the ovaries and leading to its accumulation in the target organ. Moreover, ICP-AES analysis revealed that the presence of OTC in the ovaries was not accompanied by an iron accumulation, indicating that the nanocarrier was depleted after the successful drug release into the target organ. The combination of the stability of OTC binding on SAMNs with the observed drug carrier absorption into the intestine suggests that the administration of SAMNs@OTC leads to the overcoming of biological barriers and to an improvement of the known low bioavailability of the drug[17], aspects of particular relevance for therapeutic strategy[18,19,20]. The comparable internalization in zebrafish suggests that SAMNs and SAMNs@OTC should have the same biomimetic properties, conferred by similar selectivity toward fish endogenous proteins. Therefore, protein corona was studied to explain the specific targeting abilities of SAMNs@OTC in zebrafish in comparison to neat SAMNs, as this phenomenon represents a key factor for controlling the fate of nanoparticles into an organism[21,22].

2.3.3 Protein hitch-hiking by SAMNs@OTC in fish blood serum

Ideally, the use of a selective surface, which can lead to the predictable binding of a restricted group of proteins presenting a significantly high affinity for the surface, can heavily influence the final corona composition[9,23,24]. SAMNs@OTC complex (as well as neat SAMNs) was incubated in fish blood serum and the amount and the nature of absorbed proteins on nanoparticle surface was determined by gel electrophoresis and mass spectrometry.

Electrophoretic profiles of proteins removed from SAMNs and SAMNs@OTC were similar (Fig. 3), confirming that the OTC coating does not alter the recognition properties of SAMNs toward plasma proteins. Only a slightly lower amount of proteins was observed on SAMNs@OTC, with respect to naked SAMNs. Possibly, the presence of OTC partially hindered the protein anchoring on the nanoparticle surface.

Interestingly, the electrophoretic gel of protein removed from the surface of SAMNs and SAMNs@OTC showed only one intense band at about 70 kDa (Fig. 3) and only minor other components. This most intense electrophoretic band was excised and digested by trypsin, and proteins were identified by mass spectrometry, indicating that it is attributable to Apolipoprotein A1 (Apo A1). Apo A1 is a known carrier for lipids and low polarity molecules to the ovary in fishes. This macromolecule can confer suitable biomimetic properties to the drug vehicle (as well as to neat SAMNs), and hence it can be considered an endogenous targeting functionality, promoting the specific organotropic drug delivery. In fact, during vitellogenesis, Apo A1 is sequestered via receptor-mediated uptake by the developing oocytes in the fish ovary[25]. Notably, as Apo A1 is synthesized and assembled in the liver and in the intestine, before being secreted in the plasma, SAMNs@OTC, adsorbed in fish intestine, benefits of the lipoprotein transport route. We termed this

phenomenon “protein hitch-hiking”. Thus, a bimodal nanostructured material, bearing both the antibiotic (OTC) and the targeting functionality (Apo A1) was spontaneously self-assembled as SAMNs@OTC is adsorbed.

2.4 Conclusions

Maghemite nanoparticles are able to specifically bind proteins and peptides presenting high affinities for their surface during the initial period of incubation in a biological fluid, even if present in very tiny concentrations. The emerging targeting properties, due to SAMNs binding selectivity, were studied in an animal model (*Danio rerio*, zebrafish) for the delivery of an antibiotic (oxytetracycline, OTC). Among the proteins present in the fish blood, the specific binding of apolipoprotein A1 induced the formation of a biologically recognizable protein corona. Thus, the administration of SAMNs@OTC complex, provided directly to the farming water, led to the organotropic delivery of OTC in the fish ovary. The present work offers an alternative viewpoint on protein corona formation on nanomaterial, from a detrimental uncontrollable phenomenon to new targeting opportunities.

References

1. Lundqvist M. Nanoparticles: tracking protein corona over time. Nat Nanotechnol 2013; 8: 701-702.
2. Nel AE, Mädler L, Velegol D, Xia T, Hoek EMV, Somasundaran P, et al. Understanding biophysicochemical interactions at the nano-bio interface. Nature Mater 2009; 8: 543-557.
3. Niemirowicz K, Markiewicz KH, Wilczewska AZ, Car H. Magnetic nanoparticles as new diagnostic tools in medicine. Adv Med Sci 2012; 57: 196-207.
4. Petros RA, DeSimone JM. Strategies in the design of nanoparticles for therapeutic applications. Nat Rev Drug Discov 2010; 9: 615-627.
5. Ulbrich K, Holá K, Šubr V, Bakandritsos A, Tuček J, Zbořil R. Targeted drug delivery with polymers and magnetic nanoparticles: covalent and noncovalent approaches, release control, and clinical studies. Chem Rev 2016; 116:5338-5431.
6. Mura S, Nicolas J, Couvreur P. Stimuli-responsive nanocarriers for drug delivery. Nat Mater 2013; 12: 991-1003.
7. Magro M, Valle G, Russo U, Nodari L, Vianello F. Maghemite nanoparticles and method for preparing thereof. 2015; Patent US 8,980, 218 B2.
8. Magro M, Campos R, Baratella D, Lima G, Holá K, Divoky C, et al. A magnetically drivable nanovehicle for curcumin with antioxidant capacity and MRI relaxation properties. Chem–Eur J 2014; 20: 11913-11920.
9. Venerando R, Miotto G, Magro M, Dallan M, Baratella D, Bonaiuto E, et al. Magnetic nanoparticles with covalently bound self-assembled protein corona for advanced biomedical applications. J Phys Chem C 2013; 117: 20320-20331.
10. Skopalik J, Polakova K, Havrdova M, Justan I, Magro M, Milde D, et al. Mesenchymal stromal cell labeling by new uncoated superparamagnetic maghemite nanoparticles in comparison with commercial Resovist - an initial in vitro study. Int J Nanomedicine 2014; 9: 5355-5372.

11. Chemello G, Piccinetti CC, Randazzo B, Carnevali O, Maradonna F, Magro M, et al. Oxytetracycline Delivery in Adult Female Zebrafish by Iron Oxide Nanoparticles. Zebrafish 2016; 13: 495-503.
12. Shi J, Kantoff PW, Wooster R, Farokhzad OC. Cancer nanomedicine: progress, challenges and opportunities. Nat Rev Cancer 2017; 17: 20-37.
13. Magro M, Sinigaglia G, Nodari L, Tucek J, Polakova K, Marusak Z, et al. Charge binding of rhodamine derivative to OH−stabilized nanomaghemite: universal nanocarrier for construction of magnetofluorescent biosensors. Acta Biomater 2012; 8: 2068-2076.
14. Laemmli UK. Cleavage of structural proteins during the assembly of the head of bacteriophage T4. Nature 1970; 227: 680-685.
15. Shade A, Peter H, Allison SD, Baho DL, Berga M, Bürgmann H, et al. Fundamentals of microbial community resistance and resilience. Front Microbiol 2012; 3: 417.
16. He S, Feng Y, Gu N, Zhang Y, Lin X. The effect of γ-Fe2O3 nanoparticles on Escherichia coli genome. Environ Poll 2011; 159: 3468-3473.
17. Noga EJ. Pharmacopoeia. Fish Disease: Diagnosis and Treatment (Wiley-Blackwell, Ames) 2010; pp 375-420.
18. Alonso MJ, Csaba NS. Nanostructured Biomaterials for Overcoming Biological Barriers (RSC Publishing, Cambridge) 2012.
19. Sekkim S, Kum C. Antibacterial drugs in fish farms: application and its effects. Recent Advances in Fish Farms, eds Aral F Doğu Z (InTech, Rijeka) 2011; pp 217-251.
20. Toutain PL, Ferran A, Bousquet-Melou A. Species differences in pharmacokinetics and pharmacodynamics. Handb Exp Pharmacol 2010; 199: 19-48.
21. Monopoli MP, Aberg C, Salvati A, Dawson KA. Biomolecular coronas provide the biological identity of nanosized materials. Nature Nanotech 2012; 7: 779-786.

22. Bertoli F, Garry D, Monopoli MP, Salvati A, Dawson KA. The intracellular destiny of the protein corona: a study on its cellular internalization and evolution. ACS Nano 2016; 10: 10471-10479.
23. Miotto G, Magro M, Terzo M, Zaccarin M, Da Dalt L, Bonaiuto E, et al. Protein corona as a proteome fingerprint: the example of hidden biomarkers for cow mastitis. Colloids Surf B 2016; 140: 40-49.
24. Magro M, Fasolato L, Bonaiuto E, Andreani NA, Baratella D, Corraducci V, et al. Enlightening mineral iron sensing in Pseudomonas fluorescens by surface active maghemite nanoparticles: involvement of the OprF porin. Biochim Biophys Acta 2016; 1860: 2202-2210.
25. Levi L, Ziv T, Admon A, Levavi-Sivan B, Lubzens E Insight into molecular pathways of retinal metabolism, associated with vitellogenesis in zebrafish. Am J Physiol Endocrinol Metab 2012; 302: E626-E644.

Tables

Group experimental condition	Growth (CFU/mL) of *E. coli* after incubation	
	3hrs	**18hrs**
A Control	1.3×10^8	2.5×10^9
B 4 mg/L OTC	0	0
C 2 mg/L OTC	0	0
D 100 mg/L SAMNs	3.0×10^7	1.0×10^9
E 50 mg/L SAMNs	7.4×10^7	2.2×10^9
F 100 mg/L SAMN@OTC	1.6×10^8	1.7×10^9
G 50 mg/L SAMN@OTC	2.0×10^8	2.0×10^8

Table 1. Number of *E. coli* colonies expressed as colony-forming units (CFU) grown up in LB medium after 3 and 18 hrs of incubation at 37°C at different experimental conditions: control group (A), exposed to OTC at 4 mg/L (B) and 2 mg/L (C), exposed to SAMNs at 100 mg/L (D) and 50 mg/L (E), exposed to SAMNs@OTC at 100 mg/L (F) and 50 mg/L (G).

Organ	Control (mg/Kg)	SAMNs (mg/Kg)	SAMNs@OTC (mg/Kg)
Whole organism	16.62 ± 2.58	97.72 ± 5.80	96.58 ± 9.80
Intestine	27.43 ± 7.88	574.41 ± 38.12	503.64 ± 74.92
Ovaries	19.96 ± 5.51	16.78 ± 5.15	31.34 ± 6.59
Skin	9.37 ± 3.06	21.96 ± 3.66	15.82 ± 4.81

Table 2. Distribution of iron in zebrafish organs (whole organism, intestine, ovary and skin) upon exposure to OTC, SAMNs and SAMNs@OTC**.** Animals were treated with 4 mg/L OTC, 100 mg/L SAMNs and 100 mg/L SAMN@OTC dispersed in the water. Measurements were carried out by ICP-AES.

Figures

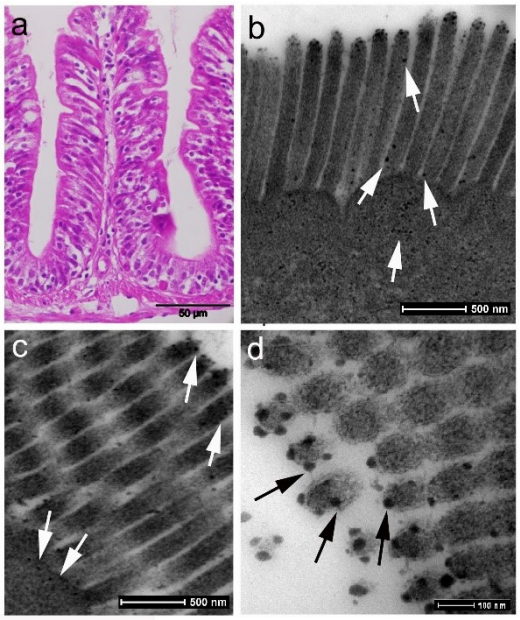

Figure 1. Optical micrographs and electron transmission microscopy (TEM) images of zebrafish intestinal tissue treated with SAMNs@OTC. **a,** Photomicrograph of cross-section of intestine showing intestinal villi in zebrafish treated with 100 mg/L SAMNs@OTC. **b**, **c**, TEM detection of single electron-dense SAMNs@OTC attached to the surface of microvilli **(b, c arrows)**. Structures resembling nanoparticles were

also observed inside gut cells (**b**: **arrows**). **d**, Higher magnification of the same region (**c**) revealing single spherical nanoparticles (**arrows**) attached to the apical region of microvilli.

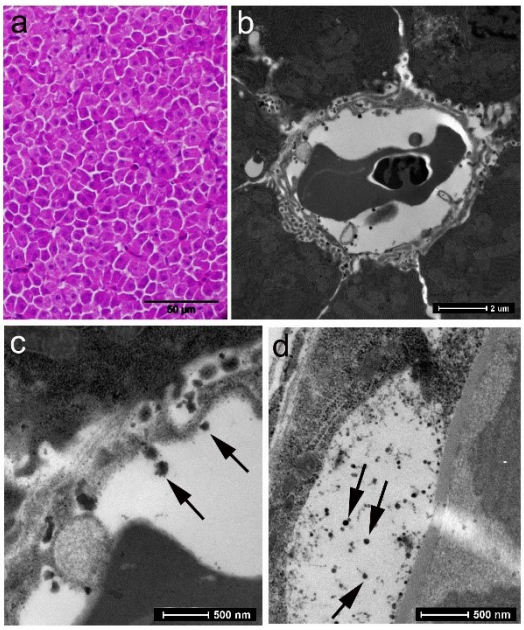

Figure 2. Optical micrographs and TEM images of zebrafish liver and ovary tissues treated with SAMNs@OTC. **a**, Photomicrograph of cross-section of liver parenchyma in 100 mg/L SAMNs@OTC administered zebrafish, showing the organization in *hepatocytes* cells. **b**, TEM detection of hepatocyte cells surrounding a capillary. **c**, Higher magnification of the same region (**b**) reveals single spherical nanoparticles (**arrows**) inside the capillary. **d**, Transmission electron microscopic detection of nanoparticles (**arrows**) in the space between the follicular epithelium and the zona radiata of zebrafish ovary.

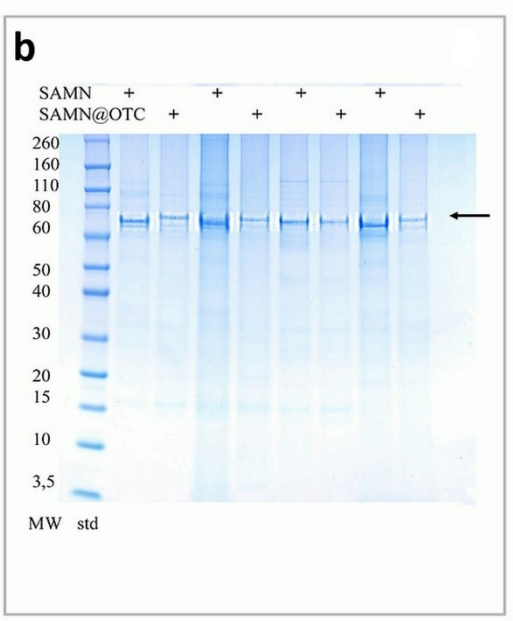

Figure 3. Gel electrophoresis of proteins bound on SAMNs after incubation in plasma from gilthead sea bream Electrophoretic profile of proteins released from the surface of SAMNs and SAMNs@OTC. Proteins bound to SAMNs or SAMNs@OTC were released by 2 M NH_4OH. The most intense bands (at about 70 kDa, marked with an arrow in the gel photograph).

Chapter 3

Safety assessment of antibiotic administration by magnetic nanoparticles in *ex vivo* zebrafish and gilthead sea bream liver and intestine cultures

Chemello G, Randazzo B, Magro M, Zarantoniello M, De Almeida Roger J, Fifi AP, Aversa S, Ballarin C, Radaelli G, Vianello F, Olivotto I.

3.1 Introduction

The number of animals used for research has significantly increased with the advancement of bio-medical technology[1].Various animals including mice, rats, rabbits, and fishes are being used for research for a long time[2].

Recently, different teleost species have been used as model organisms in different type of *ex vivo* experiments.

Zebrafish (*Danio rerio*), for instance, has become an excellent freshwater experimental model for biomedical, developmental biology, genetics and toxicology studies due to its high reproduction rate and the abundant information that has recently become available from genome sequencing[3]. Optical clarity, ease of maintenance and chemical administration, and high sensitivity also make zebrafish embryos and larvae an invaluable laboratory tool[4]. From infancy to the adult stage, it is used in a variety of experiments mainly for the detection of various toxicants and chemicals[5].

Gilthead sea bream (*Sparus aurata*) is one of the most common fish in Mediterranean aquaculture, therefore several studies have been performed to better identify the optimal quality standards for its husbandry. Thanks to in-depth knowledge of this species biology and genomics[6] it became a seawater experimental model of great interest.

For this purpose, animals are usually euthanized by established methods and either a whole animal, its organs or tissues are used for the experiment. Research involving animals is presently regulated by the Directive 2010/63/EU and besides the major concern of ethics, high maintenance costs for their housing, breeding and rearing are required[7].

To date, alternatives to animal testing are looked with great interest and the strategy of 3Rs is being applied which stands for reduction, refinement, and replacement of laboratory use of experimental animals[8]. The concept of replacement of experimental animals is extremely important and was firstly

introduced in 1957 by Charles Hume and William Russell[7]. Two types of replacements were distinguished as "relative" (in which the animals are used but not exposed to any distress during experiments) and "absolute" (in which no animals are used).

Presently different methods have been suggested to implement this strategy including *ex vivo* models, cell cultures, computer models and new analyzing or imaging techniques[9]. Efforts have been made over the past three decades to find out whether *ex vivo* toxicity assays can be used for aquatic hazard assessment as an alternative to *in vivo* tests[10].

Ex vivo models are of great interest and give the opportunity to study cellular responses in a closed system in which the experimental conditions are stable and maintained throughout the experiment[1]. Different tissues and organs like liver, kidney, intestine, and muscle are removed from an animal and can be kept outside the body in suitable growth medium for different periods of time[11,12]. These methods are particularly useful for drug and chemical testing allowing time efficiency, cost-effectiveness and less men power. For example, several cosmetics are tested for their efficacy and/or toxicity using these methods[13,14].

Organ culture is a development of tissue culture methods of research. Advantages are that the organ culture is accurately able to function as an original organ in various states and conditions maintaining the structure of the tissue and direct it towards normal development retaining its physiological features. However, even if the number of animals is not significantly reduced compared to an *in vivo* study, through this approach, animals are not directly exposed to any distress during experiments.

At date, the application of nanotechnology in both human and veterinary medicine has gained much interest, showing a wide variety of nanomaterials' application in this field[15].

At the same time, emerging nanotechnologies pose a new set of challenges for researchers, governments, and industries because of the uncertainty about the environmental, health and safety impacts of nanomaterials. Nanomaterials may constitute a new class of non-biodegradable pollutants that scientists have very little understanding of. For some of these nanoparticles (NPs), there is a set of data that already demonstrated the absence of their induced toxic effects[16–18] or their application for some emerging areas such as diagnostic, imaging and tissue engineering[19].

Among these, iron oxide nanoparticles, in their two magnetic forms, magnetite (Fe_3O_4) and maghemite (c-Fe_2O_3), are considered suitable for *in vivo* applications[17,18,20,21]. Piccinetti et al.[18], have demonstrated that iron oxide silica-coated NPs do not induce toxicity in zebrafish (*Danio rerio*), moreover, these NPs are excreted through faeces and do not activate detoxification processes or promote tissues injury[18]. *In vivo* studies showed the effectiveness of oxytetracycline (OTC) administration in adult zebrafish through the use of a new type of iron oxide nanoparticles, highlighting that NPs exposure did not cause any significant stress response in treated organisms[17].

The aim of this study is to test fish organ cultures for NPs exposure in zebrafish as fresh water model organism and gilthead sea bream as seawater model organism. In particular, liver and intestine organ cultures from both species were used to test the effects of OTC, SAMNs (surface active maghemite NPs) and SAMNs@OTC (complex constituted of SAMNs and OTC) exposure on the selected tissues. Noteworthy, SAMNs applicability range from the biomedical field [22,23], to the advanced material development[24,25] and sensoristics[26–30]. SAMNs present a high average magnetic moment and high-water stability as colloidal suspensions without any superficial modification or coating derivatization. Because of their unique physical and chemical properties, these naked iron oxide nanoparticles are currently used

to immobilize various biomolecules[31–37]. Thus, SAMNs represent an ideal material as they do not need any kind of stabilizing coating, present a very high aqueous colloidal stability and, in contrast to their surface reactivity, they are structurally conserved upon binding to target molecules[24,38,39].

A multidisciplinary approach including HPLC (high-pressure liquid chromatography), optical microscopy and Real Time PCR was used to have a comprehensive understanding of the possible effects *ex vivo*.

3.2 Materials and methods

3.2.1 Ethics

All procedures involving animals were conducted in line with Italian legislation on experimental animals and were approved by the Health Ministry's Department of Veterinary Public Health and by the ethics committee of Università Politecnica delle Marche. Optimal rearing conditions were applied throughout the study, and all efforts were made to minimize animal suffering by the use of anesthetic (MS222; Sigma-Aldrich).

3.2.2 Synthesis of Surface Active Maghemite Nanoparticles (SAMNs).

Bare NPs called surface active maghemite nanoparticles (SAMNs) constituted of stoichiometric maghemite (γ-Fe_2O_3) was synthesized as described by[38,40]. Briefly summarizing: $FeCl_3 \cdot 6H_2O$ (10.0 g, 37 mmol) was dissolved in MilliQ grade water (800 mL) under vigorous stirring at room temperature, to allow the reduction reaction occurrence $NaBH_4$ solution (2 g, 53 mmol) in ammonia (3.5 %, 100 mL, 4.86 mol/mol Fe) was quickly added to the solution. The prepared magnetic material was cured at 4900 °C for 2 hours. The final synthesis product resulted in a red brown nanopowder composed of maghemite NPs with a mean diameter of 11 ± 2 nm that showed a magnetic response when exposed to a magnetic field.

3.2.3 Formation of the complex constituted of magnetic nanoparticles and oxytetracycline (SAMNs@OTC)

OTC hydrochloride (20mg/L, O5875; Sigma-Aldrich, Italy) was incubated with various NP concentrations (0.1, 0.2, 0.5, 1.0, 1.5, and 2.0 g/L) in H_2O at room temperature. This solution was stored under overnight constant agitation to promote complex formation. Then, magnetic NPs were separated from the aqueous solution with the assistance of a magnet. Finally, OTC concentration in the supernatants was checked by spectrophotometry using the Varian Cary 60 instrument (Agilent Technologies, CA, USA).

3.2.4 Growth medium preparation

Zebrafish

The medium used for zebrafish *ex vivo* organ cultures consisted of 9 parts of DMEM–Dulbecco's Modified Eagle Medium (GIBCO, Inc., Grand Island, NY, USA) and 1 part of fetal calf serum (Hyland Laboratories, Los Angeles, CA, USA). In addition, a stabilized solution of 10,000 U of crystalline penicillin G and 0.01 g of streptomycin sulfate (Sigma-Aldrich) were added to each 100 mL of medium to avoid bacterial and fungal development.

Gilthead sea bream

The medium used for Gilthead sea bream *ex vivo* organ cultures was prepared with DMEM- Dulbecco's Modified Eagle Medium (GIBCO, Inc., Grand Island, NY, USA), NaCl (BDH CHEMICALS), $NaHCO_3$ (Sigma-Aldrich), HEPES (Sigma-Aldrich), fetal calf serum (Hyland Laboratories, Los Angeles, CA, USA). Crystalline penicillin G and 0.01 g of streptomycin sulfate (Sigma-Aldrich) were added to each 100 mL of medium.

3.2.5 Fish

Adult 6-month-old AB zebrafish were kept in a zebrafish system (Tecniplast, Varese, Italy) at 28°C, 14L/10D photoperiod, pH 7.0, NO_2 and NH_3 < 0.03 mg/L and fed with a commercial pellet (Blu Line, Italy) twice daily (2% body weight) for 1 month. The experiment started after this first period of acclimatization.

Juveniles of gilthead sea bream were purchased from a fish farm (La Rosa Orbetello, Grosseto, Italy). Acclimatization was carried out in tanks (300 liters) under the following conditions: temperature 20 ± 1 °C, salinity 35 ± 1 ppt, oxygen 6 ± 1 mg/l, and photoperiod 12hL: 12hD. Fish were fed with commercial pellet (Veronesi, Italy) twice daily (2% of body weight).

3.2.6 Experimental design

Adult zebrafish (200 animals) and juvenile sea bream (5 animals) were collected and anesthetized with a lethal dose of MS222 (1 g/L) (Sigma-Aldrich) and the liver (zebrafish), liver portions (sea bream) and posterior intestine fragments (4-5 mm length) were sampled and put in PBS 1X buffer and kept on ice until the beginning of the exposure.

Whole liver/liver portions and posterior intestine fragments were exposed to the different experimental conditions for 24 hours in sterile, tissue culture plastic plates (24 wells, flat bottom with low evaporation lid) (BECTON DICKINSON labware USA FALCON). Each fragment was placed in one well with 3 mL of the appropriate growth medium. The dishes were covered and maintained at 27°C and 20°C for zebrafish samples and sea bream respectively in a constant temperature incubator (IPP 110 Memmert GmbH, Germany) for the whole exposure time.

Four different experimental conditions were tested for both species: control (ctrl): tissues kept in growth medium; group A: tissues kept in growth medium added with SAMNs at a concentration of 100 mg/L; group B: tissues kept in

growth medium with SAMNs@OTC at a concentration of 100mg/L of SAMNs (corresponding to a 4 mg/L concentration of OTC); group C: tissues kept in growth medium with a 4 mg/L OTC. Fifty zebrafish and 9 gilthead sea bream were used for each experimental condition.

Samplings were performed at 0, 8, and 24 hours after the beginning of treatment according to Venerando et al., 2013[37] that demonstrated how the same SAMNs nanoparticles used in this study were already detectable in tissues after two hours incubation. Tissues were collected and properly stored for further analysis.

3.2.7 HPLC analysis

HPLC analysis were conducted as already described by[17].

Extraction procedure.

Tissues exposed to the different treatments (10 livers/liver portions and 10 posterior intestine fragments, 3 replicates each, at each sampling time) were triturated and homogenized in a blender, placed in a plastic tube, and dissolved in 1mL of ultrapure water acidified with 1% phosphoric acid. The tube was vigorously mixed for 2 min, treated in ultrasonic bath for 5 min, and then centrifuged at 13,000 rpm for 10min. The supernatant was collected, filtered through 0.2 μm membrane filters, and stirred before injection into the chromatograph. A 20 μL aliquot was injected. The separation conditions for the OTC were a mobile phase flow of 0.8 mL/min containing acetonitrile acidified with 0.1% phosphoric acid and ultrapure water acidified with 1% phosphoric acid (15:85, v/v) filtered through a 0.45-μm nylon filter under vacuum and degassed by ultrasonication. Column oven temperature was 25°C, and ultraviolet detector was operated at wavelength of 360 nm. The quantitation was accomplished by using an analytical calibration curve built with six concentration levels in the range 20-250 μg/L (OTC). Extraction

recoveries were determined by spiking untreated biological samples (100 mg) with a fortification solution at a limit of quantification (LOQ) and LOD levels: 500 and 100 µg/kg. The HPLC system (Agilent 1100 series with Chemstation) used for analysis consists of a quaternary pump (Agilent 1100 series), a vacuum degasser, an injector, and a wavelength ultraviolet detector (Agilent 1100 series). The chromatographic column was an analytical reversed-phase ZORBAX Eclipse XDB C18, 4.6 x 150 mm, 5 µm.

Method validation.

The method was in-house validated using the following performance criteria as already described by[17]: linearity, sensitivity and selectivity, detection and quantification limits, and accuracy and precision. The solution for calibration and fortification was prepared in ultrapure water acidified with 1% phosphoric acid and stored at temperature ≤ 18°C. Linearity, sensitivity and selectivity, and detection and quantification limits were established by the analytical curve (20, 40, 50, 80, 100, and 250 µg/L of OTC). The LOQ was obtained from the calibration curve and calculated using the following expression: $y = ax + b$, where y is the peak area of OTC and x is the amount of OTC in µg/mL; then, the LOQ was expressed in µg/kg by the following formula: OTC (µg/L) x Vex (mL)/W (g), where Vex is the extraction volume and W is the untreated sample weight. The limit of detection (LOD) was the lowest amount of an analyte in a sample that can be detected but not necessarily quantitated as an exact value and it was 100 µg/kg. The precision of the method, expressed as the relative standard deviation of peak area measurements (n=5), was evaluated by the recovery data obtained (accuracy) at the LOQ concentration level (RSD% = 6.51). The accuracy of the method, expressed as percent recovery, was determined at 500 µg/kg, the LOQ concentration level (mean recovery 95.5%).

3.2.8 Histological analysis

Ten samples of liver/liver portions and posterior intestine fragments, collected at each sampling time from control and groups A, B, C, were fixed by immersion in 4% paraformaldehyde and stored at 4°C overnight. Samples were then washed in PBS 1X, dehydrated in an ethanol series, and embedded in paraffin. Slides of 4 μm sections (cut with a microtome LEICA) were stained with Mayer's hematoxylin and eosin stain and examined under a photomicroscope (Olympus Vanox photomicroscope, Japan).

3.2.9 RNA extraction and cDNA synthesis

Total RNA extraction from single zebrafish livers and gilthead sea bream liver portions (5 replicates collected at each sampling time from control, groups A, B, and C) was optimized using the RNeasy Mini Kit (Qiagen, Italy) following the manufacturer's protocol. Total RNA extracted was eluted in 20 μL RNase-free water (Qiagen). Final RNA concentration was determined by the NanoPhotometer P-Class (Implen, Germany). RNA integrity was verified by ethidium bromide staining of 28S and
18S ribosomal RNA bands on 1% agarose gel. RNA was stored at -80°C until use. Total RNA was treated with DNAse (10 IU at 37°C for 10 min; MBI Fermentas). Then, 3 μg RNA was used for cDNA synthesis with the iScript cDNA Synthesis Kit (Bio-Rad) following the producer's instructions.

3.2.10 Real-time PCR

PCRs were performed with SYBR Green in an iQ5 iCycler thermal cycler (both from Bio-Rad) in triplicate. Reactions were set on a 96-well plate by mixing for each sample 1 μL cDNA diluted 1:20, 5 μL of 2 x concentrated iQ™ SYBR Green Supermix containing SYBR Green as the fluorescent intercalating agent, 0.3 μM forward primer, and 0.3 μM reverse primer. The

thermal profile for all reactions was 3 min at 95°C, followed by 45 cycles of 20 s at 95°C, 20 s at 60°C, and 20 s at 72°C. Fluorescence was monitored at the end of each cycle. Dissociation curve analysis showed a single peak in all cases. Relative quantification of the expression of genes involved in fish stress response (*hnf4a*, *sod1*, *sod2*, and *gsta.1*, for zebrafish) (*HNF4α*, *CuZ/SOD*, and *GST*, for sea bream) was performed using *rplp0* and *actbl* as the housekeeping genes to standardize the results (Table 1) (Table 2). Amplification products were sequenced, and homology was verified. No amplification product was detected in negative controls and no primer–dimer formation was found in control templates. Data were analyzed using the iQ5 optical system software version 2.0, including Genex Macro iQ5 Conversion and Genex Macro iQ5 files (all from Bio-Rad). Modification of gene expression is reported with respect to controls. Primer sequences were designed using Primer3 (210 v. 0.4.0) starting from zebrafish sequences available in ZFIN. Primers were used at a final concentration of 10 pmol/μL.

3.2.11 Statistical analysis

HPLC and real-time PCR data were analyzed by two-way ANOVA analysis of variance, both followed by Tukey's post-test. The statistical software package Prism5 (GraphPad Software) was used for analyses. Significance was set at $p < 0.05$.

3.3 Results

3.3.1 HPLC Analysis

Zebrafish. OTC concentration was not detectable in all analyzed tissues (control, group A, B, and C) at T0. In addition, the same result was observed in all control and group A samples (exposed to 100 mg/L of SAMNs) at T1 and T2 (Fig. 1a, b).

In liver samples (Fig. 1a), the highest OTC concentration was observed in group C at T2 (0.70 ± 0.10 μg/g). OTC concentrations were significantly higher ($p < 0.05$), for both group B and C at T2 with respect to those observed at T1 (0.2 ± 0.1 μg/g and 0.2 ± 0.02 μg/g at T1, 0.6 ± 0.1 μg/g and 0.7 ± 0.1 μg/g at T2 in group B and C, respectively). On the contrary, at both sampling times, no significant differences ($p > 0.05$) were detected in OTC concentration between group B and C (Fig. 1a).

In both group B and C intestine samples (Fig. 1b), no significant differences ($p > 0.05$) in OTC concentration were recorded at both sampling times (0.65 ± 0.06 μg/g and 0.65 ± 0.10 μg/g at T1, 0.70 ± 0.10 μg/g and 0.60 ± 0.09 μg/g at T2 in group B and C, respectively) and between group B and C samples.

Gilthead sea bream. HPLC analysis performed on sea bream samples showed that OTC concentration was not detectable in all analyzed tissues (control, group A, B, and C) at T0 as well as in all control and group A samples (exposed to 100 mg/L of SAMNs) at T1 and T2 (Fig. 2a, b).

In liver samples (Fig. 2a), OTC concentration was significantly higher ($p < 0.05$) at T1 respect to T2 for both group B and C (0.8 ± 0.4 μg/g and 0.6 ± 0.04 4 μg/g at T1, 0.07 ± 0.03 μg/g and 0.06 ± 0.02 μg/g at T2 in group B and C, respectively). At both sampling times, no significant differences ($p > 0.05$) were detected in OTC concentration between group B and C (Fig. 2a). Intestine samples analysis revealed no significant differences ($p > 0.05$) in OTC concentration between group B and C at both T1 and T2 (Fig. 2b) and within the same experimental group between the two different sampling times (0.48 ± 0.10 μg/g and 0.48 ± 0.10 μg/g at T1, 0.43 ± 0.04 μg/g and 0.41± 0.03 μg/g at T2 in group B and C respectively).

3.3.2 Histological analysis

The histological analysis of zebrafish liver (Fig. 3a, b, c, d) and intestine samples (Fig. 3e, f, g, h) did not show any significant difference in the morphological and structural integrity of the analyzed tissues respect to control group (Fig. 3). No evidence of inflammation, steatosis, vacuolation, edema, cellular atrophy or necrosis was observed in all analyzed tissues (Fig. 3). Also in gilthead sea bream samples, any significant alterations in morphological and structural integrity was observed in both liver (Fig. 4a, b) and intestine samples (Fig. 4c, d) with no evidence of inflammation, vacuolation, edema, cellular atrophy or necrosis in treated samples (Fig. 4). A widespread steatosis characterized liver samples from both controls and treatments samples analyzed (Fig. 4).

3.3.3 Real-time pcr

Zebrafish. Real time pcr analysis of liver tissues was performed to evaluate the expression of genes involved in stress response (*hnf4a*, *gsta.1, sod1* and *sod2*). *Stress response and detoxification stress markers.* As concerns to *hnf4α* gene expression, no significant differences ($p > 0.05$) were observed among controls and group A, B, and C at T0 (Fig. 5a, b, c). A similar result was evident in all treatment groups at T2 (Fig. 5a, b, c) respect to control samples. Regarding T1, a significant increase ($p < 0.05$) of *hnf4α* gene expression was observed in group A samples respect to control (Fig. 5a) while, an opposite trend was detected at the same sampling time for group B (Fig. 5b).

With regard to *gsta.1* gene expression, no significant differences ($p > 0.05$) were detected in all experimental groups (A, B and C) respect to control, at T0 (Fig. 5d, e, f). At T1, *gsta.1* gene expression in both group A and B was characterized by two opposite trends. In particular, significantly higher ($p < 0.05$) and significantly lower ($p < 0.05$) mRNA levels were observed, respect

to control, in group A (Fig. 5d) and group B (Fig. 5e), respectively. Finally, at T2, all experimental groups (A, B and C) showed a significant ($p < 0.05$) decrease in *gsta.1* gene expression with respect to control (Fig. 5d, e, f).

Sod1 gene expression analysis did not show significant differences ($p > 0.05$) during all the exposure time (T0, T1, and T2) in all experimental groups (A, B and C) (Fig. 5g, h, i). Finally, *sod2* gene expression was characterized by a significant downregulation in all treatment groups respect to control in all experimental conditions at T1 and T2 except for group A, at T1, in which *sod2* gene expression was significantly higher ($p < 0.05$) respect to control. At T0 no significant differences ($p > 0.05$) were observed in *sod2* mRNA levels in group A, B and C samples (Fig. 5l, m, n).

Gilthead sea bream. Real time pcr analysis of liver tissues was performed to evaluate the expression of genes involved in stress response (*GST*, *HNF4α* and *CuZn/SOD*) (Fig. 6). The expression of *GST* and *CuZn/SOD* didn't show any significant alteration ($p > 0.05$) among all the tested conditions, group A (Fig. 6a, g), group B (Fig. 6b, h) and group C (Fig. 6c, i) respect to the control at T0, T1, and T2. As concern *HNF4α* expression, no significant differences ($p > 0.05$) was observed in group B and C at T0, T1 and T2 (Fig. 6e, f) respect the control, while the gene expression was significantly higher ($p < 0.05$) in group A samples at T2 with respect to the control and group A at T1 and T0 (Fig.6d).

3.4 Discussion

NPs are extensively used in a variety of emerging technologies such as domestic appliances and household products, the manufacture of textiles and electronics, as well as bio-medical applications[41]. Nanotechnology has emerged as a fast-growing sector providing new-engineered nano-enabled products with novel and unique functions that reach the market every day[42].

The worldwide production of NPs is expected to increase from 225,060 metric tons in 2014 to nearly 584,984 metric tons in 2019 with an estimated annual growth rate of 21.1%[43]. However, at the same time, emerging nanotechnologies pose a new set of challenges for researchers, governments, and industries because of the uncertainty about the environmental, health and safety impacts of nanomaterials (NMs).

In particular, aquatic ecosystems are constantly under pressure due to the presence of emerging anthropogenic contaminants including NMs, posing health hazards to inhabitant organisms. Research on the ecotoxicological fate and effects of NMs have increased in recent years[44,45] and several studies demonstrated that some NPs can induce toxicity and genotoxicity under a variety of exposure scenarios[46–50]. Data on the biological effects of NPs indicate that NPs can be toxic to bacteria, algae, invertebrates, fish, and mammals[51–54]. Once introduced into aquatic ecosystems, the fate and toxicity of NPs depend on several factors such as the properties of the NPs (such as size, shape, and coatings) and water chemistry (such as dissolved organic carbon, ionic strength, pH, temperature). However, some other NPs are known to have no toxicity for living organisms and can thus be used for a wide range of applications. For example, recently Chemello and collaborators[17] showed that iron oxide nanoparticles can be used for antibiotic delivery in zebrafish, not only increasing the stability and the delivery of OTC, but also changing the target tissues of accumulation.

This study, together with a previous one performed by Piccinetti and collaborators[18], were both conducted *in vivo* and showed a successful NPs absorption *via* oral route by the fish, with no signs of toxicity or stress. At date, there is widespread agreement that the refinement of testing to reduce suffering should be an important goal for research. Various alternatives to the use of animals have been suggested[9], and the *ex vivo* models provide the

opportunity to study the cellular response in a closed system, where the experimental conditions are maintained. However, it should be pointed out that some *ex vivo* systems lack the complex, interactive effects of the immune, blood, endocrine systems, nervous system, and other integrated elements of the whole animal. Thus, *ex vivo* tests cannot always be used to study the complex nature of systemic toxicity.

In the present study, fish culture organs from two different species (zebrafish a freshwater species and gilthead seabream a seawater species) were used to investigate the effects of different delivery methods of OTC, avoiding a direct exposure of fish, and possibly reducing distress.

In this study, the effects of SAMNs exposure was tested both on a freshwater and a marine water species because despite extensive research on freshwater species, few studies have been conducted on marine organisms. At date published data are available for just eight phyla and, of these, many reports are limited to a single class, order or species[55]. It is not yet clear how best to extrapolate freshwater data for marine organisms considering that the properties of NPs could change according to exposure media such as pH, ionic strength (IS), ionic composition and NOM as well as the biological, behavioral and respiration characteristics of marine organisms[56,57].

Results, at the end of the exposure time, showed that OTC concentration was comparable in both intestine and liver samples and not dependent on the administration way (OTC in water *vs* SAMNs@OTC) for both species. However, in zebrafish samples, at T1 (8 hrs) OTC concentration was higher in intestine samples respect to liver ones. This is in accord with previous studies that demonstrated that NPs are mainly absorbed through the gastrointestinal tract *via* drinking water[58,59].The major OTC concentrations revealed in the intestine cultures can thus be associated to the high

gastrointestinal absorption rate related to the presence of intestinal microvilli and an increased surface/volume ratio of the intestinal epithelium.

However, it should be pointed out that present data are not fully in accord with a previous *in vivo* study performed in zebrafish using the same NPs, in which OTC concentrations were dependent on the way of administration as well as on the analyzed tissue. In particular, OTC delivered through NPs was able to guarantee a higher absorption efficiency of the antibiotic in the analyzed fish respect to a classical *via* water exposure[17].

On the contrary of what observed in zebrafish liver and intestine, OTC concentration detected in sea bream samples was higher in liver samples than in intestine samples after 8 hours of exposure. This result can be related to the diffuse presence of steatosis (abnormal presence of lipid vacuoles in liver tissues) detected by histological analysis. The high lipids concentration in the liver can be responsible for the faster OTC accumulation due to the antibiotic lipophilic nature[60].

Liver steatosis has been commonly observed as a consequence of artificial diets administration[61], therefore the presence of this phenomenon in liver samples (from all the experimental conditions) could be explained rather than a consequence of the exposure to the antibiotic and the nanoparticles.

In addition, molecular results obtained in the present study evidenced some alterations in the expression of the analyzed genes that were not observed in the *in vivo* study. Particularly, in the present study, an increase in *hnf4α*, *gst.1a* and *sod2* gene expression (stress and oxidative stress markers) respect to control was observed in zebrafish samples exposed to SAMNs. Contrary, a decrease of the same genes was observed in samples exposed to SAMNs@OTC complex, underlying a possible safe application of this complex for OTC delivery in organ cultures. Also results in sea bream samples underlying the safe application of SAMNs for OTC delivery. In fact, the

exposure to the complex seemed to have had no effects on the expression of genes involved in stress response in this species. Moreover, liver samples exposed to bare NPs didn't show any alteration in gene expression on the contrary of what described for zebrafish.

However, the discrepancy between *in vivo* results and *ex vivo* related to the analysis performed on zebrafish, was not obvious, and could be related to the simplicity of the organ culture system used in this study respect to the biological complexity of the whole animal, to the different exposure time of the two experiments (hours *vs* days) or to a direct contact of the NPs suspended in the culture medium with zebrafish organ cultures. Considering this last aspect, it is known that different types of NPs are able to cause intracellular oxidative stress in cell cultures by altering the expression of genes involved in stress response[62], the enzymatic response[63,64] and apoptosis[65].

These conflicting outcomes can also be attributed to typical bio-nano interactions of a whole organism (e.g., serum protein-to-particle binding) and agglomeration processes known to modulate nanomaterial surface chemistries and the kinetics of dosimetry. Therefore, these processes may affect what is presented at the cell surface and the probability that cellular uptake will occur.

In conclusion, the present *ex vivo* study provided some important data about the effects of iron oxide NPs exposure to zebrafish and gilthead sea bream liver and intestine cultures. Even if data herein obtained are not fully in accord with previous *in vivo* studies, our results showed that the complex SAMNs@OTC used in the present study may represent a valid and safe way to deliver OTC in organ cultures. However, extrapolation of *ex vivo* data to *in vivo* physiology must be cautious because the exposure of a single organ, kept under controlled conditions, cannot represent the complexity of interactions typical of a biological system.

References

1. Doke SK, Dhawale SC. Alternatives to animal testing: A review. Saudi Pharm J 2015; 23: 223-229.
2. Badyal DK, Desai C. Animal use in pharmacology education and research: the changing scenario. Indian J Pharmacol 2014; 46: 257-65.
3. Lin CY, Chang CY, Tsai HJ, Hackett PB, Hsiao CD, Hsieh FJ, et al. Zebrafish and Medaka: new model organisms for modern biomedical research. J Biomed Sci 2016; 23: 19.
4. Jungke P, Hammer J, Hans S, Brand M. Isolation of Novel CreERT2-Driver Lines in Zebrafish Using an Unbiased Gene Trap Approach. PLoS One 2015; 10: e0129072.
5. Dubińska-Magiera M, Daczewska M, Lewicka A, Migocka-Patrzalek M, Niedbalska-Tarnowska J, et al. Zebrafish: A Model for the Study of Toxicants Affecting Muscle Development and Function. Int J Mol Sci 2016; 17: 1941.
6. Marine Genomics Europe. Implementation of high-throughput genomic approaches to investigate the functioning of marine ecosystems and biology of marine organisms. Research Project. Doi:NoE, CT-2003-505403. http://www.marine-genomics-europe.org.
7. Balls M. Replacement of animal procedures: alternatives in research, education and testing. Lab Anim 1994; 28: 193-211.
8. Ranganatha N, Kuppast IJ. A review on alternatives to animal testing methods in drug development. Int J Biol Pharm Allied Sci 2012; 4: 28-32.
9. Balls M. Future Improvements: Replacement In Vitro Methods. ILAR J 2002; 43: S69-S73.
10. Taju G, Majeed SA, Nambi KSN, Sarath Babu V, Vimal S, Kamatchiammal S, et al. Comparison of in vitro and in vivo acute toxicity assays in Etroplus suratensis (Bloch, 1790) and its three cell lines in relation to tannery effluent. Chemosphere 2012; 87: 55-61.
11. Tomizawa K, Kunieda J, Nakayasu H. Ex vivo culture of isolated zebrafish whole brain. J Neurosci Methods 2001; 107: 31-38.
12. a Marca Pereira ML, Wheeler JR, Thorpe KL, Burkhardt-Holm P. Development

of an *ex vivo* brown trout (*Salmo trutta fario*) gonad culture for assessing chemical effects on steroidogenesis. Aquat Toxicol 2011; 101: 500-511.

13. Xu KP, Li XF, Yu FS. Corneal organ culture model for assessing epithelial responses to surfactants. Toxicol Sci 2000; 58: 306-14.
14. Steinhoff G, Stock U, Karim N, Mertsching H, Timke A, Meliss RR, et al. Tissue Engineering of Pulmonary Heart Valves on Allogenic Acellular Matrix Conduits. Circulation 2000; 102.
15. Can E, Kizak M, Kayim M, Can SS, Kutlu B, Ates M, et al. Nanotechnological Applications in Aquaculture-Seafood Industries and Adverse Effects of Nanoparticles on Environment. J Mater Sci Eng 2011; 5: 605-609.
16. Bacchetta C, López G, Pagano G, Muratt DT, De Carvalho LM, et al. Toxicological Effects Induced by Silver Nanoparticles in Zebra Fish (*Danio Rerio*) and in the Bacteria Communities Living at Their Surface. Bul Environ Contam Toxicol 2016; 97: 456-462.
17. Chemello G, Piccinetti CC, Randazzo B, Carnevali O, Maradonna F, Magro M, et al. Oxytetracycline Delivery in Adult Female Zebrafish by Iron Oxide Nanoparticles. Zebrafish 2016; 13: 495-503.
18. Piccinetti CC, Montis C, Bonini M, Laurà R, Guerrera Maria Cristina, Radaelli G, et al. Transfer of Silica-Coated Magnetic (Fe_3O_4) Nanoparticles Through Food: A Molecular and Morphological Study in Zebrafish. Zebrafish 2014; 0: 1-13.
19. Tay CY, Setyawati MI, Xie J, Parak WJ, Leong DT. Back to Basics: Exploiting the Innate Physico-chemical Characteristics of Nanomaterials for Biomedical Applications. Adv Funct Mater 2014; 24: 5936-5955.
20. Karlsson HL, Gustafsson J, Cronholm P, Möller L. Size-dependent toxicity of metal oxide particles—A comparison between nano- and micrometer size. Toxicol Lett 2009; 188: 112-118.
21. Soenen SJ, De Cuyper M. Assessing iron oxide nanoparticle toxicity *in vitro* : current status and future prospects. Nanomedicine 2010; 5: 1261-1275.
22. Cmiel V, Skopalik J, Polakova K, Solar J, Havrdova M, Milde D, et al. Rhodamine bound maghemite as a long-term dual imaging nanoprobe of adipose tissue-

derived mesenchymal stromal cells. Eur Biophys J 2017; 46: 433-444.

23. Skopalik J, Polakova K, Havrdova M, Justan I, Magro M, Milde D, et al. Mesenchymal stromal cell labeling by new uncoated superparamagnetic maghemite nanoparticles in comparison with commercial Resovist an initial *in vitro* study. Int J Nanomedicine 2014: 9: 5355-72.
24. Magro M, Baratella D, Jakubec P, Zoppellaro G, Tucek J, Aparicio C, et al. Triggering Mechanism for DNA Electrical Conductivity: Reversible Electron Transfer between DNA and Iron Oxide Nanoparticles. Adv Funct Mater 2015; 25: 1822-1831.
25. Magro M, Bonaiuto E, Baratella D, De Almeida Roger J, Jakubec P, Corraducci V, et al. Electrocatalytic Nanostructured Ferric Tannates: Characterization and Application of a Polyphenol Nanosensor. Chem Phys Chem 2016; 17: 3196-3203.
26. Baratella D, Magro M, Sinigaglia G, Zboril R, Salviulo G, Vianello F, et al. A glucose biosensor based on surface active maghemite nanoparticles. Biosens Bioelectron 2013; 45: 13-18.
27. Bonaiuto E, Magro M, Baratella D, Jakubec P, Sconcerla E, Terzo M, et al. Ternary Hybrid γ-Fe_2O_3/Cr^{VI}/Amine Oxidase Nanostructure for Electrochemical Sensing: Application for Polyamine Detection in Tumor Tissue. Chem-A Eur J 2016; 22: 6846-6852.
28. Magro M, Baratella D, Pianca N, Toninello A, Grancara S, Zboril R, et al. Electrochemical determination of hydrogen peroxide production by isolated mitochondria: A novel nanocomposite carbon-maghemite nanoparticle electrode. Sensors Actuators B Chem 2013; 176: 315-322.
29. Magro M, Baratella D, Salviulo G, Polakova K, Zoppellaro G, Tucek J, et al. Core-shell hybrid nanomaterial based on prussian blue and surface active maghemite nanoparticles as stable electrocatalyst. Biosens Bioelectron 2014; 52: 159-165.
30. Urbanova V, Magro M, Gedanken A, Baratella D, Vianello F, Zboril R, et al. Nanocrystalline Iron Oxides, Composites, and Related Materials as a Platform for Electrochemical, Magnetic, and Chemical Biosensors. Chem Mater 2014; 26: 6653-6673.

31. Magro M, Faralli A, Baratella D, Bertipaglia I, Giannetti S, Salviulo G, et al. Avidin Functionalized Maghemite Nanoparticles and Their Application for Recombinant Human Biotinyl-SERCA Purification. Langmuir 2012; 28: 15392-15401.
32. Magro M, Campos R, Baratella D, Ferreira MI, Bonaiuto E, Corraducci V, et al. Magnetic purification of curcumin from Curcuma longa rhizome by novel naked maghemite nanoparticles. J Agric Food Chem 2015; 63: 912-920.
33. Magro M, Moritz Denise Esteves, Bonaiuti E, Baratella D, Terzo M, Jakubec P, et al. Citrinin mycotoxin recognition and removal by naked magnetic nanoparticles. Food Chem 2016: 203: 505-512.
34. Magro M, Fasolato L, Bonaiuto E, Andreani NA, Baratella D, Corraducci V, et al. Enlightening mineral iron sensing in Pseudomonas fluorescens by surface active maghemite nanoparticles: Involvement of the OprF porin. Biochim Biophys Acta - Gen Subj 2016; 1860: 2202-2210.
35. Miotto G, Magro M, Terzo M, Zaccarin M, Da Dalt L, Bonaiuto E, et al. Protein corona as a proteome fingerprint: The example of hidden biomarkers for cow mastitis. Colloids Surf B Biointerfaces 2016; 140: 40-9.
36. Sinigaglia G, Magro M, Miotto G, Cardillo S, Agostinelli E, Zboril R, et al. Catalytically active bovine serum amine oxidase bound to fluorescent and magnetically drivable nanoparticles. Int J Nanomedicine 2012; 7: 2249-59.
37. Venerando R, Miotto G, Magro M, Dallan M, Baratella D, Bonaiuto E, et al. Magnetic Nanoparticles with Covalently Bound Self-Assembled Protein Corona for Advanced Biomedical Applications. J Phys Chem C 2013; 117: 20320-20331.
38. Magro M, Capos R, Baratella D, Lima G, Holà K, Divoky C, et al. A magnetically drivable nanovehicle for curcumin with antioxidant capacity and MRI relaxation properties. Chem - A Eur J 2014; 20: 11913-11920.
39. Magro M, Domeneghetti S, Baratella D, Jakubec P, Salviulo G, Bonaiuto E, et al. Colloidal Surface Active Maghemite Nanoparticles for Biologically Safe Cr^{VI} Remediation: from Core-Shell Nanostructures to Pilot Plant Development. Chem - A Eur J 2016; 22: 14219-14226.

40. Magro M, Sinigaglia G, Nodari L, Tucek J, Polakova K, Marusak Z, et al. Charge binding of rhodamine derivative to OH - stabilized nanomaghemite: Universal nanocarrier for construction of magnetofluorescent biosensors. Acta Biomate 2012;. 8: 2068-2076.

41. Handy RD, Henry TB, Scown TM, Johnston BD, Tyler CR. Manufactured nanoparticles: their uptake and effects on fish—a mechanis ic analysis. Ecotoxicology 2008; 17: 396-409.

42. Bour A, Mouchet F, Silvestre J, Gauthier L, Pinelli E. Environmentally relevant approaches to assess nanoparticles ecotoxicity: A review. J Hazard Mater 2015; 283: 764-777.

43. Vale G, Mehennaoui K, Cambier S, Libralato G, Jomini S, Domingos RF Manufactured nanoparticles in the aquatic environment-biochemical responses on freshwater organisms: A critical overview. Aquat Toxicol 2016; 170: 162-174.

44. Moore MN. Do nanoparticles present ecotoxicological risks for the health of the aquatic environment? Environ Int 2006; 32: 967-976.

45. Oberdörster E, Zhu S, Blickley TM, McClellan-Green P, Haasch ML. Ecotoxicology of carbon-based engineered nanoparticles: Effects of fullerene (C60) on aquatic organisms. Carbon N Y 2006; 44: 1112-1120.

46. Handy RD, Von der Krammer F, Lead JR, Hassellöy M, Owen R, Crane M. The ecotoxicology and chemistry of manufactured nanoparticles. Ecotoxicology 2008; 17: 287-314.

47. Asharani PV, Lian Wu Y, Gong Z, Valiyaveettil S. Toxicity of silver nanoparticles in zebrafish models. Nanotechnology 2008; 19: 255102.

48. Federici G, Shaw BJ, Handy RD. Toxicity of titanium dioxide nanoparticles to rainbow trout (*Oncorhynchus mykiss*): Gill injury, oxidative stress, and other physiological effects. Aquat Toxicol 2007; 84: 415-430.

49. Reeves JF, Davies SJ, Dodd NJF, Jha AN. Hydroxyl radicals (·OH) are associated with titanium dioxide (TiO_2) nanoparticle-induced cytotoxicity and oxidative DNA damage in fish cells. Mutat Res - Fundam Mol Mech Mutagen 2008; 640: 113-122.

50. Wise JP, Goodale BC, Wise SS, Craig GA, Pongan AF, Walter RB, et al. Silver nanospheres are cytotoxic and genotoxic to fish cells. Aquat Toxicol 2010; 97: 34-41.

51. Navarro E, Baun A, Behra R, Hartmann NB, Filser J. Miao AJ, et al. Environmental behavior and ecotoxicity of engineered nanoparticles to algae, plants, and fungi. Ecotoxicology 2008; 17: 372-386.

52. Ivask A, Kurvet I, Kasemet K, Balinova I, Aruoja V, Suppi S, et al. Size-dependent toxicity of silver nanoparticles to bacteria, yeast, algae, crustaceans and mammalian cells in vitro. PLoS One 20014; 9.

53. Vandebriel RJ, De Jong WH. A review of mammalian toxicity of ZnO nanoparticles. Nanotechnol Sci Appl 2012; 5: 61-71.

54. Matranga V, Corsi I. Toxic effects of engineered nanoparticles in the marine environment: Model organisms and molecular approaches. Mar Environ Res 2012; 76: 32-40.

55. Jovanović B, Palić D. Immunotoxicology of non-functionalized engineered nanoparticles in aquatic organisms with special emphasis on fish—Review of current knowledge, gap identification, and call for further research. Aquat Toxicol 2012; 118: 141-151.

56. Zhao J, Wang Z, Liu X, Xie X, Zhang K, Xing B. Distribution of CuO nanoparticles in juvenile carp (*Cyprinus carpio*) and their potential toxicity. J Hazard Mater 2011; 197: 304-310.

57. Kim S, Choi JE, Choi J, Chung KH, Park K, Yi J, et al. Oxidative stress-dependent toxicity of silver nanoparticles in human hepatoma cells. Toxicol Vitr2009; 23: 1076-1084.

58. Park EJ, Park K. Oxidative stress and pro-inflammatory responses induced by silica nanoparticles *in vivo* and *in vitro*. Toxicol Lett 2009; 184. 18-25.

59. Arora S, Jain J, Rajwade JM, Paknikar KM. Interactions of silver nanoparticles with primary mouse fibroblasts and liver cells. Toxicol Appl Pharmacol 2009; 236: 310-318.

60. Arora S, Jain J, Rajwade JM, Paknikar KM. Cellular responses induced by silver nanoparticles: In vitro studies. Toxicol Lett 2008; 179: 93-100.

Tables

Gene	Forward primer (5'- 3')	Reverse primer (5'- 3')	ZFIN ID
hnf4a	5'- ACGGTTCGGCGAGCTGCTTC-3'	5'-TCCTGGACCAGATGGGGGTGT-3'	ZDB-GENE- 030131-1077
sod1	5'-GTCGTCTGGCTTGTGGAGTG-3'	5'-TGTCAGCGGGCTAGTGCTT-3'	ZDB-GENE-990415-258
sod2	5'-CCGGACTATGTTAAGGCCATCT-3'	5'-ACACTCGGTTGCTCTCTTTTCTCT-3'	ZDB-GENE-030131-7742
gsta.1	5'-TTGAGGAAAAGGCCAAAGTG-3'	5'-AACACGGCCTTCACTGTTCT-3'	ZDB-GENE-040426-2720
rplp0	5'-CTGAACATCTCGCCCTTCTC-3'	5'-TAGCCGATCTGCAGACACAC-3'	ZDB-GENE-000629-1
actbl	5'-GGTACCCATCTCCTGCTCCAA-3'	5'-GAGCGTGGCTACTCCTTCACC-3'	ZDB-GENE-000329-1

Table 1. Primers sequences and ZFIN ID.

Gene	Forward primer (5'- 3')	Reverse primer (5'- 3')
hnf4a	5'- TTCTGAGCTGGAGGCAGTAGGC-3'	5'-GCCGATTCATAATGGTCAAATC-3'
CuZn/SOD	5'-CCATGGTAAGAATCATGGCGG -3'	5'-CGTGGATCACCATGGTTCTG -3'
Gst	5'-CCAGATGATCAGTACGTGAAGACCGTC -3'	5'-CTGCTGATGTGAGGAATGTACCGTAAC -3'
Ef1α	5'-AGTCCACCTCCACCGGTCAT -3'	5'-AGGAGCCCTTGCCCATCTC -3'
B actin	5'-GGTACCCATCTCCTGCTCCAA-3'	5'-GAGCGTGGCTACTCCTTCACC-3'

Table 2. Gilthead sea bream primers sequences.

Figures

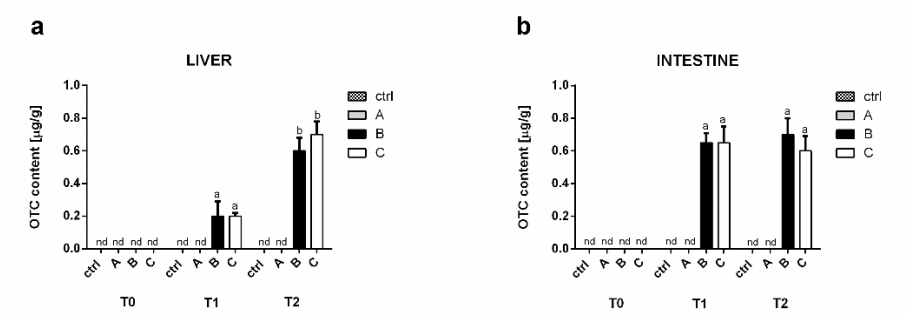

Figure 1. Mean OTC concentrations (expressed in µg/g of tissue weight) detected in zebrafish liver (a) and intestine (b) at the beginning (T0), after 8 (T1) and 24 (T2) hours of exposure. OTC content was measured in control group (ctrl), in fish tissues exposed to 100 mg/L of SAMNs (group A), in fish tissues exposed to 100 mg/L of SAMNs@OTC complex (group B) and in fish tissues exposed to 4 mg/L of OTC (group C). Samples where OTC concentration was absent or lower than the limit of detection were indicated as not detectable (nd). Different letters indicate statistically significant differences among experimental groups ($p < 0.05$). Values are presented as mean ± SD (n = 10).

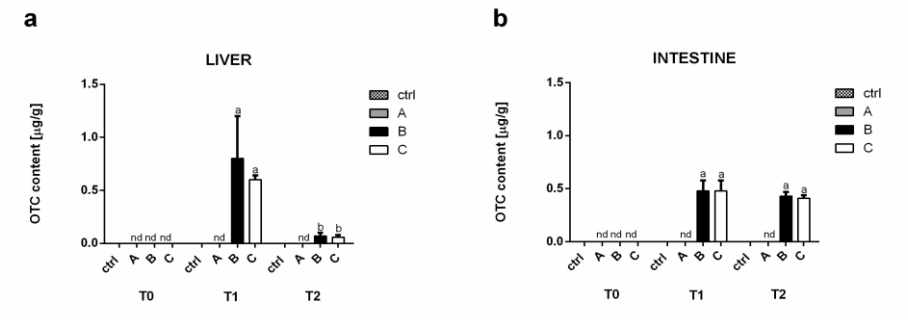

Figure 2. Mean OTC concentrations (expressed in µg/g of tissue weight) detected in gilthead sea bream liver portions (a) and intestine (b) at the beginning (T0), after 8 (T1) and 24 (T2) hours of exposure. OTC content was measured in control group (ctrl), in fish tissues exposed to 100 mg/L of SAMNs (group A), in fish tissues exposed to 100 mg/L of SAMNs@OTC complex (group B) and in fish tissues exposed to 4 mg/L of OTC (group C). Samples where OTC concentration was absent or lower than the limit of detection were indicated as not detectable (nd). Different letters indicate statistically significant differences among experimental groups ($p < 0.05$). Values are presented as mean ± SD (n = 10).

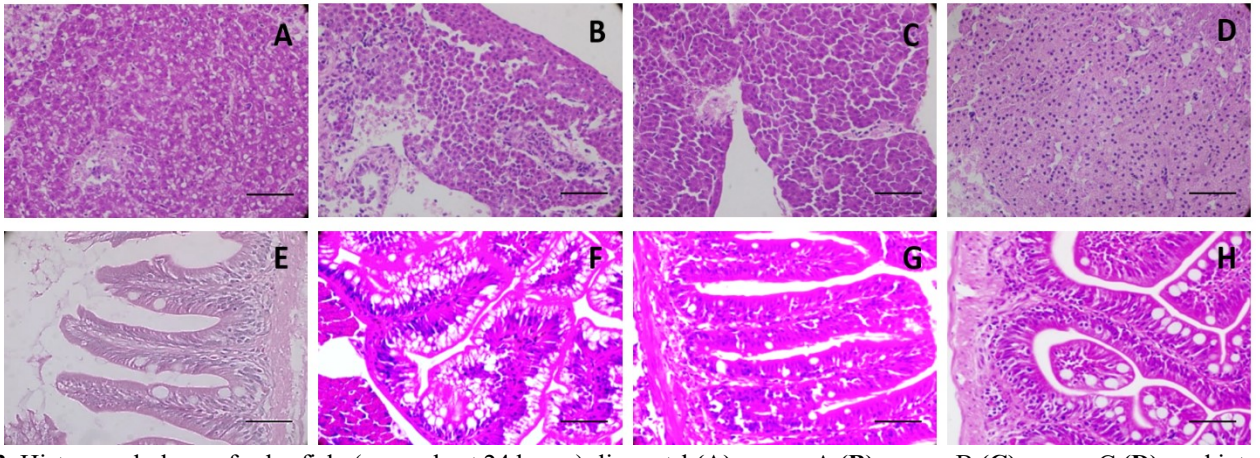

Figure 3. Histomorphology of zebrafish, (example at 24 hours): liver ctrl **(A)**, group A **(B)**, group B **(C)**, group C **(D)**; and intestine ctrl **(E)**, group A **(F)**, group B **(G)**, group C **(H)**. Scale bars: 50μm. Control group (ctrl), fish tissues exposed to 100 mg/L of SAMNs (group A), fish tissues exposed to 100 mg/L of SAMNs@OTC complex (group B) and fish tissues exposed to 4 mg/L of OTC (group C).

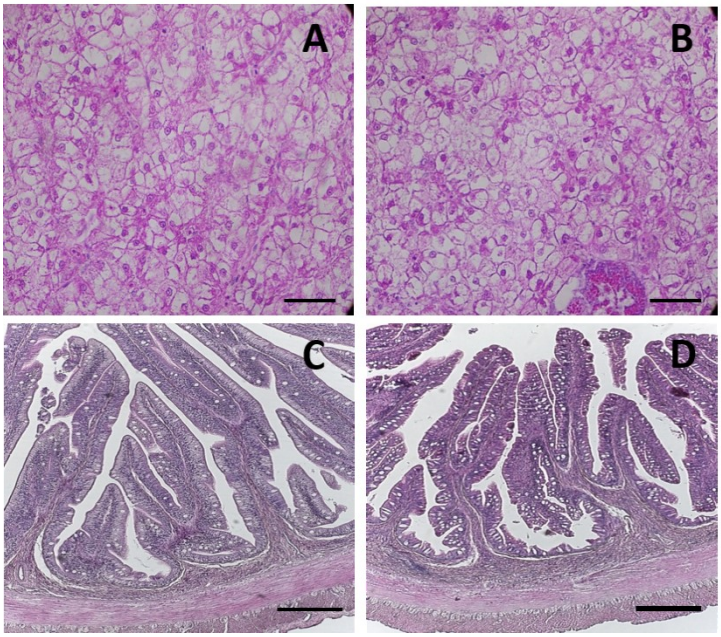

Figure 4. Histomorphology of gilthead sea bream, (example at 24 hours): liver ctrl **(A)**, an example of treated liver **(B)**, scale bars: 20 µm. Intestine ctrl **(C)**, an example of treated intestine **(D)**, scale bars: 100 µm. Control group (ctrl), treated tissues: fish tissues exposed to 100 mg/L of SAMNs (group A), to 100 mg/L of SAMNs@OTC complex (group B) and fish tissues exposed to 4 mg/L of OTC (group C).

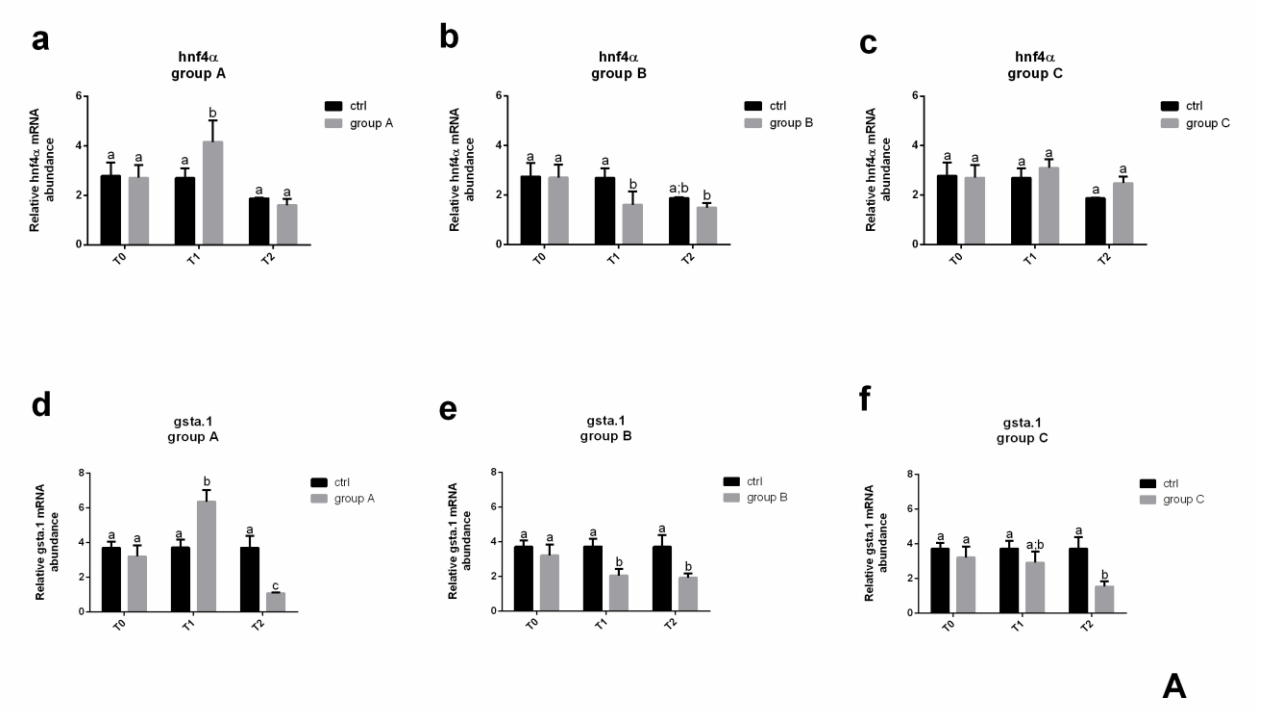

Figure 5. A. Relative mRNA levels of zebrafish genes involved in stress response and detoxification (*hnf4a* and *gsta.1*) analyzed in the liver at 0 (T0), 8 (T1), and 24 (T2) hours of exposure. *Hnf4a* and *gsta.1* expression was analyzed in control (ctrl) and group A (a, d), group B (b, e), and group C (c, f). Different letters indicate statistically significant differences among experimental groups (p <0.05). Values are presented as mean ± D (n = 5).

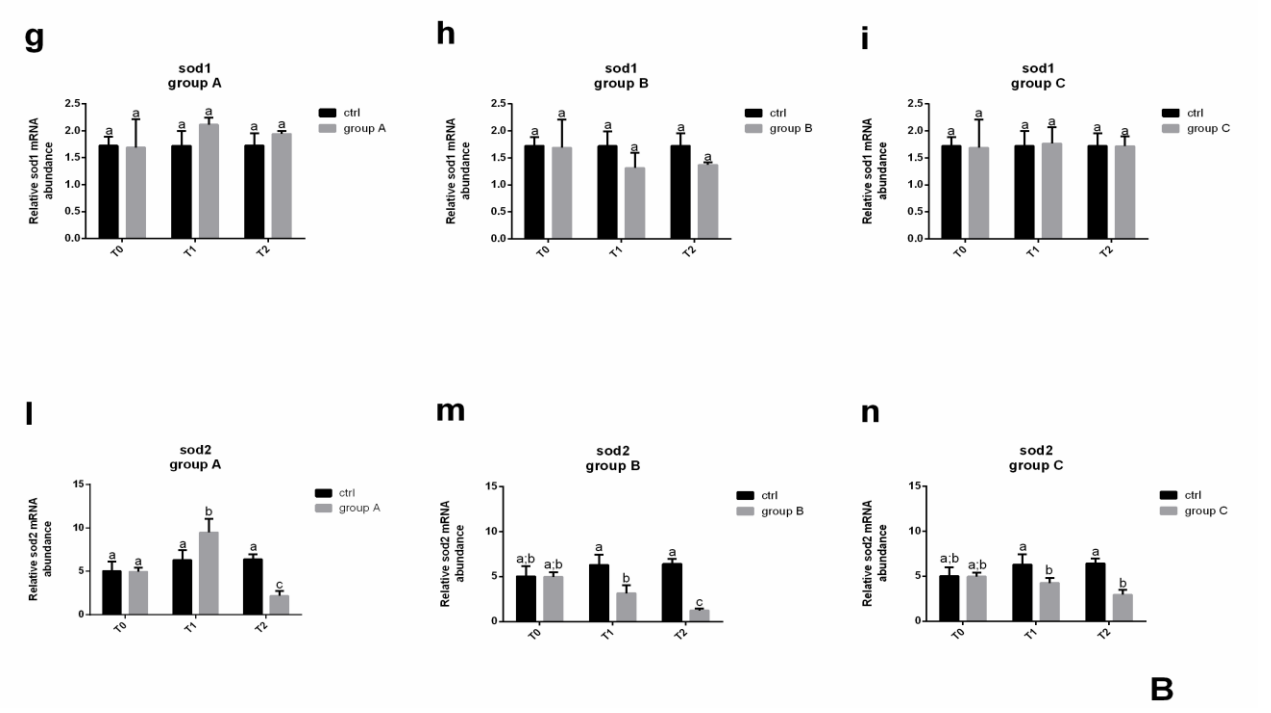

Figure 5. B. Relative mRNA levels of zebrafish genes involved in detoxification (*sod1*, *sod2*) analyzed in the liver at 0 (T0), 8 (T1), and 24 (T2) hours of exposure. *Sod1* and *sod2* expression was analyzed in control (ctrl) and group A (g, l); group B (h, m) and group C (i, n). Different letters indicate statistically significant differences among experimental groups (p <0.05). Values are presented as mean ± D (n = 5).

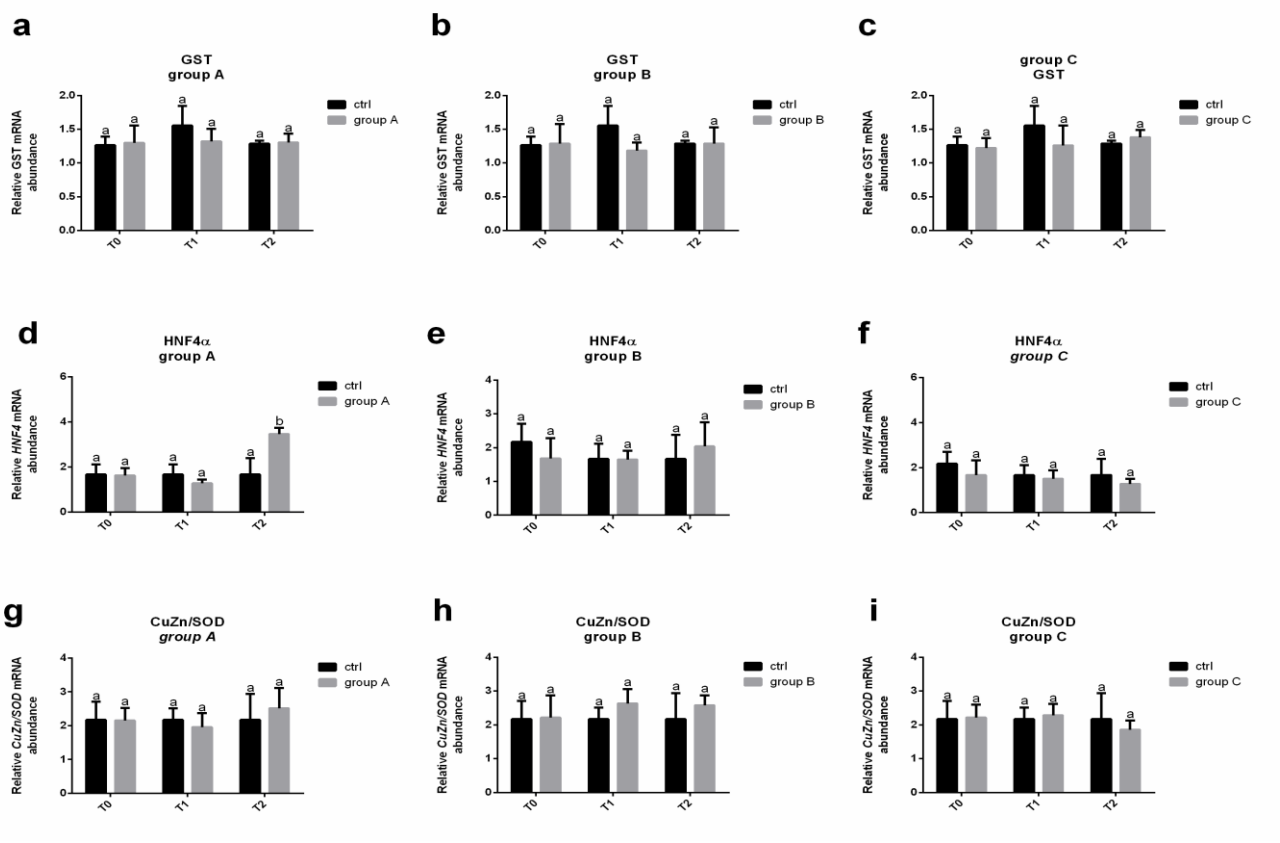
a
GST
group A
Relative GST mRNA abundance
ctrl
group A
T0
T1
T2
b
GST
group B
Relative GST mRNA abundance
ctrl
group B
c
group C
GST
Relative GST mRNA abundance
ctrl
group C
d
HNF4α
group A
Relative HNF4 mRNA abundance
e
HNF4α
group B
f
HNF4α
group C
g
CuZn/SOD
group A
Relative CuZn/SOD mRNA abundance
h
CuZn/SOD
group B
i
CuZn/SOD
group C

Figure 6. Relative mRNA levels of sea bream genes involved in stress response and detoxification (*GST*, *HNF4α* and *CuZn/SOD*) analyzed in the liver at 0 (T0), 8 (T1), and 24 (T2) hours of exposure. *GST*, *HNF4α* and *CuZn/SOD* expression was analyzed in control (ctrl) and group A (a, d, g), group B (b, e, h), and group C (c, f, i). Different letters indicate statistically significant differences among experimental groups ($p < 0.05$). Values are presented as mean ± D (n = 5). Control group (ctrl), fish exposed to 100 mg/L of SAMNs (group A), fish exposed to 100 mg/L of SAMNs@OTC complex (group B), and fish exposed to 4 mg/L of OTC (group C).

Chapter 4

A novel photocatalytic purification system for fish culture

Randazzo B, Chemello G, Tortarolo I, Chiarello GL, Zalas M, Santini S, Liberatore M, Liberatore M, Selli E, Olivotto I.

Zebrafish 2017, 14 (5): 411-421.

4.1 Introduction

One of the major negative aspects of fish culture practice is the untreated wastewater laden with uneaten feed and fish feces that might contribute to nutrient pollution[1,2,3]. These waters are particularly rich in organic compounds containing nitrogen, phosphorus, and of organic matter[2,4,5]. Organic nitrogen is potentially toxic to aquatic organisms, especially in its NH_3 form. Total ammonium nitrogen (TAN) derived from fish catabolism is the sum of NH_3 (ammonia) and NH_4^+ (ammonium ion). These two forms are in equilibrium in water with a relative preponderance of one or the other form depending on pH and temperature[6]. Ammonia represents the most toxic form for fish because of its lipophilic nature that allows its entrance through the biological membranes more easily with respect to the charged and hydrated NH_4^+ ions[7]. The main effect of ammonia exposure is the unbalance of the electrochemical gradients at the level of the central nervous system, while the ammonium ion, NH_4^+, results toxic for its capability of replacing the potassium ion K^+ in ionic transporters. Ammonium also plays a key role in inhibiting the formation of the outer protective mucus of the fishes and in acting an irritating factor for gills[8]. Although an ammonia concentration above 1.5 mg/L is considered toxic for most fishes, the toxicity threshold depends on several factors including the species and the size of the fish, the presence of surface-active compounds, nitrate, metal ions, as well as the temperature and the pH[9]. The acceptable level of unionized ammonia in aquaculture is usually fixed at only 0.025 mg/L[10,11]. Many fish culture facilities are “open-systems”, meaning that water is taken from a natural basin, is used in the tanks and finally restituted to the main water body. This system is very efficient in maintaining the water quality in the fish tanks; however, large amounts of water are used every day and discharged waters are rich in organic nutrients that may affect the aquatic environment. Therefore, alternative and proper means of disposal have to be

proposed before safely discharging these effluents into surrounding aquatic ecosystems. Consequently, nowadays closed recirculating systems are looked upon with great interest. In these systems, the same water is used for a long time because of the presence of a purification system which is usually composed of mechanical and biological units in addition to a sterilizer[6].

Biological filtration relies on the activity of specific bacteria that are able to convert ammonia to nitrite and subsequently to nitrate through a process named nitrification[12]. Nitrates are relatively non-toxic for aquatic organisms but at high concentration, they can affect fish growth[13,14,15,16]. Although at present the bacterial nitrification process is widely considered the most efficient method to convert ammonia into less toxic compounds, it still presents some disadvantages. First of all, closed recirculating systems need to undergo regular water exchange to maintain nitrates at an acceptable level[17]; secondly, biological filters require space since they need to offer a proper substrate (in terms of volume and surface) for bacterial proliferation, which is usually in relation to the water volume to treat. Furthermore, the nitrification process is affected by a variety of parameters such as substrate, dissolved oxygen concentration, organic matter, temperature, pH, alkalinity, salinity and turbulence level[18,11] with variability in the process effectiveness. Nevertheless, the desirable goal of fish culture industry is to find a method that converts TAN into non-toxic molecular nitrogen (N_2 gas), with an efficient removal of nitrogen from the aquatic system.

In the last few years, photocatalytic oxidation processes have received increasing attention in many fields [19,20]. Among the various photocatalytic oxides, titanium dioxide (TiO_2) represents the most advantageous active material for the degradation of water pollutants under ultraviolet irradiation [21,22], thanks to its low cost, chemical stability, and high photocatalytic activity [23,24,25].

In recent years, the TiO_2-assisted photocatalytic degradation process (PCD) has been showing promising results as an innovative single-step method for the removal of TAN (NH_4^+-NH_3)[26,27,28]. PCD is characterized by the production of $^{\bullet}OH$ radicals, which are very reactive and non-selective, leading to largely satisfactory results in the mineralization of organic pollutants to CO_2, water, and inorganic compounds, or in their partial degradation to less harmful and/or more biodegradable compounds. In particular, irradiation of a semiconductor oxide, such as TiO_2, leads to the formation a hole-electron pair because an electron is photopromoted from the semiconductor valence band to the conduction band. Hydroxyl anions (OH^-) and/or H_2O react with the electron deficient TiO_2 particles generating hydroxyl radicals ($^{\bullet}OH$), while $^{\bullet}O_2^-$ and other reactive oxygen species (ROS) are also produced, without any selective photocatalytic ability[29,30,31]. Ammonia conversion under UV irradiation in the presence of TiO_2 occurs in parallel and consecutive reaction steps with the formation of different products. The direct transformation to N_2 occurs in a path parallel to the main oxidation route, through a series of reactions that possibly involve the activated $(NH_2)_{ox}$ ammonia form[32]. Although photocatalytic treatments can transform ammonia into oxidized nitrogen-containing species such as nitrite and nitrate anions, Altomare and collaborators[33] demonstrated that ammonia can be selectively converted into N_2 under certain conditions in terms of pH, air bubbling rate, and TiO_2 structural features.

The new PCD based purification system proposed in this study has a small size and requires lower maintenance costs with respect to a classical biological/mechanical filtration system. To the best of our knowledge, no study has been conducted to verify the possible application of this photocatalytic purification system to zebrafish culture systems. Zebrafish (*Danio rerio*) is a widely used model for biomedical, developmental biology,

genetics, toxicology, and aquaculture studies[34], due to its high reproduction rate and to the abundant information that has recently become available from genomic sequencing.

The main goal of the present study was to investigate the efficiency of the proposed purification system in converting nitrogen-containing compounds, as well as to test possible biological effects that the contact with PCD-treated water has on a well-established experimental model such as zebrafish.

4.2 Materials and methods

4.2.1 Ethics

All procedures involving animals were conducted in line with the Italian legislation on experimental animals and were approved by the Health Ministry's Department of Veterinary Public Health and by the ethics committee of the Università Politecnica delle Marche (Authorization N° 641/2015-PR). Optimal rearing conditions (for details, see the Fish section) were applied throughout the study, and all efforts were made to minimize animal suffering by using an anesthetic (MS222; Sigma Aldrich).

4.2.2 Photoactive film deposition

All chemicals were purchased from Aldrich and used as received. A titania paste was prepared using an already described method[35], according to the following procedure. 3 g of TiO_2 powder (P25 Aeroxide, Evonik) were mixed with 0.5 mL of acetic acid and 20 mL of ethanol and kept in an ultrasonic bath for 3 h. A solution containing 1.5 g of ethyl cellulose and 10 mL of α-terpineol in 13.5 g of ethanol was prepared and then added to the former suspension. The mixture was sonicated for 1 h and then magnetically stirred overnight. Ethanol was slowly removed in a rotary evaporator and the obtained paste was ready-to-use. Titania films were deposited using the doctor blade technique

on stainless steel plates using a scotch tape mask of 62.5 μm thickness. Finally, the plates were calcined in oven with a heating ramp of 7.5 K/min up to 723 K for 2 h. Four plates were then inserted around a 36 W UVC (254 nm) lamp (Panaque©, Italy) at a 0.5 cm distance from the quartz bulb, as shown in Figure 1.

4.2.3 Purification/filtration unit

Control group. Control tanks (3 x 100 L) were equipped with an external biological/mechanical purification system (EHEIM© experience 250; flow rate: 700 L/h) and a 36 W UV sterilizer (Panaque©, Italy).

Test Group. Test group tanks (3 x 100 L) were equipped with an external mechanical purification system solely (EHEIM© experience 250; flow rate: 700 L/h) and a 36 W UVC sterilizer (Panaque©, Italy) equipped with four steel plates around the UV lamp (PCD filtration system, see Fig. 1).

4.2.4 Fish

Adult AB zebrafish were kept in a zebrafish system (Tecniplast, Varese, Italy) connected to the water line and kept at 28°C, 14L/10D photoperiod, alkalinity 120 mg/L $CaCO_3$, pH 7.0, NO_2^- and NH_3 < 0.03 mg/L and fed with a commercial pellet, protein 64%, lipids 12%, fiber 0.5%, crude ash 11%, and P total 1.4%. (BlueLine, Italy) twice daily (2% body weight) for one month. The experiment started after this first period of acclimation.

4.2.5 Experimental design

Adult zebrafish (300 animals) were kept in six tanks (100 L) divided into two experimental groups each of 150 fish (50 fish per tank) and exposed to the following conditions for 14 days:

Control group: 3 x 100 L tanks containing 50 fish each and equipped with a classical mechanical, biological, and UV purification system (Panaque, Italy) (28°C, 14L/10D photoperiod);
Test group: 3 x 100 L tanks containing 50 fish each and equipped with a PCD purification system (for details see the Purification/filtration unit section) (28°C, 14L/10D photoperiod).
Samplings were performed at 0, 7 and 14 days after the beginning of the treatment (T0, T1, and T2). The fish were collected and anesthetized with a lethal dose of MS222 (1 g/L) (Sigma-Aldrich). Liver, digestive tract, and gills were sampled and properly stored for further analysis. In addition, water samples (30 mL in three replicates) were collected from all tanks each day from the beginning of the experiment to determine the amount of NH_3, NO_2^-, and NO_3^- during the experiment, as well as temperature and pH.

4.2.6 Determination of pH and nitrogen compounds during the fish trial

Water sampling was performed twice a day before the administration of food and reported as mean value. A Jenway (Staffordshire, UK) 3510 pH-meter was used for pH measurement; instrument calibration was carried out with standard solutions at pH 7 and 4, and the measurements were done immediately after calibration.
TAN (NH_4^+/NH_3) was determined by means of a digital photometer NANOCOLOR® 500 D (Macherey-Nagel) using dedicated commercial tests (CM 0985-003), exploiting the indophenol blue reaction, with a detection range of 0.05-300 mg/L NH_4^+ and measurement at 690 nm.
An UV/Vis spectrophotometer mod. 6705 from Jenway (Staffordshire, UK) with a 1.0 cm quartz cell was used to evaluate the concentration of nitrate and nitrite anions. Each measurement was performed in triplicate for each sampling point.

The concentration of nitrite anions was determined with the procedure reported by Bendschneider and Robinson[36]. Briefly, the sample under acid conditions (super pure HCl, 34-37% Romil, Cambridge, UK) was mixed with sulphanilamide ($C_6H_8N_2O_2S$ purity ≥99.9%, Carlo Erba Milan, Italy) to form a diazo compound that then couples with N-(1-naphthyl)-ethylendiamine ($C_{10}H_7NHCH_2CH_2NH_2 \cdot 2HCl$, purity ≥ 99.9%, Carlo Erba, Milan, Italy) to form a reddish purple azo dye that was determined spectrophotometrically at 540 nm. The standard stock solution of nitrite ions was prepared by dissolving 138 mg of $NaNO_2$ (purity ≥99.9% from J.T. Baker, Phillipsburg, New Jersey) in ultrapure water (Milli-Q from Millipore, Bedford, MA, USA) in a 1000 mL volumetric flask. Working solutions were prepared daily by appropriated dilution of the standard solution; the calibration curve method was used for quantification.

Nitrate concentration in the sample was determined under acidic conditions after addition of 1 mol/L of HCl, by direct measurement of UV light absorption at 220 nm[37]. The standard stock solution of nitrate was prepared by dissolving 1.300 g of KNO_3 (purity ≥ 99.9 from Sigma Aldrich, Saint Louis, Missouri) in Milli-Q water (Millipore) in 1000 mL volumetric flask. Working solutions were prepared daily by appropriate dilution of the standard solution; the calibration curve method was used for quantification.

4.2.7 Histological analysis and TUNEL assay

At each sampling time, T0, T1, and T2, 10 fish from each of the six tanks (30 from the three control tanks and 30 from the three test group tanks) were randomly collected for histological analysis. Intestine and gills were removed, fixed were fixed by immersion in 4% paraformaldehyde (PFA 4%) and stored at 4°C overnight. Samples were then washed in PBS 1X, dehydrated in an ethanol series and embedded in paraffin. Slides of 4 μm section were stained

with Mayer's hematoxylin and eosin stain and examined under photomicroscope (Olympus Vanox photomicroscope, Japan).

After paraffin-processing, 4 µm sections from intestine and gills were mounted on aminopropyltriethoxysilane (APES)-treated slides and used for TUNEL assay (terminal deoxynucleotidyl transferase [TdT]-mediated deoxyuridine triphosphate [dUTP] nick end labeling) performed with a Roche© Molecular Biochemicals *In Situ* Cell Death Detection Kit. A TUNEL-negative control was obtained by omitting TdT from the labeling mix, and TUNEL specificity was checked by comparing labeling with cellular morphology. Briefly, after rehydration, sections were postfixed with PFA 4% and washed in 3% bovine serum albumin (BSA) and 20% normal bovine serum in PBS. Digestion was performed by mean of proteinase K (Roche Molecular Biochemicals) used at 20 µg/mL in PBT for 15 min at room temperature in a wet chamber. Incubation of sections with (TdT) in reaction buffer (containing a fixed concentration of digoxigenin-labeled nucleotides dUTP) was performed overnight at 4°C. After washing in PBS and treating with blocking solution (TBS 0.1 M, 3% BSA, 20% sheep serum), sections were incubated in a staining buffer (0.1 M Tris-HCl, pH 8.2) with prediluted alkaline phosphatase provided as Fast Red chromogen (Roche©) and the identification and quantification of apoptotic cells in tissue sections was immediately evaluated under optical photomicroscope.

4.2.8 RNA extraction and cDNA synthesis

Total RNA extraction from single zebrafish livers (10 replicates randomly collected at each sampling time from both control and test group) was optimized using the RNeasy_Minikit (Qiagen, Italy) following the manufacturer's protocol. Total RNA extracted was eluted in 20 µl RNase-free water (Qiagen, Italy). Final RNA concentration was determined by the

NanoPhotometer P-Class (Implen, Germany). RNA integrity was verified by ethidium bromide staining of 28S and 18S ribosomal RNA bands on 1% agarose gel. RNA was stored at -80°C until use. Total RNA was treated with DNAse (10 IU at 37°C for 10 min; MBI Fermentas). Then, 3 µg RNA were used for cDNA synthesis with the iScript cDNA Synthesis Kit (Bio-Rad) following the manufacturer's instructions.

4.2.9 Real-Time PCR

PCRs were performed with SYBR Green in an iQ5 iCycler thermal cycler (both from Bio-Rad), in triplicate. Reactions were set on a 96-well plate by mixing, for each sample, 1 µL cDNA diluted 1:20, 5 µL of 2x concentrated iQ TM SYBR Green Supermix containing SYBR Green as the fluorescent intercalating agent, 0.3 µM forward primer, and 0.3 µM reverse primer. The thermal profile for all reactions was 3 min at 95°C, followed by 45 cycles of 20 s at 95°C, 20 s at 60°C, and 20 s at 72°C. Fluorescence was monitored at the end of each cycle. Dissociation curve analysis showed a single peak in all cases.

Relative quantification of the expression of genes involved in fish stress response (*nr3c1*, *gsta.1*, *gsr*, *gpx1a*, *hsp70.1*, *hnf4a*) and oxidative stress (*sod1*, *sod2, cat*) was performed using *rplp0* and *ef1-α* as housekeeping genes to standardize the results (Table 1). Amplification products were sequenced, and homology was verified. No amplification product was detected in negative controls and no primer-dimer formation was found in control templates. Data were analyzed using the iQ5 optical system software version 2.0, including Genex Macro iQ5 Conversion and Genex Macro iQ5 files (all from Bio-Rad). Modification of gene expression is reported with respect to controls. Primer sequences were designed using Primer3 (210 v. 0.4.0) starting

from ZF sequences available in ZFIN. Primers were used at a final concentration of 10 pmol/μL.

4.2.10 Statistical analysis

Nitrogen-containing compounds are expressed as mean value ± s.d. (n=3) and, together with real-time PCR data, were analyzed by two-way ANOVA analysis of variance, followed by Tukey's post-test. The statistical software package Prism5 (GraphPad Software) was used for analyses. Significance was set at $p < 0.05$.

4.3 Results

4.3.1 Photocatalytic Results

The pH values remained almost constant during the whole experiment in both control and test group tanks, slightly fluctuating between 8.0 and 8.2.

The ammonia, nitrite and nitrate concentration of the control tanks and of test group (equipped with the photocatalytic system) tanks are presented in Fig. 2. Three photocatalytic phases can be distinguished for both groups with significant differences: *i*) from day 0 to day 7; *ii*) from day 7 to day 12, and *iii*) from day 12 to day 14. In the first photocatalytic activity phases (*i.e*. up to day 7), ammonia nitrogen (NH_4^+/NH_3) remained at very low levels and dropped below the detection limit after the 3rd and the 4th day in test group and control tanks, respectively. The decrease of ammonia concentration was followed by a transient formation of nitrite anions. Indeed, in test group tanks, the NO_2^- concentration significantly increased up to 2.0 ± 0.17 mg/L during the first 4 days of the experiment and then suddenly decreased to very low values (0.015 ± 0.002 mg/L) up to the end of the experiment. Moreover, the presence of nitrate was detected already from the 1st day. By contrast, in control group the nitrite ion concentration reached lower values (0.4 ± 0.17

mg/L on the 4th day), whereas the nitrate ion appeared only after the 5th day. After day 7, *i.e.* in the photocatalytic activity phase, both ammonia and nitrite concentrations dropped down to values close to 0 mg/L, whereas the nitrate ion concentration remained below 10 mg/L. The most surprising and important result in using the photocatalytic system was achieved starting from day 12 (third activity region). Indeed, while the nitrate concentration in the control tanks suddenly increased up to 56.6 ± 5.7 mg/L, in the photocatalytically treated tanks a six-fold lower concentration was retained (8.0 ± 1.0 mg/L).

4.3.2 Histology and TUNEL assay

Tissue integrity was evaluated considering the general histological aspect of gills and intestine. No alterations were observed in the gills of control group sampled at T1 and T2 (Fig. 3a, b). However, test group gills showed vessels congestion at the base of the secondary lamellae and occasionally oedema at T1, hence in correspondence of NO_2^- accumulation (Fig. 3c, d, e). Histological alterations were not observed in test group at T2 (Fig. 3f). Considering the intestinal morphology, both experimental groups did not show alteration of folds morphology or signs of inflammation during the whole experiment (data not shown).

Apoptosis was evaluated in terms of DNA fragmentation using a Roche *In Situ* Cell Death Detection Commercial Kit. At T1, gills of control group did not show apoptotic cells (Fig. 4a), while test group showed a high number of TUNEL-positive cells in the secondary lamellae (Fig. 4c). Finally, at T2 both groups did not show any sign of DNA fragmentation (Fig. 4b, d).

4.3.3 Real-time PCR results

Real-time PCR analysis were performed on genes involved in general stress response (*nr3c1, gsta.1, gsr, gpx1a, hsp70.1, hnf4a*) and oxidative stress (*sod1*, *sod2, cat*).

Stress and detoxification stress markers

Considering the genes involved in stress response, it was evident that most of the differences among control and test group were detectable at T1. In particular at T1, a significantly higher gene expression ($p < 0.05$) was evidenced in test group with respect to control for *nr3c1*, *gsr*, *hsp70.1*, *hnf4a* and *sod2* (Fig. 5a, c, e, f, h). The remaining genes did not show any significant difference ($p > 0.05$) with respect to the control group at this sampling time (Fig. 5b, d, g, i). Considering T2, only *gsta.1, sod1*, and *hsp70.1* gene expression was significantly ($p < 0.05$) lower in test group compared to control group (Fig. 5b, e, g). Finally, *nr3c1*, *gpx1a,* and *hnf4a* did not show any significant difference with respect to control at this sampling time (Fig. 5a, d, f).

4.4 Discussion

Long-term growth of the aquaculture industry requires both ecologically sound practices and sustainable resource management. Such practices can be encouraged by mandating treatment and recirculation of wastewater[38,39]. Despite significant improvements in the industry, a considerable distance remains between ecologically sound technologies on the shelf and those actually implemented in the field. At present, fish culture is mainly based on open or recirculating systems, both of which produce large amounts of discharged waters rich in organic nutrients that may affect the aquatic environment.

For this main reason, the desirable goal of the fish culture industry is to find a method that efficiently removes TAN from the water, reducing wastewater production over the time.

A number of new approaches, including physical, chemical and biological treatments for wastewater purification have been investigated. For example, ultralow-pressure polyethersulfone (PES) membranes were found to exert excellent performances in terms of reduction of total ammonium[40]. Moreover, nearly emission-free aquaponics systems have proved to be useful in transforming fish nitrogen compounds in an organic food source for the growing plants, with the plants providing a natural filter for the water[41,42]. Despite this, the efficiency of these different categories of treatment is questionable because of maintenance costs and/or efficiency over the time[43]. The present study investigated for the first time the possible application of a novel photocatalytic purification system, useful in recirculating systems in reducing water replacement and thus management costs.

Photocatalytic oxidation processes can be considered as a novel and unconventional way to purify water from TAN in a single-step process[44,45]. It is presently one of the most advantageous systems because of its low cost, chemical stability, and high photocatalytic activity[25,26]. In the present study, the photocatalytic system showed excellent performances in reducing nitrogen compounds produced by a constant bio-load of fish and its ideal safe placement is after the mechanical/biological filtration.

Zebrafish is a widely used model for biomedical, developmental biology, genetics, toxicology, and aquaculture studies[34], due to its high reproduction rate and to the abundant information that has recently become available from genomic sequencing. As a consequence, results obtained in the present study may be useful for both aquarium fish systems and the aquaculture industry

As described in the results section, three photocatalytic activity areas were detected. The first one was characterized by the prevalent photocatalytic conversion of NH_4^+/NH_3 in NO_2^- anions at least until the 4th day of experimentation. At this time NO_2^- was significantly higher than the suggested value for aquaculture systems. This transitory condition is a consequence of TAN partial oxidation into nitrite ions, which occurs at a higher rate under photocatalytic conditions with respect to the classical purification treatment.

In the second activity phase, both ammonia and nitrite concentrations dropped down to values close to 0 mg/L, whereas the nitrate concentration remained below 10 mg/L. In the last photocatalytic activity phase the most interesting result was obtained: NO_2^- and NO_3^- were still close to 0 mg/L while NO_3^- was six folds lower with respect to the control group, underlining the efficiency of the present system.

These results suggest that TAN continuously produced in the tanks undergoes photoinduced oxidation on the photocatalyst surface starting from the very beginning of the experiment (first activity region). Full ammonia oxidation up to nitrate proceeds through nitrite formation as intermediate species, according to the following consecutive reactions scheme[32,33]:

$$NH_3 \xrightarrow{O_2 + h\nu} NO_2^- \xrightarrow{O_2 + h\nu} NO_3^-$$

As shown in Fig. 2, the amount of nitrite ions accumulated under photocatalytic conditions is higher with respect to that accumulated in the tank under control experiments. After this period, steady-state conditions are probably reached, and the further produced TAN does not accumulate in water anymore. One possibility is that TAN undergoes a redox reaction with nitrite ions according to the following thermodynamically allowed process:

$$NH_4^+ + NO_2^- \rightarrow N_2 + H_2O$$

By this reaction, TAN is transformed into innocuous gas phase dinitrogen. Nitrogen oxides are other possible gas-phase products of the photocatalytic process, also leading to the removal of nitrogen-containing compounds from the aqueous phase. The higher transient concentration of nitrite ions obtained by photocatalytic treatment ensures the overall transformation of almost all TAN subsequently produced in the aqueous-phase into gas-phase nitrogen-containing products, with its consequent removal from water. This explains why the amount of nitrate ions accumulating in water at the end of the test was much higher in classically treated tanks with respect to the photocatalytically treated ones[46]. These nitrate ions are produced from full oxidation of the TAN persisting in the aqueous phase, which was much lower in the photocatalytically treated tanks. Indeed, an almost constant nitrate ion concentration below 10 mg/L was attained in this case and no sudden rise of nitrate ion concentration after day 12 was observed, which was observed instead in control tanks.

It should be pointed out that the present photocatalytic system was characterized by the production of reactive oxygen species (ROS) and in particular $^{\bullet}OH$ radicals. These radicals react indiscriminately with virtually all organic molecules[47]. Any process that leads to increased ROS production in recirculating systems, either directly, or indirectly *via* organic radical formation or other mechanisms, can potentially be harmful for living organisms[48]. Consequently, it is obvious to hypothesize that the exposure of a living organism such as zebrafish to ROS can lead to the activation of different stress/antioxidant pathways. While at T1 a general overexpression of most of the genes involved in both generic stress response (*nr3c1, gsr*, *hsp70.1*, *hnf4α*) and oxidative stress (*sod2*) was observed in test group with respect to control, at T2 only oxidative stress markers (*sod2*, *cat*) were still significantly higher in test group with respect to control. On the contrary, general stress markers

reached normal values. These results could be related to the different chemical activity phases observed during the experiment rather than to a possible direct ROS involvement. Accumulation of NO_2^- is known to impact the well-being of fish, specifically by changing the balance of intra- and extracellular electrolytes, which causes damage to liver cell mitochondria and repression of the immune system [49,50]. While one of the main toxic effects of nitrite exposure in fish is hypoxia, at a histological level hyperplasia, hypertrophy, vacuolization and an increase in numbers of chloride cells are the main alterations that can be observed in the gills[51,52]. These alterations are usually coupled with an increase in haematocrit, red blood cells count and in haemoglobin concentration.

While no histological changes were generally observed in the gills of control group, test group gills showed vessels congestion at the base of the secondary lamellae and occasionally oedema, suggesting a possible involvement of NO_2^-. This result was in agreement with the TUNEL assay which showed an increase of apoptotic activity only in test group samples at T1. The involvement of NO_2^- in this first phase is also supported by the fact that these negative effects observed in fish were no more evident in the same experimental group in the last activity region (14 days) of the experiment in which all nitrogen concentrations dropped to desirable levels. These data are supported also by molecular results that showed that general stress markers reached normal values at this time. However, at this same time oxidative stress markers were still significantly higher with respect to control. This result was not obvious but suggested a possible ROS exposure of the fish. In fact, it is well established that fish facing ROS activate the antioxidant defenses that mainly include superoxide dismutase (SOD1 and SOD2), catalase and glutathione peroxidase[46].

Finally, considering nitrates at the end of the experiment, their values were six folds lower in tanks equipped with a photocatalytic purification unit with respect to control, underlying the efficiency of the PCD system in TAN removal. Toxicity of nitrates to fish has been traditionally considered to be irrelevant and usually physiological effects can only be observed after a long period of exposure[53,54]. In fact, it is known that fish can chronically be exposed to NO_3^- levels up to 70 mM (1000 mg N/L). Uptake of NO_3^- via the gills is low compared to that of ammonia and nitrite due to an apparently low branchial permeability for NO_3^- [55]. However, chronic exposure to high NO_3^- can lead to reduced feed intake and growth[56]. Because of the short experimental period of the present study (14 days), no effects on molecular growth markers were detectable.

Overall, the photocatalytic purification system proposed in the present study showed excellent performances in removing TAN from the tank water with no significant adverse effects on the cultured fish. This purification system has both the potentiality to be applied to recirculating systems (helping in saving water and reducing costs for the facility) and as a wastewater treatment system in aquaculture facilities, reducing environmental impacts. The reduction of nitrate in a recirculating system is desirable but may have some undesired side effects. Nitrates are often considered as an "Indicator Species" for all pollutants, representing an important overall readout of the pollutant equilibrium. As a consequence, the strong reduction of nitrate by the photocatalytic purification unit may make it harder to accurately gauge the level of water contamination in a recirculating system, and thus a water exchange program should be developed through further studies to assure optimal rearing water quality conditions. Finally, further studies should evaluate the performances of the present purification unit over a longer period

of time (i.e. years) to better understand if ROS formation may have adverse effects on fish.

References

Brune DE, Schwartz G, Eversole AG, Collier JA, Schwedler TE. Intensification of pond aquaculture and high rate photosynthetic systems. Aquac Eng 2003; 28: 65-86.

Piedrahita RH. Reducing the potential environmental impact of tank aquaculture effluents through intensification and recirculation. Aquaculture. 2003; 226: 35-44.

Gutierrez-Wing MT, Malone RF. Biological filters in aquaculture: trends and research directions for freshwater and marine applications. Aquac Eng 2006; 34: 163-171.

Sugiura SH, Marchant DD, Wigins T, Ferraris RP. Effluent profile of commercially used low-phosphorus fish feeds. Environ Pollut 2006; 140: 95-101.

Read P, Fernandes T. Management of environmental impacts of marine aquaculture in Europe. Aquaculture 2003; 226: 139-163.

Timmons MB, Ebeling JM, Wheaton FW, Summerfelt ST, Vinci BJ. Recirculating aquaculture systems, 2nd edition. NRAC Publication, vol. 01-002. 2002.

Körner S, Das SK, Veenstra S, Vermaat JE. The effect of pH variation at the ammonium/ammonia equilibrium in wastewater and its toxicity to *Lemna gibba*. Aquat Bot 2001; 71: 71-78.

Randall DJ, Tsui TKN. Ammonia toxicity in fish. Mar Pollut Bull 2002; 45: 17-23.

Colt J. Water quality requirements for reuse systems. Aquac Eng 2006; 34: 143-156.

Neori A, Chopin T, Troell M, Buschmann AH, Kraemer GP, Halling C, Shpigel M, Yarish C. Integrated aquaculture: rationale, evolution and state of the art emphasizing seaweed biofiltration in modern mariculture. Aquaculture 2004; 231: 361-391.

Chen S, Ling J, Blancheton JP. Nitrification kinetics of biofilm as affected by water quality factors. Aquac Eng 2006; 34: 179-197.

Killham K. Heterotrophic nitrification, p. 117–126. In J. I. Prosser (edn), Nitrification. IRL Press, Oxford. 1986.

Kamstra A, van der Heul JW. The effect of denitrification on feed intake and feed conversion of European eel *Anguilla anguilla* L. In Grizel, H, Kestermont P

(eds.), Aquaculture and Water: Fish Culture, Shellfish Culture and Water Usage. European Aquaculture Society Special Publication no. 26, Oostende, Belgium, pp. 128-129 1998.

Hyrayama K. Influences of nitrate accumulated in culturing water on Octopus vulgaris. Bull Jpn Soc Sci Fish 1966; 32: 105-111.

Berka R, Kujal B, Lavicky J. In Recirculating systems in Eastern European Proceeding World Symposium on Aquaculture in Heated Effluents and Recirculation Systems vol. 2, Stavanger, 28 Berlin, 1980.

Muir PR, Sutton DC, Owens L. Nitrate toxicity to *Penaeus monodon* protozoea. Mar Biol 1991; 108: 67-71.

Masser MP, Rakocy J, Losordo TM. Recirculating aquaculture tank production systems - management of recirculating systems. SRAC Publication, vol. 452. 1999.

Satoh H, Okabe N, Watanabe Y. Significance of substrate C/N ratio on structure and activity of nitrifying biofilms determined by in situ hybridization and the use of microelectrodes. Water Sci Technol 2000; 41: 317-321.

Seyedjamali H, Pirisedigh A. In situ sol-gel fabrication of new poly(amide-ether-imide)/titania (TiO_2) nanocomposite thin films containing L-leucine moieties. Colloid Polym Sci 2011; 289: 15-20.

Sun D, Sun W, Yang W, Li Q, Shang JK. Efficient photocatalytic removal of aqueous NH_4^+/NH_3 by palladium-modified nitrogen-doped titanium oxide nanoparticles under visible light illumination, even in weak alkaline solutions. Chem Eng J 2015; 264: 728-734.

Linsebigler AL, Lu GQ, Yates JT. Photocatalysis on TiO_2 surfaces - principles, mechanisms, and selected results. Chem Rev 1995; 95(3): 735-758.

Fujishima A, Zhang XT, Tryk DA. TiO_2 photocatalysis and related surface phenomena. Surf Sci Rep 2008; 63(12): 515-582.

Ohko Y, Ando I, Niwa C. Degradation of bisphenol A in water by TiO_2 photocatalyst. Environ Sci Technol 2001; 35: 2365-2368.

Dozzi MV, Saccomanni A, Selli E. Cr(VI) photocatalytic reduction: effects of simultaneous organics oxidation and of gold nanoparticles photodeposition on TiO_2. J. Hazard Mater 2012; 211-212, 188-195.

Daghrir R, Drogui P, Robert D. Modified TiO_2 for environmental photocatalytic applications: A review. Ind Eng Chem Res 2013; 52: 3581-3599.

Luo X, Chen C, Yang J, Wang J, Yan Q, Shi H, Wang C. Characterization of La/Fe/TiO_2 and its photocatalytic performance in ammonia nitrogen wastewater. Int J Environ Res Public Health 2015; 12(11): 14626-14639.

Vohra MS, Selimuzzaman SM, Al-Suwaiyan MS. NH_4^+-NH_3 Removal from simulated wastewater using UV-TiO_2 photocatalysis: Effect of co-pollutants and pH. Environ Technol 2010; 31(6): 641-654.

Zhu X, Nanny MA, Butler EC. Photocatalytic oxidation of aqueous ammonia in model gray waters, Wat Res 2008; 42(10): 2736-2744.

Turchi CS, Ollis DF. Photocatalytic degradation of organic water contaminants: Mechanisms involving hydroxyl radical attack. J Catal 1990; 122: 178-192.

Mrowetz M, Selli E, Enhanced photocatalytic formation of hydroxyl radicals on fluorinated TiO_2, Phys Chem Chem Phys 2005; 7: 1100-1102.

Jie W, Guo CJ. Photocatalysis degradation of inorganic nitrogen. Water Sci Tech Inf Dev Econ 2005; 15: 173-175.

Altomare M., Chiarello GL, Costa A, Guarino M, Selli E. Photocatalytic abatement of ammonia in nitrogen-containing effluents. Chem Eng J. 2012; 191: 394-401. Altomare M, Selli E. Effects of metal nanoparticles deposition on the photocatalytic oxidation of ammonia in TiO_2 aqueous suspensions. Cat Tod 2013; 209: 127-133.

Chemello G, Piccinetti C, Randazzo B, Carnevali O, Maradonna F, Magro M, *et al*. Oxytetracycline delivery in adult female zebrafish by iron oxide nanoparticles. Zebrafish 2016; 13(6): 495-503.

Sobuś J, Kubicki J, Burdziński G, Ziółek M. Carbazole dye-sensitized solar cells studied from femtoseconds to seconds - Effect of additives in cobalt- and iodide-based electrolytes. Chem Sus Chem 2015; 8(18): 3118-3128.

Bendshneider K, Robinson RJ. A new spectrophotometric method for the determination of nitrite in seawater. J Mar Res 1952; 11: 87-96.

Takeda K, Fujiwara K. Determination of nitrate in natural waters with photo-induced conversion of nitrate and nitrite. Anal Chim Acta 1993; 276: 25-32.

Cao L, Wang W, Yang Y, Yang C, Yuan Z, Xiong S, Diana J. Environmental impact iof aquaculture and countermeasures to aquaculture pollution in China. Environ Sci Pollut Res Int 2007; 14(7): 452-462.

Antelo LT, Lopes C, Franco-Uría A, Alonso AA. Fish discards management: pollution levels and best available removal techniques. Mar Pollut Bull 2012; 64(7): 1277-1290.

Nora'aini A, Mohammad AW, Jusoh A, Hasan MR, Ghazali N, Kamaruzaman K. Treatment of aquaculture wastewater using ultra-low pressure asymmetric polyethersulfone (PES) membrane. Desalination 2005; 185: 317-326.

Reyes LD, Slinkert T, Cappon HJ, Baganz D, Staaks G, Keesman KJ. Model of an aquaponic system for minimised water, energy and nitrogen requirements. Water Sci Technol 2016; 74(1): 30-7.

Nozzi V, Parisi G, Di Crescenzo D, Giordano M, Carnevali O. Evaluation of *Dicentrarchus labrax* meats and the vegetable quality of *Beta vulgaris* var. *cicla* farmed in freshwater and saltwater aquaponic systems. Water 2016; 8: 423.

Camargo JA, Alonso A. Ecological and toxicological effects of inorganic pollution in aquatic ecosystems: A global assessment. Environ Int 2006; 32(6): 831-839.

Kamat PV. Photochemistry on nonreactive and reactive (semiconductor) surfaces. Chem Rev 1993; 93(1): 267-300.

Hoffman MR, Martin ST, Choi W, Bahnemann DW. Environmental application of semiconductor photocatalysis. Chem Rev 1995; 95: 69-96.

Lee DK, Cho JS, Yoon WL. Catalytic oxidation of ammonia: why is N_2 formed against preferentially against NO_3^-? Chemosphere 2005; 61(4): 573-578.

Farhataziz PC, Ross AB, Selective specific rates of reactions of transients in water and aqueous solutions. Part III. Hydroxyl radical and perhydroxyl radical and their radical ions, Natl Stand Ref Data Ser 59, USA Natl Bur Stand. 1977.

Livingstone DR. Oxidative stress in aquatic organisms in relation to pollution and aquaculture. Revue Méd Vét 2003; 154(6): 427-430.

Lewis WM, Morris DP. Toxicity of nitrite to fish: A review. T Am Fish Soc 1986; 115: 83-95.

Jensen FB. Nitrite disrupts multiple physiological functions in aquatic animals. Comp Biochem Phys A 2003; 135: 9-24.

Svobodova Z, Machova J, Drastichova J, Groch L, Luskova V, Poleszczuk G, *et al*. Haematological and biochemical profile of carp blood following nitrite exposure at different concentration of chloride. Aquac Res 2005; 36: 1177-1184.

Michael MI, Hilmy AM, el-Domiaty NA, Wershana K. Serum transaminases activity and histopathological changes in *Clarias lazera* chronically exposed to nitrite. Comp Biochem and Physiol 1987; 86: 255-262.

Russo RC. Ammonia, nitrite and nitrate. In: Rand GM, Petrocelli SR, editors. Fundamental of aquatic toxicology. Washington DC: Hemisphere Publishing Corporation 1985; 455-71.

Camargo JA, Alonso A, Salamanca A. Nitrate toxicity to aquatic animals: a review with new data for fresh water invertebrates. Chemosphere 2005; 58: 1255-67.

Stormer J, Jensen FB, Rankin JC. Uptake of nitrite, nitrate, and bromide in rainbow trout, *Oncorhynchus mykiss*: effects on ionic balance. Can J Fish Aquat Sci 1996; 53: 1943-1950.

Schram E, Roques JAC, van Kuijk T, Abbink W, van de Heul, de Vries P, Bierman S, *et al*. The impact of elevated water ammonia and nitrate concentrations on physiology, growth and feed intake of pikeperch (*Sander lucioperca*). Aquaculture 2014; 420-421: 95-104.

Tables

Gene	Forward primer (5'- 3')	Reverse primer (5'- 3')	ZFIN ID
rplp0	5'-CTGAACATCTCGCCCTTCTC-3'	5'-TAGCCGATCTGCAGACACAC-3'	ZDB-GENE-000629-1
eef1a	5'-AGTCCACCTCCACCGGTCAT-3'	5'-AGGAGCCCTTGCCCATCTC-3'	ZDB-GENE-030131-8278
nr3c1	5'-AGACCTTGGTCCCCTTCACT-3'	5'-CGCCTTTAATCATGGGAGAA-3'	ZDB-GENE-050522-503
gsta.l	5'-TTGAGGAAAAGGCCAAAGTG-3'	5'-AACACGGCCTTCACTGTTCT-3'	ZDB-GENE-040426-2720
gsr	5'-AGACCTTGGTCCCCTTCACT-3'	5'-CGCCTTTAATCATGGGAGAA-3'	ZDB-GENE-050522-116
gpx1a	5'-ACCTGTCCGCGAAACTATTG-3'	5'-TGGAGAC C GAC CAC CTTTTC-3'	ZDB-GENE-030410-1
hsp70.1	5'-AAAGCACTGAGGGACGCTAA-3'	5'-TGTTCAGTTCTCTGCCGTTG-3'	ZDB-GENE-990415-91
hnf4a	5'-ACGGTTCGGCGAGCTGCTTC-3'	5'-TCCTGGACCAGATGGGGGTGT-3'	ZDB-GENE-030131-1077
sod1	5'-GTCGTCTGGCTTGTGGAGTG-3'	5'-TGTCAGCGGGCTAGTGCTT-3'	ZDB-GENE-990415-258
sod2	5'-CCGGACTATGTTAAGGCCATCT-3'	5'-ACACTCGGTTGCTCTCTTTTCTCT-3'	ZDB-GENE-0301131-7742
cat	5'-CCAAGGTCTGGTCCCATAAA-3'	5'-GCACATGGGTCCATCTCTCT-3'	ZDB-GENE-000210-20
igf1	5'-GGCAAATCTCCACGATCTCTAC-3'	5'-CGGTTTCTCTTGTCTCTCTCAG-3'	ZDB-GENE-010607-2
igf2a	5'-GAGTCCCATCCATTCTGTTG-3'	5'-TCCTTTGTTTGTTGCCATTTG-3'	ZDB-GENE-991111-3
mstnb	5'-GGACTGGACTGCGAT GAG-3'	5'-GATGGGTGTGGGGATACTTC-3'	ZDB-GENE-990415-165

Table 1. Primer Sequences and ZFID used in the present study.

Figures

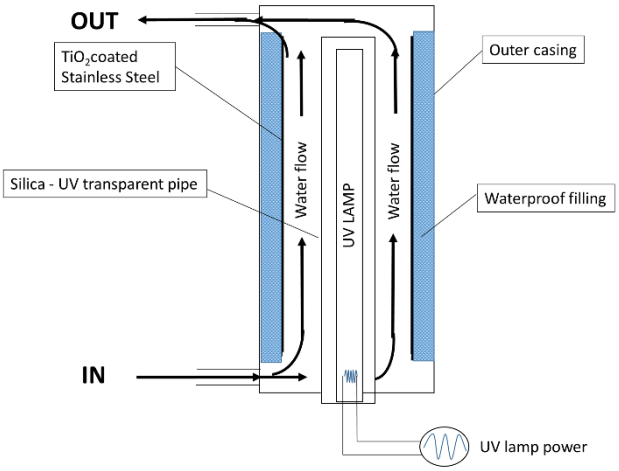

Figure 1. Schematic representation of the TiO_2 photocatalytic system used in this study.

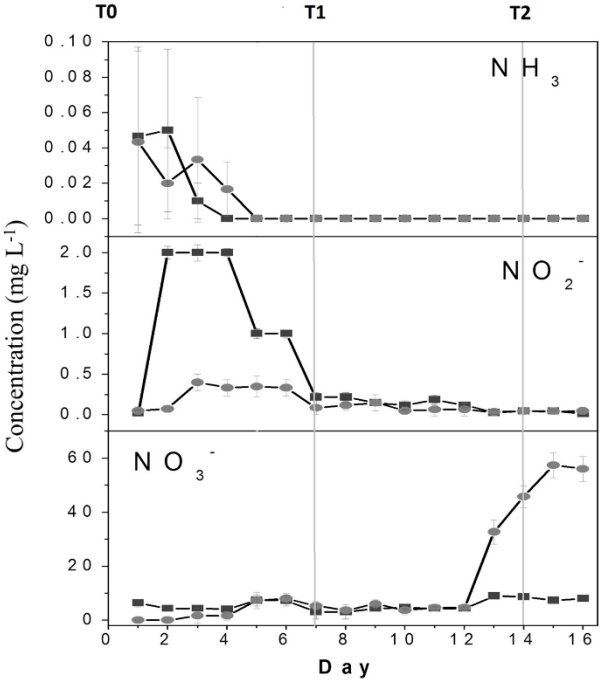

Figure 2. Ammonia, nitrite and nitrate ions mean concentration (mg/L) measured during the experiment for the control (•) and TiO_2 photocatalytic system (■) tanks. Bars indicate standard errors.

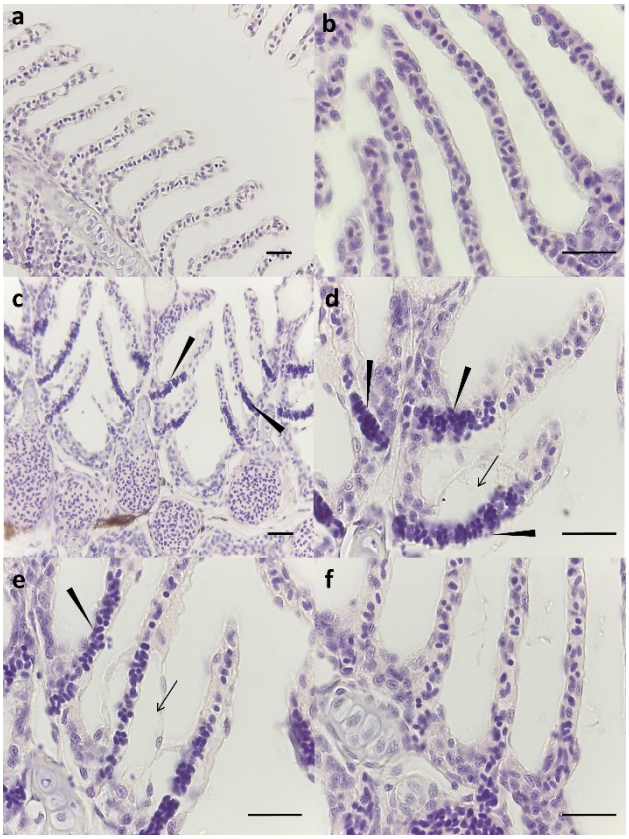

Figure 3. Histology of gills. Control group at T1 (a) and at T2 (b); test group at T1 (c, d, e) and at T2 (f). Arrow heads indicate vessel congestion, arrows indicate oedema. Scale bar = 10 µm.

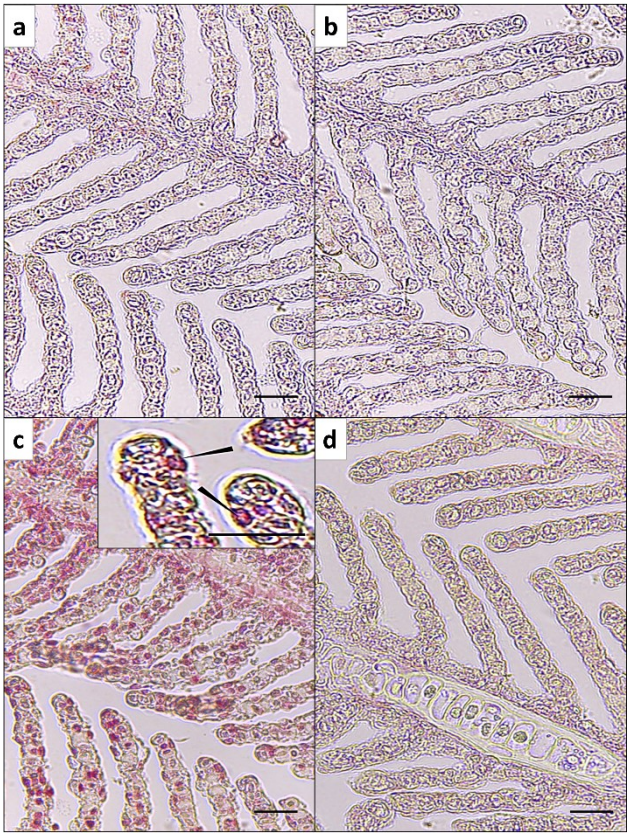

Figure 4. Detection of apoptotic cells in gills by mean of TUNEL assay. Control group at T1 (a) and at T2 (b) and test group at T1 (c) and T2 (d). Arrow heads in the insert indicate epithelial TUNEL-positive cells. Scale bar = 10 µm.

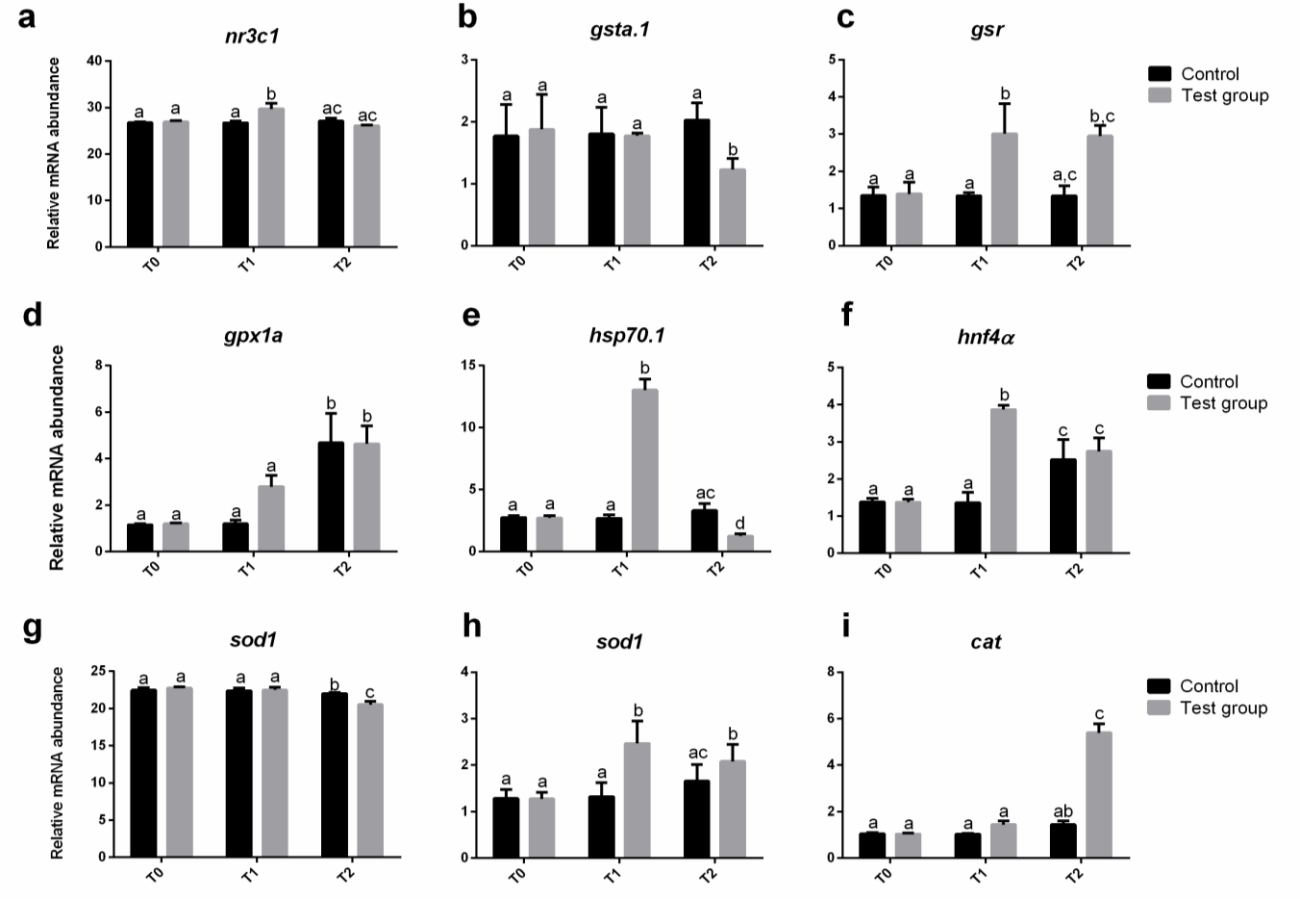
a
nr3c1
Relative mRNA abundance
b
gsta.1
c
gsr
Control
Test group
d
gpx1a
Relative mRNA abundance
e
hsp70.1
f
hnf4α
Control
Test group
g
sod1
Relative mRNA abundance
h
sod1
i
cat
Control
Test group
T0
T1
T2

Figure 5. Relative mRNA abundance of genes involved in fish stress response (*nr3c1*, *gsta.1*, *gsr*, *gpx1a*, *hsp70.1*, *hnf4a*, *sod1*, *sod2*, *cat*) analyzed in the liver at 0 (T0), 7 (T1) and 14 (T2) days of exposure of test group compared to control group. Different letters indicate statistically significant differences between the two experimental groups (p <0.05). Values are presented as mean ± SD.

Chapter 5

Larvicidal activity of a new nano-photosensitizer complex tested on *Aedes aegypti* larvae

Chemello G, Randazzo B, Zarantoniello M, Magro M, Ballarin C, Radaelli G, Rossi P, Vianello F,Olivotto I.

5.1 Introduction

Insect-transmitted diseases represent a major cause of illness and death around the world, especially in tropical countries where the favorable environmental conditions are responsible for the proliferation of disease vectors, such as mosquitoes, lice, fleas, and ticks[1,2].

Mosquitoes alone, transmit disease to more than 700 million people annually[3], therefore, their control is an important public health concern.

Aedes aegypti is a day-biting mosquito, which often feeds on multiple hosts during a single gonotrophic cycle. Females preferentially lay eggs in man-made or artificial containers including water tanks, flower vases, pot plant bases, discarded tires, and buckets[4].

Ae. aegypti occurs in Asia, Africa, Central and South America and transmits the Flavivirus genus virus, etiologic agents of human diseases like dengue and yellow fever[5]. Together with others mosquitoes of the *Aedes genus*, it is also the main vector of Zika virus[6] now causing the recent explosive outbreaks in French Polynesia (2013-2014) and South America (2015-2016)[7].

The World Health Organization (WHO) has recognized dengue fever as one of the fastest-growing viral threats globally. Fifty million dengue infections and about 500,000 cases requiring hospitalization occur each year worldwide[8]. To date, according to the WHO (2016), severe dengue mostly affects Asian and Latin American countries and has become a leading cause of hospitalization and death among children and adults in these regions. The only method to minimize the virus transmission is through vector control since to date, there is no vaccine for dengue fever[1].

Measures to control this vector, often include the application of chemical or biological agents for both immature and adult mosquito stages control and environmental control of mosquitoes' breeding sites[9]. However, the efficacy of vector control strategies in terms of reduction of dengue transmission is still

unclear. Most insecticides indeed, are non-selective, harmful to non-target organisms and can adversely affect the environment by contaminating soil, water, and air[10]. Large amounts of organic solvents are usually employed to dissolve these materials in order to achieve effective and uniform application in the field[11]. Organic solvents are much more expensive than water and many of the resultant organic solutions are incompatible with the aquatic environment causing their possible application in aquatic pool, pond, basin or aquaculture system to be useless.

Different insecticides that are still in use against mosquitos' populations can reach the aquatic environment at high enough concentrations to affect aquatic life[12]. Moreover, long-term exposure to a toxicant eventually selects for mutations, conferring a level of resistance to that toxicant. Indeed insecticide-resistant mosquito populations are now threatening the control programs[13]. Mosquitoes resistance to current commercial insecticides such as organochlorides, organophosphates, carbamates and also to biological insecticides is well established[10]. The organophosphate Temephos, for example, is widely used in Brazil to control *Ae. aegypti* proliferation, however, a decrease in its effectiveness has already been described due to larval tolerance[13]. Therefore, the developing of new methods for controlling mosquitoes in an environmentally safer way is of primary importance.

In this direction, nanotechnologies may be exploited for the development of novel larvicides. Over the years, nanometric systems as carriers to reduce the concentration of applied pesticides have been developed in order to obtain safer agricultural products[14–16]. The application of nanomaterial-based formulations can produce several benefits such as improving the product efficacy due to a higher surface area to volume ratio and increasing the systemic activity due to smaller particle size and higher mobility[17]. Moreover, the application of nanoparticles allows a significant increase in water

solubility, dissolution rate and dispersion of the insecticide with no chemical alteration to its molecule[11]. When compared with the bulk material, nanoparticles are also much more mobile, enabling better penetration into insect tissues and increasing the insecticide activity. This can be achieved either by faster penetration by direct contact through the insect's cuticle or by ingestion through the digestive tract[17].

Photosensitizing agents activated by sunlight or artificial light have been considered as a tool to control several types of insects. Different compounds have been examined in both laboratory experiments[18,19] and field studies[20]. Some of these molecules, called photo-insecticides, have been successfully used in agriculture to fight insect pests[21].

Most investigations have been performed by using photoactivatable polycyclic aromatic dyes that absorb near-UV light wavelengths. All of these dyes require the presence of molecular oxygen to express their phototoxic action and undergo to photodynamic reactions in which a substrate is destroyed only in the presence of a chromophoric molecule called a photosensitizer that absorbs light[22]. Among other processes, light absorption promotes the photosintetizer in a long-lived excited state called a triplet state. When a photosensitizer is in its excited state it can interact with molecular triplet oxygen ($^3O_2$) and produce radicals and reactive oxygen species (ROS). These species include singlet oxygen ($^1O_2$), hydroxyl radicals (•OH) and superoxide (O_2^-) ions. They can interact with cellular components including unsaturated lipids, amino acid residues, and nucleic acids. If sufficient oxidative damage ensues, this will result in target-cell death (only within the illuminated area). Well known photosensitizers include several families of aromatic and heterocyclic compounds such as pyrenes, xanthenes, phenothiazines, porphyrins and chlorins (Kohen et al., 1995).

In the present study, the efficacy of a new complex made of magnetic nanoparticles and photosensitizer molecule (under evaluation for a patent method) to mosquitoes' proliferation control was tested. *Aedes aegypti* larvae were exposed to the complex in water solution, and larvicidal activity of a new type of magnetic nanoparticles, new molecule, and the complex was compared. The accumulation of the new complex was evaluated by optic and transmission electron microscopy (TEM).

5.2 Materials and Methods

5.2.1 *Aedes aegypti*

Laboratory strain of *Aedes aegypti* eggs was provided by Camerino University (Italy) and kept dry until the time of hatching. Larvae were reared in water tanks at 28 °C with a controlled amount of food (yeast suspension) for 5 days (fourth stage) before exposure to the different experimental conditions.

5.2.2 Formation of the complex magnetic nanoparticles and new photosensitizer molecule

The new complex tested in this study is actually under patent pending method.

5.2.3 Experimental design

Twenty mosquito larvae (3 days post hatching) were exposed to a total volume solution of 50 ml in a petri dish (5 petri dishes each experimental conditions) at the following conditions: control group (ctrl) water; group A: 20 mg/L new complex, group B: 50 mg/L new complex, group C: 100 mg/L new complex, group D: 20 mg/L magnetic nanoparticles, group E: 50 mg/L magnetic nanoparticles, group F: 100 mg/L magnetic nanoparticles, group G: 9 mg/L photosensitizer molecule, group H: 22.5 mg/ photosensitizer molecule, group I: 45 mg/L photosensitizer molecule.

All treatments were conducted under constant light (Photon flux density: 2384 µmol/m2/s) and in complete dark continuously for 4 hrs. All treatments were constantly monitored during the experimental time and the mortality was registered every 30 minutes, All the death larvae were collected and properly stored for further analysis.

5.2.4 Survival rate

Dead larvae were identified during the exposure to all different experimental conditions each 30 min., larvae were considered dead when they failed to move after probing with a needle in the siphon or cervical region. Results on larval survival rate were expressed as the mean ± s.d. (n=5).

5.2.5 Histological analysis

Larvae were fixed in 4% paraformaldehyde at 4°C overnight, washed in phosphate-buffered saline (PBS, 0.1 M, pH 7.4) and dehydrated through a graded series of ethanol before being embedded in paraffin following the procedures to routine optical microscopy. Sections of 4 µm were stained with hematoxylin and eosin (HE) and observed with an Olympus® Vanox AHBT3 photomicroscope coupled to an Olympus camera and CellB Olympus software.

5.2.6 Transmission electron microscopy analysis (TEM)

Larvae of *Aedes aegypti* from all experimental conditions were collected at every sampling time and immediately fixed in 2,5% glutaraldehyde in 0.1 M Sorensen's buffer (pH 7.4) for 3h at 4°C for primary fixation. Successively larvae were washed in 0.1 M Sorensen's buffer and then post-fixed in osmium tetroxide (1% in 0.2 M Sorensen's buffer) for 1h at 4°C and in dark conditions. After 1h, all the osmium tetroxide was removed, and larvae were washed in

0.1 M Sorensen's buffer to completely remove osmium tetroxide excess. Larvae were dehydrated and embedded in araldite. Sections of 400 Å were cut using an ultracut and stained with uranyl acetate-lead citrate 23. TEM micrographs of biological samples were acquired by a FEI Tecnai 12 microscope operating at 120 Kv.

5.2.7 Statistical analysis

Results on larval survival rate were expressed as the mean ± s.d. (n=5). Statistical differences were determined using one-way ANOVA analysis of variance, followed by Tukey's multiple comparison test. All statistical analyses were performed using Prism 6 (GraphPad Software, San Diego, CA, USA). Significance was set at $p < 0.05$.

5.3 Results

5.3.1 Survival rate

The analysis of the survival rate performed on larvae exposed to different concentrations of magnetic nanoparticles (group D, group E, and group F) and the photosensitizer molecule (group G, group H, and group I) both in complete dark and under constant light irradiation, showed a 100% survival rate at the end of the exposure time (4 hrs). The same result was observed for larvae exposed, in complete dark, to the new complex formed by magnetic nanoparticles and the photosensitizer molecule (data not shown).

The analysis of larvae exposed to the new complex under constant light irradiation showed a time-concentration correlation in the decrease of survival rate (Figure 1).

Larvae exposed to the highest concentration of the new complex (100 mg/L, group C) showed a survival percentage of 0% after 1 hour and 20 minutes of exposure, while a survival of 0% was observed in larvae exposed to 50 mg/L

of the new complex (group B) after 3 hours. Finally, group A (20 mg/L of the new complex) was characterized by a mean survival percentage of 27 ± 8,7% at the end of the exposure time (4 hrs).

5.3.2 Histological analysis

Histological analysis, performed in groups exposed to 50 mg/L of bare nanoparticles (group E) under constant light irradiation, showed nanoparticles (np) accumulation in the midgut lumen after 1 hour of exposure (Fig. 2C).
Similarly, histological analysis performed on larvae exposed to, constant light irradiation to the highest concentration (100 mg/L) of the new complex (Fig. 2 A, B, D) and bare magnetic nanoparticles (Fig. C) revealed the accumulation of NPs after 1hour exposure.

5.3.3 Transmission electron microscopy analysis (TEM)

Images from TEM analysis showed the presence of a small aggregates of magnetic nanoparticles in the larval gut lumen (Fig.4A, B) of animals exposed to 50 mg/L of the bare NPs and a bigger aggregate (Fig. 4C) in the gut of those exposed to the highest NPs concentrations (100 mg/L). NPs aggregates were detectable also in the gut of larvae exposed to 100 mg/L of the new complex (Fig. 4D).

5.4 Discussion

Mosquitoes (especially those belonging to *Aedes* genus) are vectors of several human arboviruses, the most important of which are dengue and yellow fever viruses[24]. *Ae. aegypti* represents the main dengue vector species, because of its marked anthropophily and for its ability to proliferate in proximity to human communities by using artificial water storages such as tanks, drums, buckets, flower vases, etc. as breeding sites[25]. Since a vaccine against dengue

is still lacking, control of the vector proliferation is considered the most effective strategy for the prevention of disease breakout. However, present methods used to prevent disease vector proliferation, are often toxic and induce the emergence of insecticide resistance.

The present study evaluated the potential of a new alternative method for mosquitoes' proliferation control, through the use of a photosensitizer molecule bind to a new type of magnetic nanoparticle, obtaining interesting preliminary results.

Several synthetic and naturally derived photosensitizers, such as thiophenes, xanthenes, phenothiazines, furocoumarins, acridines, tetraethynylsilanes, and porphyrins, have been demonstrated to be effective photo-insecticides against a range of harmful insects, including flies[26,27] and mosquitoes[28]. Their activity depends on the photoactivation by visible light, while they are completely harmless at dark. A similar result was demonstrated in this study with a 100% survival rate in all groups treated both with the new complex and the photosensitizer molecule subjected to darkness.

Photo-activated processes have been demonstrated to be very harmful and cause irreversible damages to cells by reactive singlet oxygen ($^1O_2$) intermediate produced under aerobic conditions[29]. Despite the present study did not aim to study the molecular mechanisms behind the just-mentioned damages, it is likely that the larvicidal activity of the new compound herein tested be explained by their onset, as already broadly detailed in literature (see below for references).

A variety of biological molecules are susceptible to photosensitized oxidation, including acids, alcohols, amines, carbohydrates, esters, ketones, nitrogen heterocycles, nucleic acids, unsaturated lipids, phenols, proteins, pyrroles, steroids, and vitamins[30]. Major targets are unsaturated membrane lipids (fatty acids, neutral fats, phospholipids, and steroids) that are photooxidized to

allylic hydroperoxides and their breakdown products, and membrane-associated proteins, in which the most common sites of damage are cysteinyl, histidyl, methionyl, tryptophyl, and tyrosyl residues. Photooxidative damage results in both loss of structural integrity of the membrane and loss of biological function of associated molecules such as enzymes, hormones, and receptors[31]. Lipid peroxidation, as a result of photooxidative damage, has been observed in mosquito larvae[32].

Moreover, photosensitizer molecule (like the one used in this study) present a great advantage because they are harmless in case of ingestion by humans and, in general, by non-translucent organisms.

The new complex formed by magnetic nanoparticles and the photosensitizer molecule showed a larvicidal activity in a relative short period of time-related to the concentration tested, while the exposure to the photosensitizer molecule alone didn't show the same results during the same exposure time. These different outcomes can be related to the difficulty of driving the photosensitizer molecule to a specific location in cells and tissues. Magnetic nanoparticles, increased the accumulation rate efficacy of the photosensitizer molecule acting as vectors to the larvae's midgut as showed in histological and TEM images. Insect midgut has been identified as a major site of accumulation for several photosensitizers as demonstrated in *Ceratitis capitata* (the Mediterranean fruit fly) adults, which shown to accumulate hematoporphyrin in the midgut, as well as in the fat body, malpighian tubules and cuticle after feeding on porphyrin-containing baits[33]. Also, larvae of the culicid *Eretmapodites quinquevittatus* accumulated porfimer sodium in the gastric caeca, gut, rectum, malpighian tubules, and anal papillae[34]. The accumulation of both bare NPs and the complex, into the larva body, can be considered as the evidence that the bond between the photosensitizer molecule and magnetic nanoparticle didn't change the NPs target accumulation organ.

Actually, the NP acted as a carrier for the photosensitizer molecule into the larva midgut.

5.5 Conclusions

The preliminary results obtained from this study highlighted, for the first time, the efficient larvicidal activity of this new photosensitizer complex under controlled laboratory conditions. However, future field studies are required to assess the potential of this approach in natural conditions. *Aedes aegypti* breeding sites are found both outdoors and indoors[35]. While the photosensitization approach is expected to be effective on larvae located in outdoor containers, which are common productive breeding sites, a major challenge is represented by the breeding sites receiving little sunlight because of their shape or because of indoor or shaded location, a condition that for *Aedes aegypti* is not infrequent.

References

1. El-Sheikh, T. M. Y., Al-Fifi, Z. I. A. & Alabboud, M. A. Larvicidal and repellent effect of some *Tribulus terrestris* L., (Zygophyllaceae) extracts against the dengue fever mosquito, *Aedes aegypti* (Diptera: Culicidae). J. Saudi Chem. Soc 2016; 20, 13–19.
2. Jawale, C., Kirdak, R. & Dama, L. Larvicidal activity of Cestrum nocturnum on *Aedes aegypti*. Bangladesh J. Pharmacol. 5, 39–40 (2010).
3. Taubes, G. Vaccines. Searching for a parasite's weak spot. Science 2000; 290, 434–7.
4. Jansen, C. C. & Beebe, N. W. The dengue vector *Aedes aegypti*: what comes next. Microbes Infect 2010; 12, 272–279.
5. Roberts, L. Mosquitoes and disease. Science 2002; 298, 82–3.
6. Ioos, S. et al. Current Zika virus epidemiology and recent epidemics. Médecine Mal. Infect 2014; 44, 302–307.
7. Liu, Y. et al. Evolutionary enhancement of Zika virus infectivity in *Aedes aegypti* mosquitoes. Evolutionary increases in the infectivity of mosquito-borne viruses within their vectors results in high epidemic potential. We speculate that the adaptability and infectivity of ZIKV within its mosquito vectors. Nat. Publ. Gr 2017; 545.
8. WHO. Dengue and severe dengue. WHO (World Health Organization, 2017).
9. George, L. et al. Community-Effectiveness of Temephos for Dengue Vector Control: A Systematic Literature Review. PLoS Negl. Trop. Dis. 9, e0004006 (2015).
10. Dharmagadda, V. S. S., Naik, S. N., Mittal, P. K. & Vasudevan, P. Larvicidal activity of *Tagetes patula* essential oil against three mosquito species. Bioresour. Technol 2005; 96, 1235–1240.
11. Margulis-Goshen, K. & Magdassi, S. Nanotechnology: An Advanced Approach to the Development of Potent Insecticides. in Advanced Technologies for Managing Insect Pests 295–314 (Springer Netherlands, 2013). doi:10.1007/978-94-007-4497-4_15

12. Monteiro, D. A., de Almeida, J. A., Rantin, F. T. & Kalinin, A. L. Oxidative stress biomarkers in the freshwater characid fish, *Brycon cephalus*, exposed to organophosphorus insecticide Folisuper 600 (methyl parathion). Comp. Biochem. Physiol. Part C Toxicol. Pharmacol 2006; 143, 141–149.

13. Poupardin, R. et al. Cross-induction of detoxification genes by environmental xenobiotics and insecticides in the mosquito *Aedes aegypti*: Impact on larval tolerance to chemical insecticides. Insect Biochem. Mol. Biol 2008; 38, 540–551.

14. de Oliveira, J. L., Campos, E. V. R., Bakshi, M., Abhilash, P. C. & Fraceto, L. F. Application of nanotechnology for the encapsulation of botanical insecticides for sustainable agriculture: Prospects and promises. Biotechnol. Adv 2014; 32, 1550–1561.

15. Campos, E. V. R., de Oliveira, J. L. & Fraceto, L. F. Applications of Controlled Release Systems for Fungicides, Herbicides, Acaricides, Nutrients, and Plant Growth Hormones: A Review. Adv. Sci. Eng. Med 2014; 6, 373–387.

16. Kah, M. & Hofmann, T. Nanopesticide research: Current trends and future priorities. Environ. Int 2014; 63, 224–235.

17. Sasson, Y., Levy-Ruso, G., Toledano, O. & Ishaaya, I. Nanosuspensions: Emerging Novel Agrochemical Formulations. in Insecticides Design Using Advanced Technologies 1–39 (Springer Berlin Heidelberg, 2007). doi:10.1007/978-3-540-46907-0_1.

18. Heitz, J. R. Development of Photoactivated Compounds as Pesticides. in 1–21 (1987). doi:10.1021/bk-1987-0339.ch001.

19. Rebeiz, C. A., Reddy, K. N., Nandihalli, U. B. & Velu, J. Tetrapyrrole-dependent photodynamic herbicides. Photochem. Photobiol. 52, 1099–1117 (1990).

20. Lemke, L. A., Koehler, P. G., Patterson, R. S., Feger, M. B. & Eickhoff, T. Field Development of Photooxidative Dyes as Insecticides 1987; 10, 156–167 doi:10.1021/bk-1987-0339.ch010.

21. Moreno, D. S., Celedonio, H., Mangan, R. L., Zavala, J. L. & Montoya, P. Field Evaluation of a Phototoxic Dye, Phloxine B, Against Three Species of Fruit Flies (Diptera: Tephritidae). J. Econ. Entomol 2001; 94, 1419–1427.

22. Dondji, B. et al. Assessment of Laboratory and Field Assays of Sunlight-Induced Killing of Mosquito Larvae by Photosensitizers. J. Med. Entomol 2005; 42, 652–656.

23. Reynolds, E. S. The use of lead citrate at high pH as an electron-opaque stain in electron microscopy. J. Cell Biol 1963; 17, 208–12.

24. Kraemer, M. U. et al. The global distribution of the arbovirus vectors Aedes aegypti and *Ae. albopictus*. Elife 2015; 4, e08347.

25. Lucantoni, L. et al. Novel, Meso-Substituted Cationic Porphyrin Molecule for Photo-Mediated Larval Control of the Dengue Vector *Aedes aegypti*. PLoS Negl. Trop. Dis 2011; 5, e1434.

26. Ben Amor, T. & Jori, G. Sunlight-activated insecticides: historical background and mechanisms of phototoxic activity. Insect Biochem. Mol. Biol 2000; 30, 915–925.

27. Amor, T. Ben, Bortolotto, L. & Jori, G. Symposium-in-Print Porphyrins and Related Compounds as Photoactivatable Insecticides. 3. Laboratory and Field Studies. Photochem. Photobiol 2000; 71, 124.

28. Dosdall, L. M., Galloway, M. M. & Arnason, J. T. Toxicity and residual action of the photoactivated compound, cyano-alpha-terthienyl, and its efficacy for reducing pre-imaginal populations of mosquitoes. J. Am. Mosq. Control Assoc 1992; 8, 166–72.

29. Ricchelli, F. Photophysical properties of porphyrins in biological membranes. J. Photochem. Photobiol. B Biol 1995; 29, 109–118.

30. Marles, R. J. et al. Thiophenes as mosquito larvicides: Structure-toxicity relationship analysis. Pestic. Biochem. Physiol 1991; 41, 89–100.

31. Girotti, A. W. Photosensitized oxidation of membrane lipids: reaction pathways, cytotoxic effects, and cytoprotective mechanisms. J. Photochem. Photobiol. B Biol 2001; 63, 103–113.

32. Hasspieler, B. M., Arnason, J. T. & Downe, A. E. R. Modes of action of the plant-derived phototoxin α-terthienyl in mosquito larvae. Pestic. Biochem. Physiol 1990; 38, 41–47.

33. Amor, T. Ben, Bortolotto, L. & Jori, G. Porphyrins and Related Compounds as Photoactivatable Insecticides. 2. Phototoxic Activity of Meso-Substituted Porphyrins. Photochem. Photobiol 1998; 68, 314–318.

34. Helleck, A. M. & Hartberg, W. K. Site of Photofrin II photosensitization in larvae of *Eretmapodites quinquevittatus* Theobald. J. Am. Mosq. Control Assoc 1999; 15, 437–45.

35. Strickman, D. & Kiooayapong, P. Dengue and its vectors in Thailand: Calculated Transmission Risk From total pupal counts of *Aedes aegypti* and association of wing-length measurements with aspects of the larval habitat. Am. J. Trop. Med. Hyg 2003; 68, 209–217.

Figures

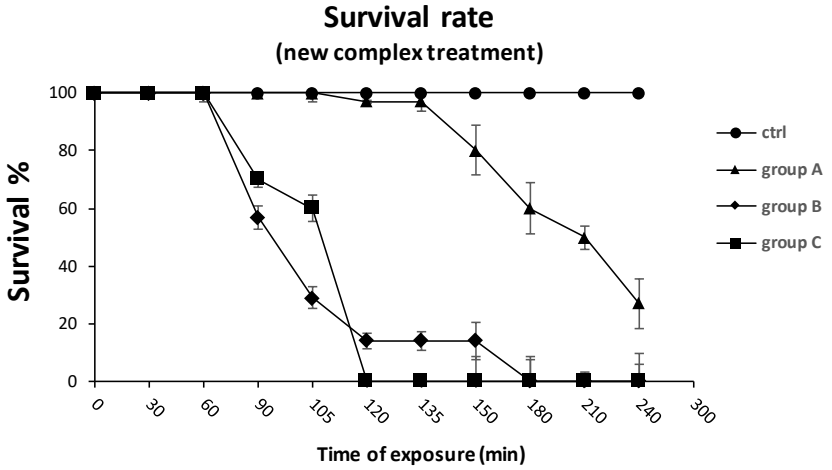

Figure 1. Survival rate (%) of *Aedes aegypti* larvae exposed to the new complex at different concentrations: group A (20mg/L), group B (50 mg/L), group C and control group (ctrl). Results are expressed as the mean ± s.d. (n=5).

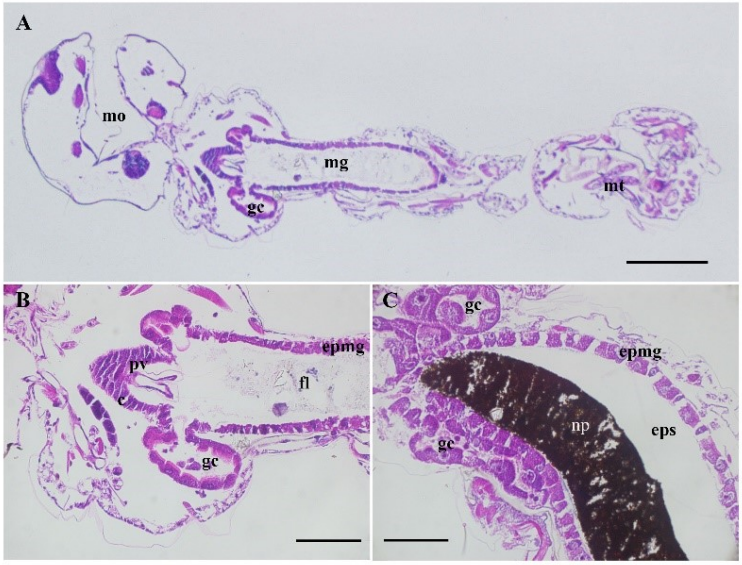

Figure 2. Histological sections of *Aedes aegypti* larvae. Examples of sagittal sections of a control larva (ctrl) (**A**). Section through proventriculus, anterior end of mid-gut and gastric caeca (**B**), portion of the midgut (**C**) of a larva exposed to 50 mg/L of bare magnetic nanoparticles for 1 hour. (mo), mouth; (mg), midgut; (mt), Malpighian tubules; (gc), gastric caeca; (pv), proventriculus; (fl), food in gut lumen; (epmg,) epithelium of the midgut; (eps), ectoperitrophic space; (np), nanoparticles. Scale bars: **A**=250 μm, **B** and **C** = 100 μm.

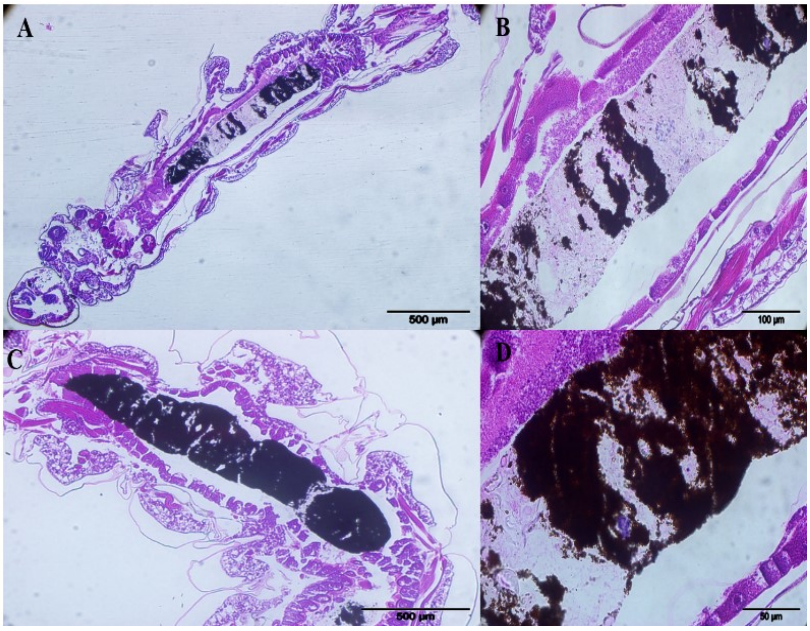

Figure 3. Histological sections of *Aedes aegypti* larvae. Examples of sagittal sections of a larva exposed to 100 mg/L of the new complex for 1 hour (**A**) (**B**) (**D**); sagittal section of a larva exposed to 100 mg/L of bare magnetic nanoparticles for 1 hour (**C**). Scale bars: **A** and **C** = 500 µm, **B** = 100 µm, **D** = 50 µm.

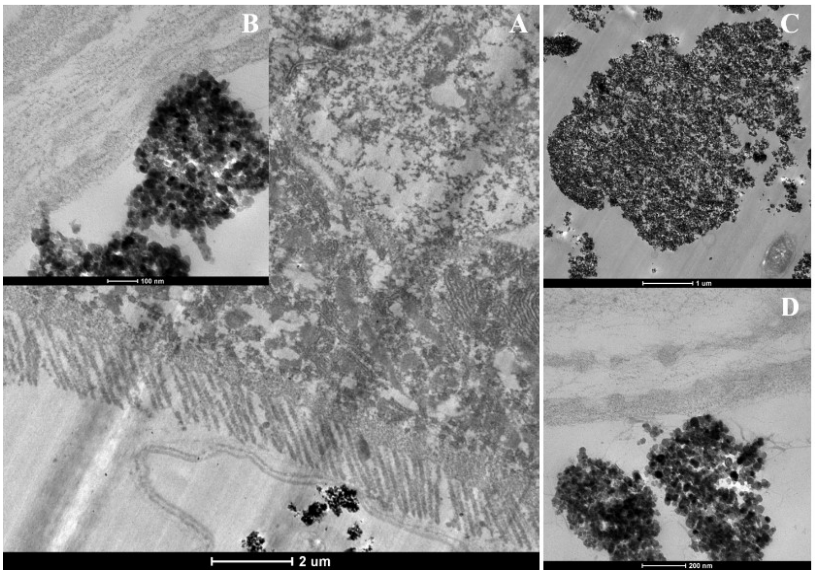

Figure 4. Transmission electron microscopic detection of nanoparticles in the gut of *Aedes aegypti* larvae. Example images of a small aggregate (**A**)(**B**) of bare nanoparticles in a larva exposed to 50 mg/l of magnetic NPs and a big aggregate (**C**) in larva exposed to 100 mg/L of magnetic NPs. Example image of nanoparticles aggregates in the gut of a larva exposed to 100 mg/L of the new complex (**D**). Scale bars: **A** = 2 μm, **B** = 100 nm, **C** = 1 μm, **D** = 200 nm.

Conclusions

In the present doctoral thesis, the application of nanotechnology in different aquaculture sectors was investigated. Nanotechnology offers the opportunity to control properties without changing the chemical composition of the material, as a consequence, nanomaterials (including nanoparticles) show unique and different properties if compare to the same material on the macroscale. These innovative features can offer new solutions to existing limits and problems in several industry and research fields including aquaculture activity.

In particular, a new type of iron oxide nanoparticles called SAMNs (surface active magnetic nanoparticles), TiO_2 nanoparticles and a new complex made of magnetic nanoparticle and a photosensitizer molecule were chosen as tools for our studies due to their unique characteristics which make them suitable for our purposes.

Thanks to the shared financial support between Polytechnic University of Marche and BioTecnologie BT company (Pantalla di Todi, Italy) multidisciplinary studies were performed and interesting and promising results were obtained. This research was divided into five chapters each of them focused on testing an innovative application of a new nanomaterial to a specific aquaculture aspect. Different model organisms were chosen, after the evaluation of various scientific and practical factors and according to data present in scientific literature to find the most relevant and useful species to the present research. Zebrafish was used as experimental model due to its advantageous features which made it suitable for biomedical, molecular, genetic, development and toxicology studies. Gilthead sea bream was select as seawater model because of the numerous information already gained on its biology and rearing methods and for the high interest as a commercial species due to its good market price and high survival rate and feeding habits.

Aedes aegypti is responsible of the most dangerous disease outbreaks of dengue and yellow fever and Zika virus, therefore the prevention of this species proliferation is of global concern. *Escherichia coli* was used as one of the representative species of aquatic microflora community and considering as the most finely understood and extensively studied free-living organism on our planet.

The results obtained from this study revealed, for the first time, the safety application of SAMNs as an alternative OTC delivery method in both *in vivo* and *ex vivo* exposure studies. Moreover, *in vivo* tests detected a higher absorption rate (particularly in zebrafish ovary samples) of the antibiotic administered through SAMNs@OTC complex highlighting the possible reduction of antibiotic utilization in aquaculture activity and the consequent environmental impacts. However, results obtained from *ex vivo* exposure, of both zebrafish and sea bream organs, also revealed that the extrapolation of *ex vivo* data to *in vivo* physiology must be cautious because the exposure of a single organ cannot represent the complexity of interactions typical of a biological system.

SAMNs were also observed to be involved in the "protein hitch-hiking" mechanism, binding plasma apolipoprotein A1 which acts as a carrier for the complex SAMNs@OTC into the ovary, demonstrating the great potential of SAMNs in future application for drug delivery. Moreover, this result rises ulterior questions on the Apo A1 mediate transport of the complex (once in the ovary) inside the oocytes. Therefore, the study of the actual OTC accumulation into the oocytes and the consequent effects on their maturation and/or fish reproduction represent a matter of study of great interest, especially regarding future drug delivery applications.

TiO_2 based purification system was successfully tested showing both the potentiality to be applied in recirculating systems (helping in saving water and

reducing costs for the facility) and as a waste water treatment system in aquaculture facilities, reducing environmental impacts. Finally, magnetic nanoparticles used in this study revealed their functionality in controlling mosquitoes' proliferation when it is bound to a photosensitizer molecule. The complex between the NPs and this molecule (now under patent pending) increase the larvicidal effect of the molecule itself on *Aedes aegypti* larvae. This doctoral thesis highlighted at first, the great versatility of SAMNs; secondly, the safe application of an alternative purification system based on TiO_2 NPs, and finally the possible application of a new complex (magnetic NPs and photosensitizer molecule) in mosquitoes' proliferation control. Both SAMNs and TiO_2 systems' behavior was studied in a controlled aquatic environment laying the foundations for future studies aiming to a practical consequence in aquaculture activity.